

**Transition Metal-Containing Brønsted Acids as Single Component Cationic Initiators for
Olefin Polymerization**

by

Anna Louise Bennett

B.Sc. (Hons.), University of Birmingham, 2016

A THESIS SUBMITTED IN PARTIAL FULFILLMENT OF
THE REQUIREMENTS FOR THE DEGREE OF

MASTER OF SCIENCE

in

THE FACULTY OF GRADUATE AND POSTDOCTORAL STUDIES
(Chemistry)

THE UNIVERSITY OF BRITISH COLUMBIA

(Vancouver)

October 2018

© Anna L. Bennett, 2018

The following individuals certify that they have read, and recommend to the Faculty of Graduate and Postdoctoral Studies for acceptance, a thesis/dissertation entitled:

Transition Metal-Containing Brønsted Acids as Single Component Initiators for Olefin
Polymerization

submitted by Anna L. Bennett in partial fulfillment of the requirements for

the degree of Master of Science

in Chemistry

Examining Committee:

Prof. Derek. Gates

Supervisor

Prof. Parisa Mehrhodovandi

Supervisory Committee Member

Prof. Pierre Kennepohl

Supervisory Committee Member

Prof. Geoffrey Herring

Additional Examiner

Additional Supervisory Committee Members:

Supervisory Committee Member

Supervisory Committee Member

Abstract

Butyl rubber is a polymer commonly found in everyday life and produced solely by cationic polymerization at $-100\text{ }^{\circ}\text{C}$. The cationic polymerization of olefin monomers, like isobutylene and isoprene in butyl rubber, is very challenging. It is prone to side reactions which can lead to low molecular weight polymers with broad dispersities if the temperature of polymerization is not kept extremely low. Using Brønsted acids incorporating weakly coordinating anions (WCAs) as single component initiators has been an area of growing interest over recent years. WCAs are commonly comprised of main group elements, however in this thesis transition metal complexes are implemented instead to increase the steric bulk of the anions. A series of four Brønsted acids containing Group 5 metals have been synthesized, isolated and characterized. The cationic polymerization of *n*-butyl vinyl ether, styrene, α -methylstyrene and isoprene is studied for each of isolated single component initiators and have been shown to produce high molecular weight polymers at temperatures above $-100\text{ }^{\circ}\text{C}$.

Lay Summary

Butyl rubber is the synthetic alternative to natural rubber and is made of repeat units of organic molecules. To produce this long chain of repeat units (*i.e.* a polymer) an initiator must be used and, in the case of butyl rubber, one with a positively charged functionality. The positive charge must be balanced with a negative charge. The better initiators incorporate a large negatively charged molecule that is not strongly attracted to the positive charge. The strength of the interaction between the positive and negative charge will dictate the length of polymer chain and is therefore often critical. Syntheses and characterizations of initiators containing the positively charged and negatively charged portion in the same system is outlined in this thesis, as well as the successful polymerization of a range of repeat units to evaluate the efficiency of these initiators to produce butyl rubber.

Preface

All compounds and polymers reported in this thesis were prepared and characterized by me. All Chapters were written by me with the intention for Chapters 2 and 3 to be submitted for publication in a peer reviewed journal. Crystal structure data for Chapters 2 and 3 were collected and solved by Brian O. Patrick.

Table of Contents

Abstract.....	iii
Lay Summary	iv
Preface.....	v
Table of Contents	vi
List of Tables	x
List of Figures.....	xi
List of Schemes	xiv
List of Symbols and Abbreviations	xvi
Acknowledgements	xxi
Dedication	xxii
Chapter 1: Introduction	1
1.1 A History of Rubber.....	1
1.2 Cationic Polymerization.....	3
1.2.1 Cationic Chain Polymerization	3
1.2.2 Coordination Polymerization	8
1.3 Initiators Used in Cationic Polymerization.....	9
1.4 Weakly Coordinating Anions	10
1.4.1 Weakly Coordinating Anions in Cationic Polymerization	10
1.4.2 Weakly Coordinating Anions Containing Group 5 Metals.....	15
1.4.3 Brønsted Acids Utilizing Weakly Coordinating Anions	16
1.5 Outline of Thesis.....	18

Chapter 2: Hexacoordinate Niobium(V) Weakly Coordinating Anions and their

Application as Single Component Cationic Initiators for Olefin Polymerization19

2.1	Introduction.....	19
2.2	Results and discussion	22
2.2.1	Synthesis of H(OEt ₂) ₂ [2.1].....	22
2.2.2	H(OEt ₂) ₂ [2.1]-initiated polymerizations of <i>n</i> -butyl vinyl ether and styrene.....	25
2.2.3	Synthesis of H(OEt ₂) ₂ [2.2].....	26
2.2.4	H(OEt ₂) ₂ [2.2]-initiated polymerizations	31
2.2.5	Summary	41
2.3	Experimental	42
2.3.1	General Procedures	42
2.3.2	X-ray Structure Determination	43
2.3.3	Differential Scanning Calorimetry.....	44
2.3.4	Synthesis of H(OEt ₂) ₂ [2.1].....	45
2.3.5	Representative procedure for H(OEt ₂) ₂ [2.1]-initiated polymerization of <i>n</i> -butyl vinyl ether.....	45
2.3.6	Representative procedure for H(OEt ₂) ₂ [2.1]-initiated polymerization of styrene	46
2.3.7	Synthesis of H(OEt ₂) ₂ [2.2].....	46
2.3.8	Representative procedure for H(OEt ₂) ₂ [2.2]-initiated polymerization of <i>n</i> -butyl vinyl ether.....	47
2.3.9	Representative procedure for H(OEt ₂) ₂ [2.2]-initiated polymerization of styrene	48
2.3.10	Representative procedure for H(OEt ₂) ₂ [2.2]-initiated polymerization of α -methylstyrene	48

2.3.11	Representative procedure for H(OEt ₂) ₂ [2.2]-initiated polymerization of isoprene.....	49
--------	---	----

Chapter 3: Hexacoordinate Perfluorinated Weakly Coordinating Anions Using Group 5

Metals as Solid Brønsted Acids as Cationic Initiators for Olefin Polymerization50

3.1	Introduction.....	50
3.2	Results and discussion	52
3.2.1	Synthesis of H(OEt ₂) ₂ [3.1].....	52
3.2.2	Synthesis of H(OEt ₂) ₂ [3.2].....	55
3.2.3	H(OEt ₂) ₂ [3.1] and H(OEt ₂) ₂ [3.2]-initiated polymerizations.....	61
3.3	Summary	74
3.4	Experimental	74
3.4.1	General procedures	74
3.4.2	X-ray structure determination.....	76
3.4.3	Differential Scanning Calorimetry.....	77
3.4.4	Synthesis of H(OEt ₂) ₂ [3.1].....	78
3.4.5	Synthesis of H(OEt ₂) ₂ [3.2].....	78
3.4.6	Representative procedure for H(OEt ₂) ₂ [3.1]-initiated polymerization of <i>n</i> -butyl vinyl ether.....	79
3.4.7	Representative procedure for H(OEt ₂) ₂ [3.1]-initiated polymerization of styrene	80
3.4.8	Representative procedure for H(OEt ₂) ₂ [3.1]-initiated polymerization of α -methylstyrene	80
3.4.9	Representative procedure for H(OEt ₂) ₂ [3.1]-initiated polymerization of isoprene ..	81

3.4.10	Representative procedure for H(OEt ₂) ₂ [3.2]-initiated polymerization of <i>n</i> -butyl vinyl ether	81
3.4.11	Representative procedure for H(OEt ₂) ₂ [3.2]-initiated polymerization of styrene.....	82
3.4.12	Representative procedure for H(OEt ₂) ₂ [3.2]-initiated polymerization of <i>α</i> -methylstyrene	82
3.4.13	Representative procedure for H(OEt ₂) ₂ [3.2]-initiated polymerization of isoprene.....	83
Chapter 4: Conclusion.....		84
4.1	Introduction.....	84
4.2	Group 5 Hexacoordinate WCAs	84
References.....		87
Appendices.....		95
Appendix A Supplementary Information for Chapter 2		95
Appendix B Supplementary Information for Chapter 3		99

List of Tables

Table 2.1 H(OEt ₂) ₂ [2.1]-initiated polymerizations of <i>n</i> -butyl vinyl ether and styrene.	25
Table 2.2 Polymerization of <i>n</i> -butyl vinyl ether initiated with H(OEt ₂) ₂ [2.2].	32
Table 2.3 Cationic polymerization of styrene, α -methylstyrene, and isoprene initiated with H(OEt ₂) ₂ [2.2].	41
Table 2.4 Crystallographic parameters for H(OEt ₂) ₂ [2.2].	44
Table 3.1 H(OEt ₂) ₂ [3.1]-initiated polymerization of <i>n</i> -butyl vinyl ether, styrene, α -methylstyrene and isoprene.	61
Table 3.2 H(OEt ₂) ₂ [3.2]-initiated polymerization of <i>n</i> -butyl vinyl ether, styrene, α -methylstyrene and isoprene.	62
Table 3.3 Crystallographic parameters for H(OEt ₂) ₂ [3.2].	77

List of Figures

Figure 1.1 <i>cis</i> -1,4-polyisoprene monomer units of natural rubber.	1
Figure 1.2 Solvent association of the carbocation ($\overset{\sim}{\text{C}}^{\oplus}$) and the counter anion (A^{\ominus}).	6
Figure 1.3 Electrostatic interaction between a cation and a counter ion.	10
Figure 1.4 A selection of boron-containing WCAs.	12
Figure 1.5 A selection of aluminum-containing WCAs.	13
Figure 1.6 A selection of phosphorus-containing WCAs.	15
Figure 1.7 A selection of Group 5 containing WCAs, where M = Nb, and Ta.	16
Figure 2.1 Examples of WCAs containing hexacoordinate Nb(V) anions.	20
Figure 2.2 Previously reported Brønsted acids $\text{H}(\text{OEt}_2)_2[\mathbf{Ta.1}]$ and $\text{H}(\text{OEt}_2)_2[\mathbf{Ta.2}]$ and the Brønsted acids $\text{H}(\text{OEt}_2)_2[\mathbf{2.1}]$ and $\text{H}(\text{OEt}_2)_2[\mathbf{2.2}]$ pertaining to this thesis.	22
Figure 2.3 ^1H NMR (400 MHz, CD_2Cl_2 , $-85\text{ }^\circ\text{C}$) spectrum of $\text{H}(\text{OEt}_2)_2[\mathbf{2.1}]$	24
Figure 2.4 ^1H NMR (400 MHz, CD_2Cl_2 , $-85\text{ }^\circ\text{C}$) spectrum of $\text{H}(\text{OEt}_2)_2[\mathbf{2.2}]$	27
Figure 2.5 Molecular structure of $\text{H}(\text{OEt}_2)_2[\mathbf{2.2}]$	30
Figure 2.6 ^1H NMR spectrum (400 MHz, CDCl_3 , $25\text{ }^\circ\text{C}$) of poly(<i>n</i> -butyl vinyl ether) initiated with $\text{H}(\text{OEt}_2)_2[\mathbf{2.2}]$ at a) $21\text{ }^\circ\text{C}$ and b) $-84\text{ }^\circ\text{C}$	33
Figure 2.7 DSC traces of poly(<i>n</i> -butyl vinyl ether) initiated with $\text{H}(\text{OEt}_2)_2[\mathbf{2.2}]$ showing glass transition temperature (T_g) as a function of the temperature of polymerization.	35
Figure 2.8 ^1H NMR spectrum (400 MHz, CDCl_3 , $25\text{ }^\circ\text{C}$) of polystyrene initiated with $\text{H}(\text{OEt}_2)_2[\mathbf{2.2}]$ at $-50\text{ }^\circ\text{C}$	36
Figure 2.9 ^1H NMR spectrum (400 MHz, CDCl_3 , $25\text{ }^\circ\text{C}$) of poly(α -methylstyrene) initiated with $\text{H}(\text{OEt}_2)_2[\mathbf{2.2}]$ at $-78\text{ }^\circ\text{C}$	38

Figure 2.10 ^1H NMR spectrum (400 MHz, CDCl_3 , 25 °C) of oligoisoprene initiated with $\text{H}(\text{OEt}_2)_2$ [2.2] at -78 °C.....	40
Figure 3.1 Examples of Group 5 WCAs.....	51
Figure 3.2 Brønsted acids $\text{H}(\text{OEt}_2)_2$ [3.1] and $\text{H}(\text{OEt}_2)_2$ [3.2].....	52
Figure 3.3 ^1H NMR (400 MHz, CD_2Cl_2 , -85 °C) spectrum of $\text{H}(\text{OEt}_2)_2$ [3.1].....	54
Figure 3.4 $^{19}\text{F}\{^1\text{H}\}$ NMR (376 MHz, CD_2Cl_2) spectrum of $\text{H}(\text{OEt}_2)_2$ [3.1] at a) 25 °C, and b) -85 °C.....	55
Figure 3.5 ^1H NMR (400 MHz, CD_2Cl_2 , -85 °C) spectrum of $\text{H}(\text{OEt}_2)_2$ [3.2].....	57
Figure 3.6 $^{19}\text{F}\{^1\text{H}\}$ NMR (376 MHz, CD_2Cl_2) spectrum of $\text{H}(\text{OEt}_2)_2$ [3.2] at a) 25 °C, and b) -85 °C.....	57
Figure 3.7 Molecular structure of $\text{H}(\text{OEt}_2)_2$ Λ -[3.2].....	59
Figure 3.8 Metrical parameters [Å] for the cation in $\text{H}(\text{OEt}_2)_2$ [3.2].....	60
Figure 3.9 ^1H NMR spectrum (400 MHz, CDCl_3 , 25 °C) of poly(<i>n</i> -butyl vinyl ether) initiated with: a) $\text{H}(\text{OEt}_2)_2$ [3.1] at 21 °C and b) $\text{H}(\text{OEt}_2)_2$ [3.1] at -84 °C.....	65
Figure 3.10 ^1H NMR spectrum (400 MHz, CDCl_3 , 25 °C) of poly(<i>n</i> -butyl vinyl ether) initiated with: a) $\text{H}(\text{OEt}_2)_2$ [3.2] at 21 °C and b) $\text{H}(\text{OEt}_2)_2$ [3.2] at -84 °C.....	66
Figure 3.11 DSC traces of poly(<i>n</i> -butyl vinyl ether) initiated with $\text{H}(\text{OEt}_2)_2$ [3.2] showing glass transition temperature (T_g) as a function of the temperature of polymerization.....	67
Figure 3.12 ^1H NMR spectrum (400 MHz, CDCl_3 , 25 °C) of polystyrene initiated with a) $\text{H}(\text{OEt}_2)_2$ [3.1] and b) $\text{H}(\text{OEt}_2)_2$ [3.2].....	69
Figure 3.13 ^1H NMR spectrum (400 MHz, CDCl_3 , 25 °C) of poly(α -methylstyrene) initiated with a) $\text{H}(\text{OEt}_2)_2$ [3.1] and b) $\text{H}(\text{OEt}_2)_2$ [3.2].....	71

Figure 3.14 ^1H NMR spectrum (400 MHz, CDCl_3 , 25 °C) of oligoisoprene initiated with a) $\text{H}(\text{OEt}_2)_2[\mathbf{3.1}]$ and b) $\text{H}(\text{OEt}_2)_2[\mathbf{3.2}]$	73
Figure A.1 GPC trace of $\text{H}(\text{OEt}_2)_2[\mathbf{2.1}]$ -initiated poly(<i>n</i> -butyl vinyl ether).....	95
Figure A.2 GPC trace of $\text{H}(\text{OEt}_2)_2[\mathbf{2.1}]$ -initiated poly(styrene).....	95
Figure A.3 $^{13}\text{C}\{^1\text{H}\}$ NMR (100 MHz, CD_2Cl_2 , -85 °C) spectrum of $\text{H}(\text{OEt}_2)_2[\mathbf{2.2}]$	95
Figure A.4 GPC traces of $\text{H}(\text{OEt}_2)_2[\mathbf{2.2}]$ -initiated poly(<i>n</i> -butyl vinyl ether).....	96
Figure A.5 GPC traces of $\text{H}(\text{OEt}_2)_2[\mathbf{2.2}]$ -initiated polystyrene.....	97
Figure A.6 GPC traces of $\text{H}(\text{OEt}_2)_2[\mathbf{2.2}]$ -initiated poly(α -methylstyrene).....	98
Figure A.7 GPC trace of $\text{H}(\text{OEt}_2)_2[\mathbf{2.2}]$ -initiated poly(isoprene).....	98
Figure B.1 GPC traces of $\text{H}(\text{OEt}_2)_2[\mathbf{3.1}]$ -initiated poly(<i>n</i> -butyl vinyl ether).....	99
Figure B.2 GPC traces of $\text{H}(\text{OEt}_2)_2[\mathbf{3.1}]$ -initiated polystyrene.....	100
Figure B.3 GPC traces of $\text{H}(\text{OEt}_2)_2[\mathbf{3.1}]$ -initiated poly(α -methylstyrene).....	101
Figure B.4 GPC traces of $\text{H}(\text{OEt}_2)_2[\mathbf{3.1}]$ -initiated polyisoprene.....	102
Figure B.5 GPC traces of $\text{H}(\text{OEt}_2)_2[\mathbf{3.2}]$ -initiated poly(<i>n</i> -butyl vinyl ether).....	103
Figure B.6 GPC traces of $\text{H}(\text{OEt}_2)_2[\mathbf{3.2}]$ -initiated polystyrene.....	104
Figure B.7 GPC traces of $\text{H}(\text{OEt}_2)_2[\mathbf{3.2}]$ -initiated poly(α -methylstyrene).....	105
Figure B.8 GPC traces of $\text{H}(\text{OEt}_2)_2[\mathbf{3.2}]$ -initiated polyisoprene.....	105

List of Schemes

Scheme 1.1 Synthesis of butyl rubber.....	2
Scheme 1.2 General mechanism of cationic chain polymerization.	3
Scheme 1.3 Example of initiation of isobutylene by Lewis acid (BF ₃) and co-initiator (H ₂ O) to form a carbocation.	4
Scheme 1.4 a) Resonance stabilization of carbocationic intermediate of vinyl ether polymerization, and b) Stability of a tertiary carbocation vs. a primary carbocation.....	5
Scheme 1.5 Chain transfer reactions via hydrogen abstraction to a) the anion, and b) another monomer molecule.....	7
Scheme 1.6 Side reactions in the cationic polymerization of styrene via a) ring alkylation or b) branching or crosslinking.....	8
Scheme 1.7 Mechanism for the homogeneous metallocene polymerization of ethylene.	9
Scheme 1.8 Equilibrium of solvated protons and counterions.	16
Scheme 2.1 Synthesis of Brønsted acid H(OEt ₂) ₂ [2.1].....	23
Scheme 2.2 Synthesis of Brønsted acid H(OEt ₂) ₂ [2.2].....	26
Scheme 2.3 H(OEt ₂) ₂ [2.2]-initiated cationic polymerization of <i>n</i> -butyl vinyl ether.	31
Scheme 2.4 H(OEt ₂) ₂ [2.2]-initiated cationic polymerization of styrene.	35
Scheme 2.5 H(OEt ₂) ₂ [2.2]-initiated cationic polymerization of α -methylstyrene.....	37
Scheme 2.6 H(OEt ₂) ₂ [2.2]-initiated cationic polymerization of isoprene.	39
Scheme 3.1 Synthesis of Brønsted acid H(OEt ₂) ₂ [3.1].....	53
Scheme 3.2 Synthesis of H(OEt ₂) ₂ [3.2].....	55

Scheme 3.3 H(OEt ₂) ₂ [3.1] and H(OEt ₂) ₂ [3.2]-initiated cationic polymerization of <i>n</i> -butyl vinyl ether.....	63
Scheme 3.4 H(OEt ₂) ₂ [3.1] and H(OEt ₂) ₂ [3.2]-initiated cationic polymerization of styrene.	68
Scheme 3.5 H(OEt ₂) ₂ [3.1] and H(OEt ₂) ₂ [3.2]-initiated cationic polymerization of α -methylstyrene.....	70
Scheme 3.6 H(OEt ₂) ₂ [3.1] and H(OEt ₂) ₂ [3.2]-initiated cationic polymerization of isoprene.	72

List of Symbols and Abbreviations

α	alpha
Å	Angstrom (1×10^{-10} metres)
A	anion
Ar	aryl
avg.	average
ax	axial
BAr^{F}_4	tetrakis[3,5-bis(trifluoromethyl)phenyl]borate anion
br	broad
Bu	butyl, C_4H_9^-
c	centi (1×10^{-2})
C	Celsius; cation
<i>ca.</i>	circa
calc	calculated
<i>cis</i>	same side
Cp	cyclopentadienyl ligand
Cp^*	pentamethylcyclopentadienyl
°	degree
δ	NMR shift in parts per million (ppm)
d	doublet (NMR spectroscopy)
<i>d</i>	deuterated
DCC	<i>N,N'</i> -dicyclohexylcarbodiimide
DMF	dimethylformamide, $(\text{CH}_3)_2\text{NCH}$

Đ	dispersity
dn/dc	differential refractive index
DSC	differential scanning calorimetry
ed.	edition
Ed.	editor(s)
<i>e.g.</i>	exempli gratia (for example)
ESI	electrospray ionization
eq	equatorial
equiv	equivalent
Et	ethyl, CH_3CH_2-
et al.	and others
Et_2O	diethyl ether
g	gram
GOF	goodness of fit (crystallography)
GPC	gel permeation chromatography
$\{^1\text{H}\}$	proton decoupled (NMR spectroscopy)
Hz	Hertz (s^{-1})
<i>i</i>	iso
<i>i.e.</i>	id est (for example)
<i>in vacuo</i>	in a vacuum
<i>J</i>	coupling constant (NMR spectroscopy)
$\text{K}\alpha$	spectral line
Λ	lambda

L	generic ligand; litre
LLS	laser light scattering
m	milli (1×10^{-3}); multiplet (NMR spectroscopy)
<i>m</i>	meta
M	generic metal
MAO	methylaluminoxane, $-\text{[O-Al(CH}_3\text{)]}_n-$
Me	methyl, CH_3-
MeOH	methanol, CH_3OH
MHz	megahertz
mid	midpoint (DSC)
min	minutes
μ	micro (1×10^{-6})
[M]:[I]	monomer to initiator ratio
M_n	number average molecular weight
M_w	weight average molecular weight
mol	mole
MS	mass spectrometry
<i>m/z</i>	mass to charge ratio
μ	bridging ligand
<i>n</i>	number; normal (in <i>n</i> -butyl)
n.d.	not determined
NMR	nuclear magnetic resonance
<i>p</i>	para

%	percent (parts per hundred)
ppm	parts per million
Ph	phenyl
ⁱ Pr	isopropyl
q	quartet (NMR spectroscopy)
R	generic substituent; residual factor (crystallography)
R ^F	generic fluorinated ligand
<i>rr</i>	syndiotactic triad
rt	room temperature
<i>r</i> _{vdw}	van der Waals radii
s	second; singlet (NMR spectroscopy)
σ	sigma
SADABS	Siemens area detector absorption correction program
t	<i>tert</i> (in <i>t</i> -butyl); triplet (NMR spectroscopy)
T	temperature
T _g	glass transition temperature
THF	tetrahydrofuran, (CH ₂) ₄ O
<i>trans</i>	opposite side
TRISPHAT	tris(tetrachlorobenzenediolato)phosphate anion
USD	United States Dollar
V	volume
vol	volume
WCA	weakly coordinating anion

X

generic halogen

Z

number of units in a cell (crystallography)

Acknowledgements

Firstly, I would like to thank my supervisor, Professor Derek P. Gates for this opportunity to learn from you. Your support, guidance and knowledge have been invaluable on my journey.

Khatera Hazin, thank you for guiding me through the past two years, both in and out of the lab. You have been a great mentor.

To past and present Gates group members, thank you for making the lab a fun and enjoyable place to be: Khatera Hazin, Ben Rawe, Zeyu Han, Leixing Chen, Chuantian Zhan, Jeffrey Suen, Harvey MacKenzie, Kerim Samedov, and Henry Walsgrove.

Khatera Hazin, Henry Walsgrove, Jennifer Yuan and Kerim Samedov, thank you for efforts in proof-reading this thesis.

I would like to thank NMR, Mass-Spec, the X-ray lab and Chemistry Shops and Services for everything they do. Dr. Brian O. Patrick, thank you for your work collecting and refining data for the crystal structures.

Last, but not least, to my family and friends, thank you for always being there.

For the strength of the pack is the wolf, and the strength of the wolf is the pack.

- *Rudyard Kipling*

Chapter 1: Introduction

1.1 A History of Rubber

A tree native to South America, *Hevea brasiliensis*, produces a milky-white sap, known as latex, or natural rubber, that can be tapped, collected and processed into a versatile product.¹ The earliest reports of natural rubber date back 3600 years to the indigenous people of the Amazon, who used the sap as primitive forms of rubber.² Natural rubber was introduced to Europe by Christopher Columbus in 1496, after he returned from a voyage to the West Indies, bringing back bouncy rubber balls.³ In 1818, Charles Macintosh discovered one of the first uses for natural rubber. By bonding two layers of cotton together with rubber, a method that is still used today, the first waterproof raincoat, or ‘mackintosh’, was born. These coats were used by Sir John Franklin on his 1924 Arctic expedition and the British Army during World War I.⁴

With the growth of the rubber trade, many researchers became focused on rubber and its products. Charles Goodyear and Thomas Hancock were simultaneously seeking to minimize the change in physical properties dependent on temperature of natural rubber and in 1839 discovered vulcanization, a heat treatment in the presence of sulfur.^{5, 6} Crosslinking by vulcanization of the unsaturated groups in the polymers creates a harder, more durable material with more versatility. This caused a rapid expansion in the rubber industry and specifically in its uses in the automobile industry as car tires and sealants.⁷

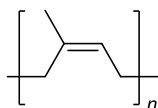


Figure 1.1 *cis*-1,4-polyisoprene monomer units of natural rubber.

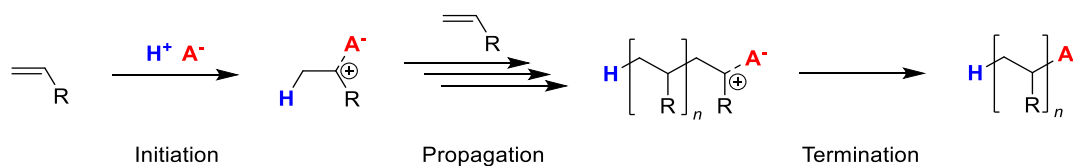
rubber production, a projected 7 million additional hectares of plantations would be necessary in the next five years, threatening biodiversity by deforestation.^{14, 15}

The goal of this thesis is to investigate possible improvements to the synthesis of butyl rubber, principally the development of new initiators that produce high molecular weight polymers without the necessity of extremely low temperatures.

1.2 Cationic Polymerization

1.2.1 Cationic Chain Polymerization

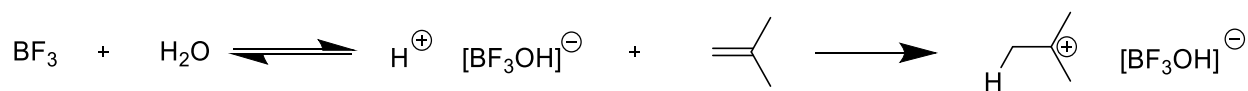
To understand the essential low temperatures during butyl rubber production, the mechanism of cationic olefin polymerization must be understood. Cationic chain polymerization of olefins is an ionic polymerization of high industrial relevance as butyl rubber is produced solely by cationic polymerization.¹⁶ The mechanism follows three main stages (Scheme 1.2). A cation, ordinarily a proton source, is attacked by the nucleophilic olefin portion of the monomer creating a carbocation. The polymerization is propagated by sequential attack by other olefin monomers to the electrophilic carbocation. The stability of the highly reactive carbocationic intermediate can affect the resulting polymers, therefore the nature of the charge balancing anion is often critical. Propagation continues until side reactions or termination occurs.



Scheme 1.2 General mechanism of cationic chain polymerization.

Cationic polymerization occurs on the timescale of seconds, orders of magnitudes faster than anionic (minutes) and radical (hours) polymerizations.¹⁷ The rapid rate leads to uncontrolled polymerization producing polymers with low molecular weights and broad dispersities.¹⁸ The

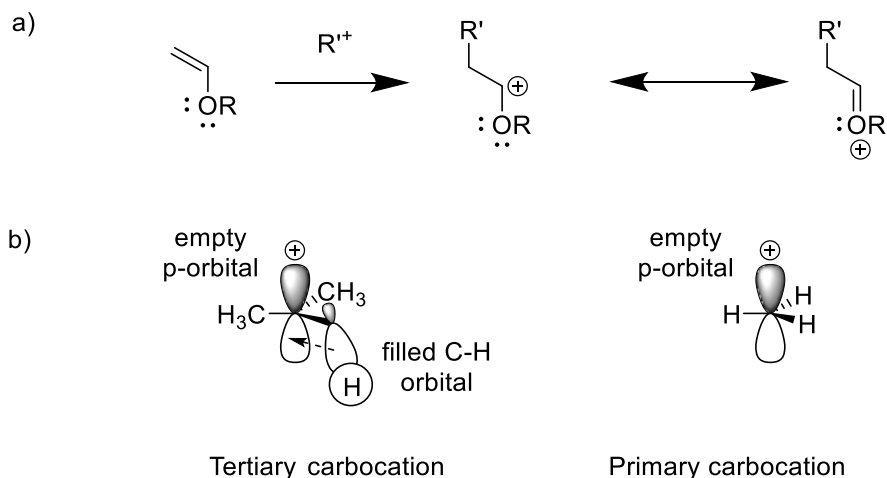
stability of the propagating carbocation can often affect the polymer by promoting side reactions including chain transfer processes and termination, which results in low molecular weight polymers.¹⁹ These potential side reactions contribute to the challenging nature of cationic polymerization compared to anionic or radical polymerizations.



Scheme 1.3 Example of initiation of isobutylene by Lewis acid (BF₃) and co-initiator (H₂O) to form a carbocation.

Initiation requires a cation source with a charge balancing anion. Commonly used initiators for cationic polymerization involve a Lewis acid and a co-initiator.^{20, 21} The Lewis acid, such as AlCl₃, BF₃, and TiCl₄, is activated by a proton source such as water or alcohols to form an electrophilic species (Scheme 1.3).^{19, 22} Protic acids including phosphoric acid, sulfuric acid and triflic acid have also been reported as cationic initiators, albeit with only low molecular weight polymers isolated.^{18, 23-25} The stability of the carbocationic intermediate is crucial to the propagation of a polymerization. Intermediates that are more stable lead to a greater rate of polymerization. For example, vinyl ethers are particularly reactive due to the resonance stabilized intermediate resulting from the lone pair of the oxygen (Scheme 1.4 a). The stability of the carbocation also greatly increases with the number of substituents, therefore a tertiary carbocation is more stable than a secondary carbocation, and a primary carbocation is least stable (Scheme 1.4 b). The stabilization by hyperconjugation in a tertiary carbocation originates from C-H σ donation into the empty p-orbital of a planar carbocation. In a primary carbocation, C-H bonds and the empty p-orbital are orthogonal and no donation is possible,²⁶ and therefore the carbocationic intermediate is significantly less stable. Carbocations of lower stability are more prone to side

reactions and termination during the polymerization, resulting in low molecular weight polymers with broad dispersity.



Scheme 1.4 a) Resonance stabilization of carbocationic intermediate of vinyl ether polymerization, and b) Stability of a tertiary carbocation vs. a primary carbocation.

Propagation of the carbocationic polymer can be influenced by external factors such as temperature, the counterion and the solvent used. Low temperatures during polymerization will afford higher molecular weight polymers. This is due to the activation energy for termination reactions being higher than the activation energy for propagation reactions. Therefore, the low temperature suppresses termination reactions and the polymer chain length increases.^{17, 27} If termination reactions and chain transfer processes are eliminated completely, the resulting polymerization is referred to as “living polymerization”.^{17, 28, 29}

The counter anion can also significantly affect the rate of propagation. A small, charge localized anion will have a strong electrostatic interaction with the carbocation, leading to recombination of the charges and therefore termination. Larger, more charge delocalized anions will have a much weaker electrostatic interaction with the growing cationic chain and will therefore promote propagation. However, an anion too large and electron diffuse will not be able to stabilize the reactive carbocation, leading to side reactions, such as chain transfer. Therefore, finding the

anion with correct interaction to the highly reactive cation is important to the production of high molecular weight polymers.^{17, 30}

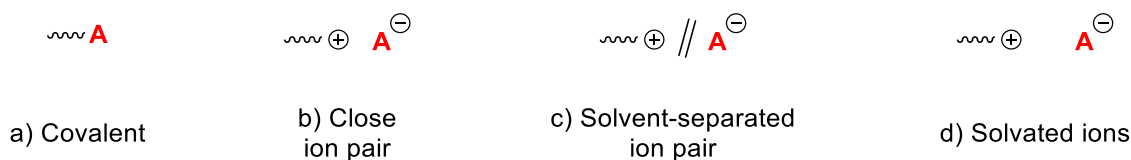
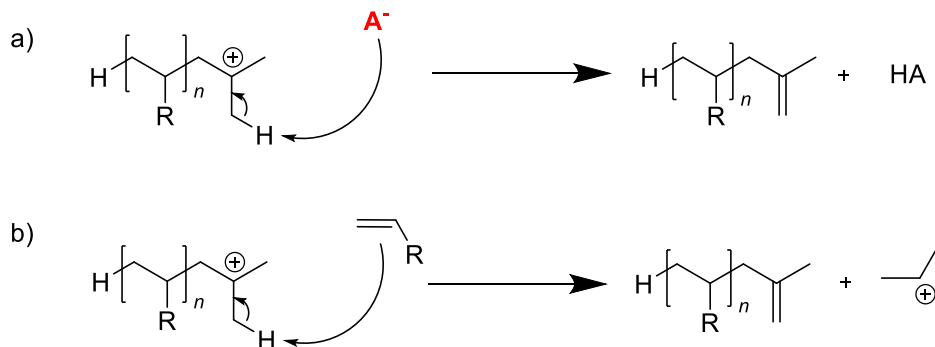


Figure 1.2 Solvent association of the carbocation ($\sim\oplus$) and the counter anion ($A\ominus$).

The rate of propagation can additionally be altered by considering the polarity of the solvent used. Polar solvents, such as water and alcohols commonly react with the initiator and propagating chain, preventing initiation or high degrees of polymerization therefore low polarity solvents are necessary. Even in low polarity solvents, a continuum of states of separation between the cation and anion are possible, from covalently bound (a), to close ion pairs (b), solvent-separated ion pairs (c) and finally fully solvated ions (d) (Figure 1.1). In the covalently bound pair, there is no opportunity for reaction of the cation with surrounding monomers leading to it becoming inactive as an initiator. When the ions are fully solvated, the cation is no longer reactive and propagation will also be significantly decreased. Propagation is favoured in solvent polarities where close ion pairs or solvent-separated ion pairs may form, such as methylene chloride and ethylene dichloride.^{9, 19, 31-33}

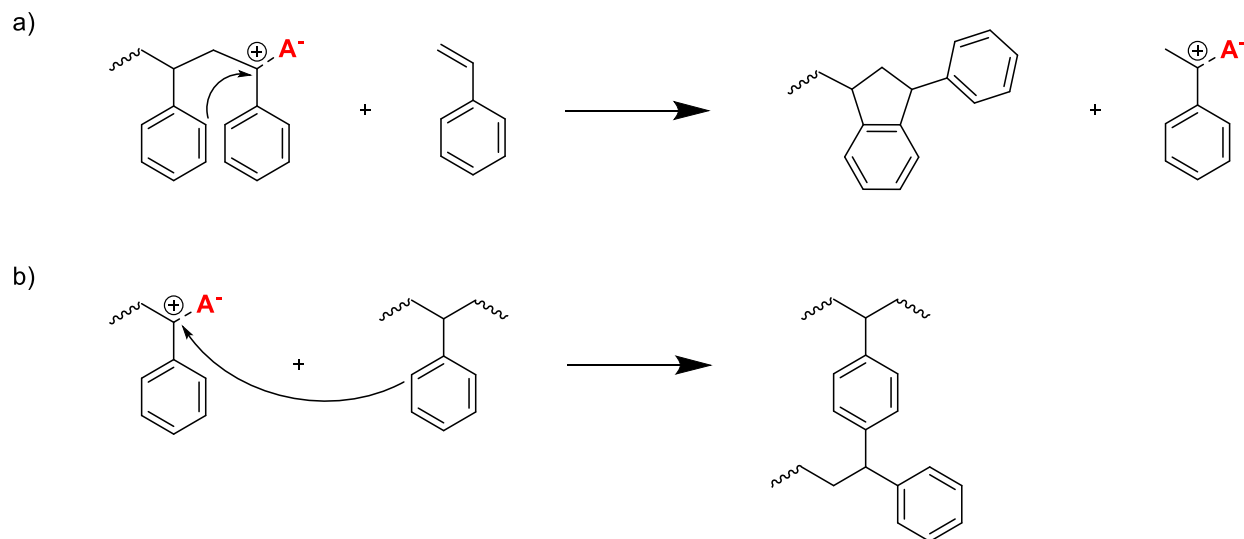
Termination involves the recombination of the cation and the counter anion inactivating the growing polymer chain. Linear chain growth can also be reduced through chain transfer processes.³⁴ Chain transfer can occur by hydrogen abstraction to the counterion.^{19, 35} The growing chain is terminated and the active initiator system can be regenerated (Scheme 1.1 Scheme 1.5 a). Hydrogen abstraction can also occur to another monomer molecule, creating a carbenium ion that becomes the new propagating chain (Scheme 1.5 b). In both these cases only low molecular weight polymers are achieved, which is undesirable in the production of butyl rubber.^{17, 27} In attempts to

reduce the chain transfer to monomer reaction proton traps, such as 2,6-di-*t*-butyl pyridine, are added to intercept the proton before chain transfer occurs.^{19, 36, 37} This normally results in a loss in overall yield of the polymerization. However, higher molecular weight polymers with lower dispersities can often be isolated. Obtaining high molecular weight polymers in a high yield with narrow dispersity is very challenging as a result of chain transfer processes.



Scheme 1.5 Chain transfer reactions via hydrogen abstraction to a) the anion, and b) another monomer molecule.

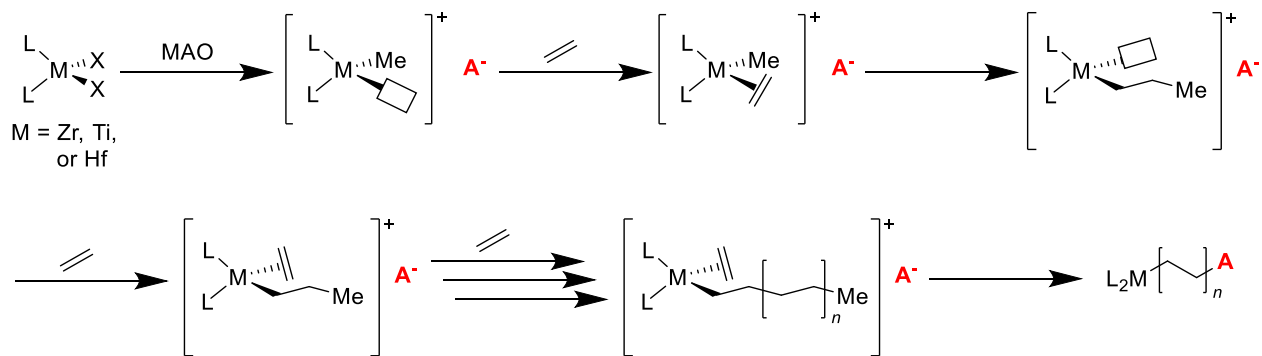
Chain transfer reactions in cationic polymerizations involving aromatic monomers such as styrene and its derivatives are common.¹⁹ This has been observed by intramolecular ring alkylation via electrophilic aromatic substitution to create cyclized structures (Scheme 1.6 a).^{38, 39} Chain transfer reactions lead to low molecular weight polymers. Branching can additionally occur through intermolecular aromatic substitution by a propagating carbocation onto the aromatic ring of another polymer chain (Scheme 1.6 b).^{40, 41} Both chain transfer and branching reactions give an additional layer of complexity to controlling cationic polymerization making it very challenging.



Scheme 1.6 Side reactions in the cationic polymerization of styrene via a) ring alkylation or b) branching or crosslinking.

1.2.2 Coordination Polymerization

The polymerization of olefins can also proceed by a metal-mediated mechanism, for example Ziegler-Natta polymerization (Scheme 1.7).⁴²⁻⁴⁴ Formation of the active site occurs by complexation between the catalyst and methylaluminoxane (MAO), followed by methyl-halogen exchange to form a dimer. Reaction with MAO occurs again to form the active site on the metallocene. An olefin monomer undergoes *cis* addition to the empty orbital on the metal centre.⁴⁵ A polymer chain grows through the successive migratory insertion of alkene molecules into the M-C bond. By changing the identity of the ligands on the metal centre, the stereospecificity of the polymers obtained can be controlled.⁴⁵⁻⁴⁹ Transition metal-mediated polymerization is often applied for the polymerization of terminal alkenes, such as ethylene and propylene.⁵⁰⁻⁵²



Scheme 1.7 Mechanism for the homogeneous metallocene polymerization of ethylene.

1.3 Initiators Used in Cationic Polymerization

The most common type of initiators used for cationic olefin polymerization have been developed from Lewis acids and are binary, or two-component systems requiring a co-initiator.²² A Lewis acid initiating system ($\text{AlCl}_3/\text{H}_2\text{O}$) is currently employed in the industrial polymerization of butyl rubber.^{9, 10} Vinyl ethers have been polymerized by HCl , HI , or RCOOH in conjunction with a Lewis acid, such as: ZnI_2 , ZnBr_2 , ZnCl_2 , SnI_2 , SnCl_2 , SnCl_4 , TiCl_4 or MgCl_2 .⁵³⁻⁵⁵ It has been shown that styrene can be polymerized by $\text{B}(\text{C}_6\text{F}_5)_3$ with water as a co-initiator.⁵⁶ Poly(isobutylene) can be isolated upon initiation of isobutylene with $\text{TiCl}_4/(t\text{-Bu-}m\text{-DCC})$,⁵⁷ and $\text{Cp}^*\text{TiMe}_3/\text{B}(\text{C}_6\text{F}_5)_3$.⁵⁸ $\text{H}(\text{OEt}_2)_2[\text{Al}(\text{OR}^F)_4]$ has been shown to polymerize isobutylene in the presence of AlCp_3 .⁵⁹ Two-component systems such as these do not have a clear initiating species making the study of polymerization challenging.

Single component initiators contain a protic source and a counter anion in the same species, therefore single component initiators are solids that can be isolated. This gives greater control over the monomer to initiator ratio during polymerization. High molecular weight poly(isobutylene) was isolated with zirconocene trihydrides, such as $[\text{Cp}'_4\text{Zr}_2\text{H}(\mu\text{-H})_2]^+$, with a variety of weakly coordinating anions⁶⁰ and $[\text{M}(\text{NCCH}_3)_6]^+$ ($M = \text{Mn, Ni, Cu, and Ag}$).⁶¹ It was also possible to use

Much of this research has been focused on Group 13 elements which give 4-coordinate WCAs.^{59, 67} Most studied is tetrakis[3,5-bis(trifluoromethyl)phenyl]borate WCA ($[\text{BAr}^{\text{F}}_4]^-$) (Figure 1.3, **[1.2]**).⁶⁸ Prior to the prevalence of **[1.2]**⁻ as a counter ion, simpler molecules were used, for example: tetrafluoroborate ($[\text{BF}_4]^-$) **[1.1]**⁻ and hexafluorophosphate ($[\text{PF}_6]^-$). The reduced steric bulk of these classical WCAs lead to electron density that is more localized and therefore they are more coordinating.⁶⁹ **[1.2]**⁻ has been used as a counter ion for many syntheses since the 1990s when it was first reported and improvements to the previously explosive synthesis now allow a relatively safe process.⁷⁰ It is a highly fluorinated borate anion and is a popular choice in many applications from synthesis to catalysis.⁷¹

The developments in the synthesis of **[1.2]**⁻ and other related WCAs such as tetrakis(pentafluorophenyl)borate ($[\text{B}(\text{C}_6\text{F}_5)_4]^-$) **[1.3]**⁻ and BOB ($[\text{B}(\text{C}_2\text{O}_2)]^-$) **[1.4]**⁻ have enabled the isolation of more electrophilic cations.⁷¹⁻⁷⁷ $\text{Ph}_3\text{C}[\mathbf{1.3}]$ has been synthesized and incorporated into a zirconocene complex, which was highly effective initiator for the cationic polymerization of propylene.^{78, 79} Furthermore, a series of alkyl borates $[\text{B}(\text{OR})_4]^-$ **[1.5]**⁻ have been reported,⁸⁰⁻⁸⁴ including the chelated perfluoropinacol borate $[\text{B}(\text{OC}(\text{CF}_3)_2)_4]^-$ **[1.6]**⁻.^{85, 86} Many of these anions have found applications in ionic liquids and lithium batteries.^{59, 87, 88}

Another concept to reduce the coordination of a WCA to a cation is by enlarging the anion was by bridging, as the negative charge can then be spread over a larger number of atoms.⁵⁹ The reaction of the corresponding Lewis acid with imidazole afforded the bridged anion **[1.7]**⁻ as an amine salt.⁸⁹ This salt was shown to initiate ethylene in conjunction with $\text{Me}_2\text{Si}(\eta^5\text{-Me}_4\text{C}_5)(t\text{-BuN})\text{TiMe}_2$. Similarly, $[\text{Ph}_3\text{C}][\mathbf{1.8}]$ was shown to be an effective catalyst activator for the polymerization of propylene.⁹⁰ A bridged species was also obtained using *n*-decanoic acid giving

$[n\text{-C}_{17}\text{H}_{35}\text{CO}_2\text{H}][\text{B}(\text{C}_6\text{F}_5)_3]_2$. Of particular note, the polymerizations of both isobutylene and isobutylene/isoprene gave high molecular weight polymers, via coordination polymerization.^{91, 92}

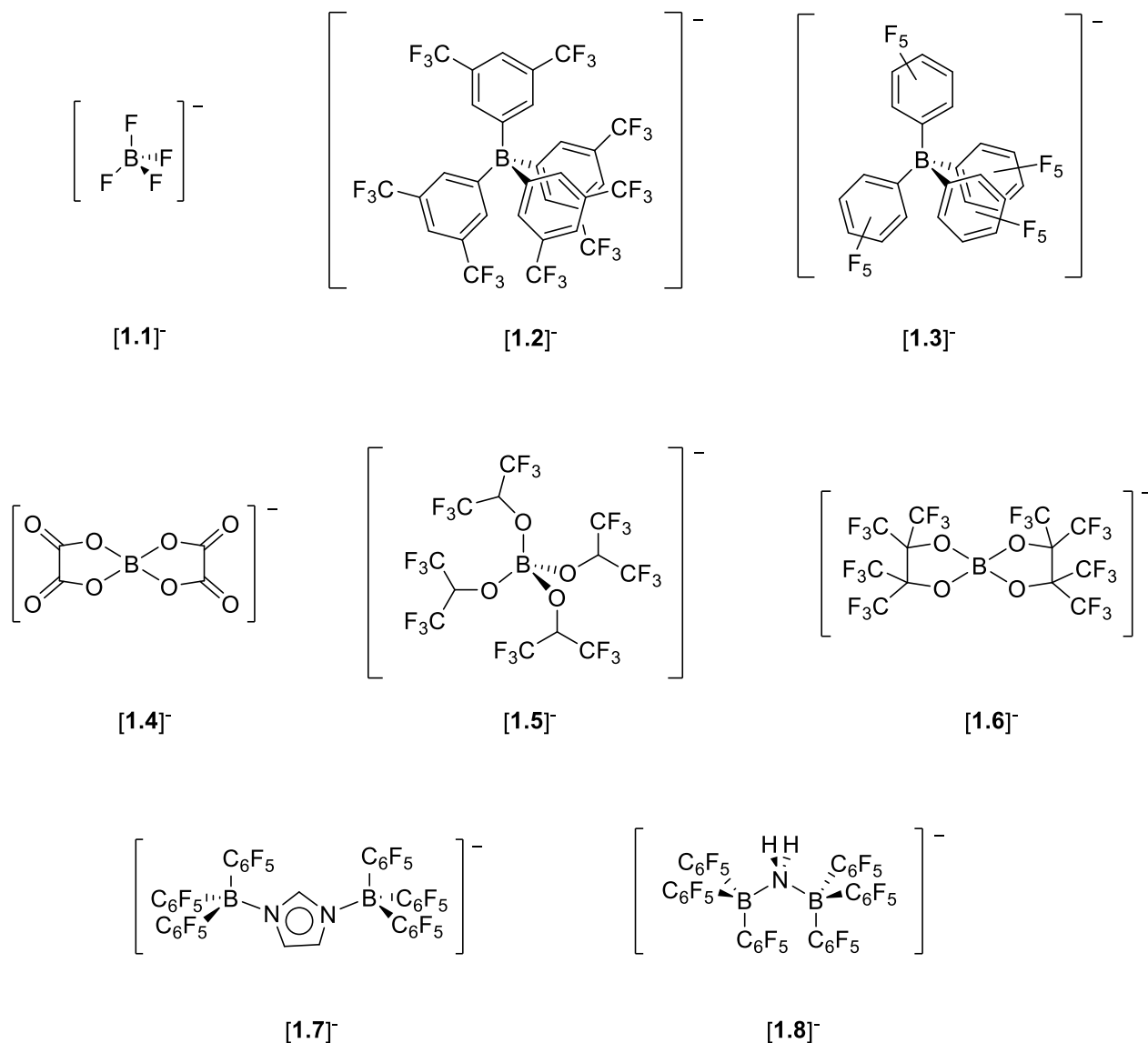


Figure 1.4 A selection of boron-containing WCAs.

Carborane anions are covalently bonded clusters consisting primarily of carbon and boron atoms and are of interest as they have a larger steric bulk than other boranes. The first prepared carborane anion was $[\text{HCB}_{11}\text{H}_{11}]^-$, in 1986.⁹³⁻⁹⁶ This carborane was shown to coordinate to a variety of zirconocenes and initiate the cationic polymerization of olefins.⁹⁷ Development of this anion further has led to the halogenated derivatives $[\text{CHB}_{11}\text{Cl}_{11}]^-$ and $[\text{CHB}_{11}\text{F}_{11}]^-$, with H^+ , Ph_3C^+

and R_3Si^+ cations, and the introduction of “superacids”.⁹⁸⁻¹⁰² A superacid is a molecule with a higher acidity than neat sulfuric acid.^{29, 103, 104} Carborane anions are often seen as the least coordinating anions which is demonstrated by the high acidity observed, however they are costly to obtain and therefore not widely implemented.^{59, 67, 105}

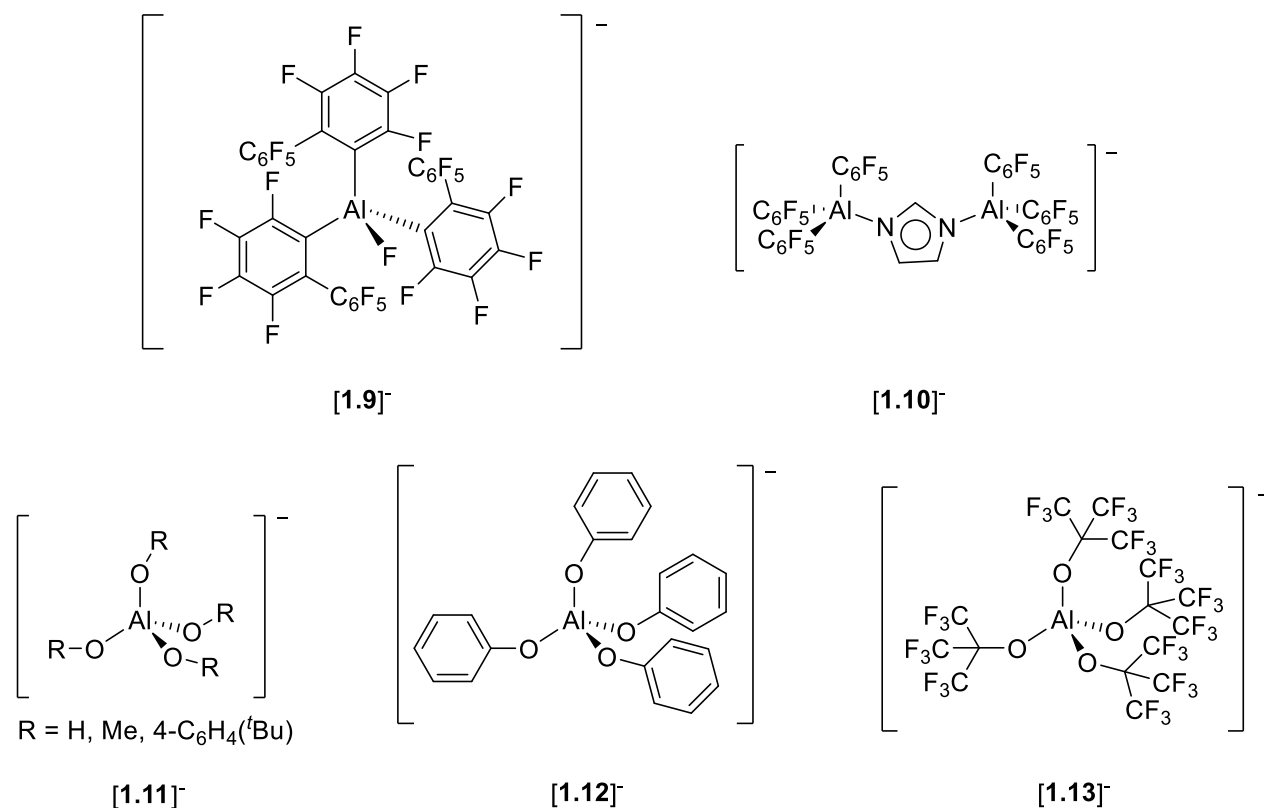


Figure 1.5 A selection of aluminum-containing WCAs.

Aluminium has also been used in the design of WCAs, as the size of the element increases as the group is descended, increasing the steric bulk to obtain a less coordinating anion. Analogues of the previously seen boron-containing WCAs are common. Marks and coworkers have shown that the anion **[1.9]⁻** is active as a co-catalyst for the zirconocene-mediated polymerization of propylene.^{44, 106, 107} Bridging is also observed in the anions to increase bulk. Upon comparing **[1.10]⁻** to **[1.7]⁻**, a higher catalytic activity for the cationic initiation of ethylene was observed with the larger aluminium-containing WCA.⁸⁹

Alkoxyaluminates $[\text{Al}(\text{OR})_4]^-$ [**1.11**]⁻ and aryloxyaluminates $[\text{Al}(\text{OAr})_4]^-$ [**1.11**]⁻ were first synthesized by Strauss et al. in the late 1990's.¹⁰⁸⁻¹¹⁰ Further development of these aluminium-containing anion systems has been undertaken by the group of Krossing.^{59, 111} Similar to boron-containing WCAs, perfluorination of alkyl and aryl aluminates has been pursued to give $[\text{Al}(\text{OR}^{\text{F}})_4]^-$ where R^{F} is $\text{C}(\text{CF}_3)_3$ ([**1.12**]⁻).¹¹¹ The $[\text{Al}(\text{OR}^{\text{F}})_4]^-$ anion has been studied in great detail by Krossing as it has a simple and scalable procedure. It is easy to convert from the lithium salt to other salts with the cations $[\text{Ph}_3\text{C}]^+$, $[\text{NO}]^+$, $[\text{Ag}]^+$ and $[\text{H}(\text{OEt}_2)_2]^+$.^{62, 109} The salts of this anion have applications in ionic liquids, batteries and catalysis, including ethylene polymerization when coupled with zirconocene cation, and cationic ring-opening polymerization.^{80, 112-116}

Group 13 elements are exclusively 4-coordinate anions. To obtain a larger and more electron diffuse anion that is less coordinating it is possible to increase the steric bulk by including a Group 15 element. These elements are stable in the +5 oxidation state resulting in the synthesis of hexacoordinate WCAs with a single negative charge. This facilitates the design of larger anions that are more charge delocalized. Therefore, these anions should have a lower electrostatic attraction to the cations and be less coordinating. Traditionally a non-coordinating anion, $[\text{PF}_6]^-$ (Figure 1.5, [**1.14**]⁻) has been widely used in lithium batteries and ionic liquids.^{117, 118}

As with other WCAs, phosphorus(V)-based anions can be made more weakly coordinating by incorporating larger and more electron-withdrawing substituents on the anion.¹¹⁹ Hellwinkel began investigating phosphorus(V) anions pioneering several anionic biphenyl phosphates.^{119, 120} He also utilized diols as substituents for phosphorus, for example benzenediolato ligands (Figure 1.5, [**1.17**]⁻, $\text{R} = \text{H}$).¹²¹ Furthermore, the halogenated tris(tetrachlorobenzenediolato)phosphate anion (TRISPHAT) ([**1.17**]⁻, $\text{R} = \text{Cl}$) has been well studied by Lacour leading to the separation of the enantiomers.¹²²⁻¹²⁵ The fluorinated derivative of [**1.17**]⁻ ($\text{R} = \text{F}$) has also been reported with

both Li^+ and $\text{H}(\text{OEt}_2)_2^+$.^{126, 127} Although the oxonium cation was shown to initiate the polymerization of THF, this was not investigated further, as the intended application was as an ionic liquid in lithium batteries. More recently, the hexacoordinate derivative of BOB can be isolated with three oxalato ligands [**1.15**]⁻ and the protonated diethyl ether Brønsted acid has shown to be catalyst for Friedel-Crafts type reactions.¹²⁸ Partially fluorinated derivatives [**1.16**]⁻ have also been isolated.¹²⁹ These anionic compounds containing P-O are easy to synthesize and original one-pot procedures can often be followed, starting with diols and PCl_5 .^{121, 130-132}

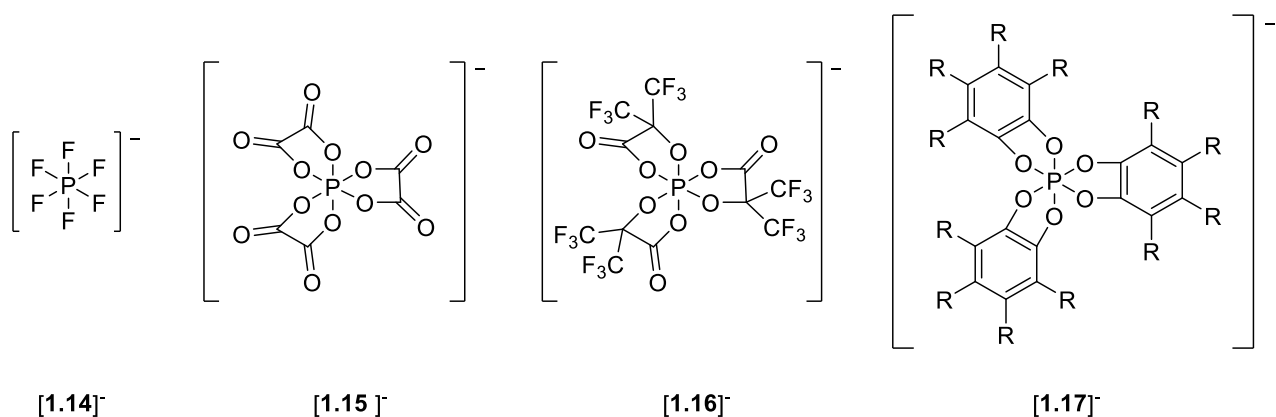


Figure 1.6 A selection of phosphorus-containing WCAs.

1.4.2 Weakly Coordinating Anions Containing Group 5 Metals

Whilst WCAs containing main group elements are common in literature, they are prone to hydrolysis.⁶⁷ Other WCAs have been isolated containing Group 5 metals. Group 5 metals form stronger bonds to oxygen, and therefore may be more stable.¹³³ The larger ionic radii of transition metals can also allow the use of more sterically bulky ligands.¹³⁴ Both niobium and tantalum have been utilized in WCAs with a range of ligands, including sterically bulky and perfluorinated options (Figure 1.7). [**1.20**]⁻¹³⁵ and [**1.21**]⁻¹³⁶ have been fully structurally characterized. However, these have not been investigated as single component initiators for the polymerization. To the best of

our knowledge the only Group 5-containing complex to be studied as a single component initiator is $[\text{Ph}_3\text{C}][\text{TaF}_6]$.¹³⁷

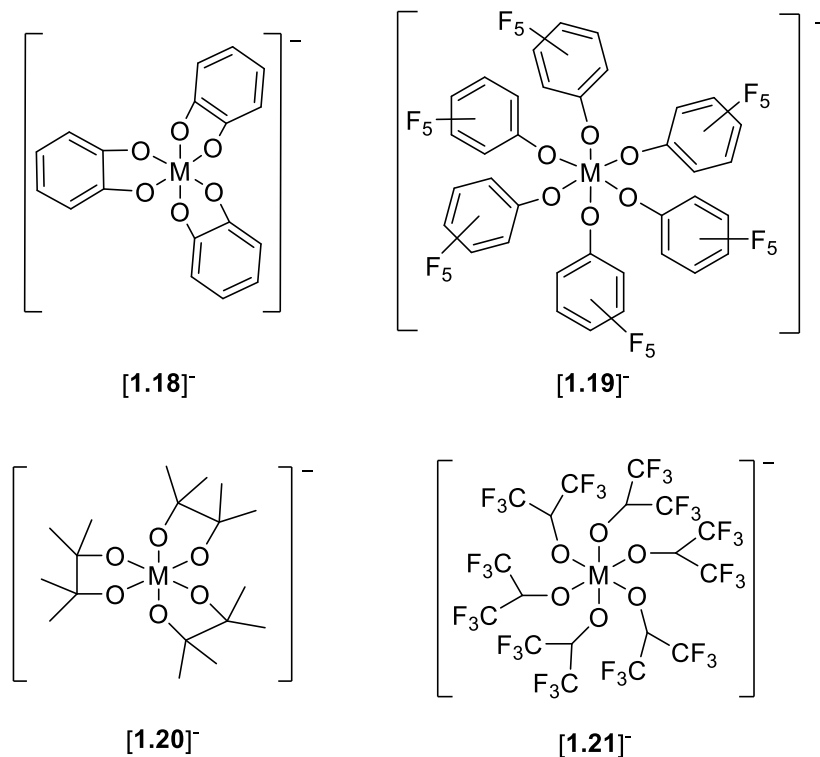


Figure 1.7 A selection of Group 5 containing WCAs, where M = Nb, and Ta.

1.4.3 Brønsted Acids Utilizing Weakly Coordinating Anions

A Brønsted acid (HA) is a compound that readily dissociates to give a proton (H^+) and counterion (A^-).¹³⁸ Fundamentally, when considering a Brønsted acid the more readily a H^+ dissociates from the counter anion, the stronger the acid is considered to be.^{29, 104} Solvation effects must also be considered and therefore Krossing has developed a new unified Brønsted acidity scale in an attempt to determine true acidities of these species, by considering gaseous phase H^+ .^{104, 139}



Scheme 1.8 Equilibrium of solvated protons and counterions.

A common cation for a strong Brønsted acids utilizing WCAs is an oxonium cation, HL_2^+ where L is a weakly basic solvent molecule.⁵⁹ Brønsted acids have been isolated in this form using BAr^F_4 as an anion by Brookhart et al. (L = Et₂O). The high acidity was demonstrated by generation of a positively charged palladium species on protonolysis of Pd-C bonds which was an active initiator for the copolymerization of olefins and CO as well as olefins and methyl acrylate.¹⁴⁰⁻¹⁴² Oxonium cations have also been isolated for **[1.3]**⁻ (L = Et₂O) and **[1.12]**⁻ (R = C(CF₃)₃ (L = Et₂O), with the latter being an effective single component initiator for the ring opening polymerization of 2-alkyl-2-oxazolines.^{59, 77} Research by the Gates group has resulted in the isolation of the Brønsted acid of **[1.17]**⁻ (R = H) (L = DMSO, DMF)¹⁴³ as a protonolysis reagent. More recently, the TRISPHAT anion **[1.17]**⁻ (R = Cl) (L = Et₂O, THF, DMF) was isolated as a Brønsted acid and shown to be an effective initiator for cationic polymerization of vinyl monomers.^{64, 65}

Neutral acids, in the form H[WCA] are rare, although a few have been observed indirectly. These are among some of the strongest acids known, and therefore are desired as the ultimate Brønsted acid. Neutral acids are often formed with carborane anions. The strength of the acid increases as the coordinating nature of the anion decreases. H[HCB₁₁F₁₁] is known as one of the strongest neutral acids known, a superacid,¹⁰³ along with its chlorinated derivative H[HCB₁₁Cl₁₁].¹⁴⁴ These species have been shown to protonate extremely weak bases, such as alkanes.¹⁰¹ Carborane superacids have also been observed to initiate ring-opening polymerization of cyclic chlorophosphazene.¹⁴⁵ A true unshielded H⁺ in combination with a WCA would represent the ultimate Brønsted acid, but remains elusive.

1.5 Outline of Thesis

The Gates group has previously reported the synthesis of Brønsted acids and their applications as single component initiators utilizing the phosphorus(V)-based TRISPHAT anion ($[\mathbf{1.17}]^-$, R = Cl) with HL_2 (L = Et₂O, THF, DMF) as the cation.^{64, 65, 122} These solid weighable Brønsted acids polymerized a range of vinyl monomers (*n*-butyl vinyl ether, styrene, α -methylstyrene, *p*-methoxystyrene, and isoprene). Furthermore, an introduction to Group 5 metal-containing anions has been discussed with the synthesis of single component initiators $H(OEt_2)_2[Ta(1,2-O_2C_6Cl_4)_3]$ and $H(OEt_2)_2[Ta(1,2-O_2C_6Cl_4)_2(1,2OC_6Cl_4OH)_2]$ for the cationic polymerization of *n*-butyl vinyl ether, styrene, α -methyl styrene and isoprene.^{146, 147} Chapter 2 advances on this chemistry and describes the syntheses and characterization of the niobium(V) analogues. Their application as single component initiators for the cationic polymerization of olefin monomers is evaluated. Chapter 3 discusses the syntheses and characterization of two strong Group 5 metal-containing Brønsted acids with perfluorinated ligands. The polymerization of vinyl monomers (*n*-butyl vinyl ether, styrene, α -methylstyrene and isoprene) with the Brønsted acids is also examined. Chapter 4 is a summary of the research contained in this thesis and the possible directions for future work are considered.

Chapter 2: Hexacoordinate Niobium(V) Weakly Coordinating Anions and their Application as Single Component Cationic Initiators for Olefin Polymerization

2.1 Introduction

Weakly coordinating anions (WCAs) can be paired with a proton source and the resulting Brønsted acids can be applied as single component initiators for cationic olefin polymerization. The interaction between the anion and the cation strongly influences the polymerization ability of an initiator. An interaction that is too strong leads to termination of the polymerization, whilst an interaction that is too weak leads to undesirable side reactions, such as chain transfer processes and branching. As a consequence, anion design is critical. WCAs that are electron diffuse and sterically bulky usually offer better activity as cationic initiators for polymerization. This reduces the interaction between cation and anion, which leads to its weakly coordinating nature.

Main group elements, such as boron and aluminium, are traditionally found in the spotlight of WCA centred research and have been heavily studied as counterions for the stabilization of highly reactive cations.^{63, 66-68, 93, 99, 110, 111, 113, 122, 140, 148-154} Other elements, such as phosphorus, have also been studied.^{64, 119-121, 125, 143, 147} The use of phosphorus permits access to the more sterically bulky hexacoordinate species, as opposed to 4-coordinate anions.⁶⁷ However, the Brønsted acids are less common and their use as single component initiators for cationic olefin polymerization is limited to a few examples ($\text{H}[\text{B}\{\text{C}_2\text{O}_4\}_3]$, $\text{H}(\text{OEt}_2)_2[\text{B}(\text{Ar}_F)_4]$, and $\text{H}(\text{OEt}_2)_2[\text{Al}\{\text{OC}(\text{CF}_3)_3\}_4]$).^{63, 140, 141, 155, 156} including $\text{HL}_2[\text{P}(1,2\text{-O}_2\text{C}_6\text{Cl}_4)_3]$ ($\text{L} = \text{Et}_2\text{O}$, THF, DMF) previously by the Gates group utilizing the tris(tetrachlorobenzenediolato)phosphate(V) (TRISPHAT, **[1.17]**⁻, $\text{R} = \text{Cl}$) anion.^{119, 122} The solid Brønsted acids were shown to initiate vinyl

monomers.^{64, 65} Solid single component systems are increasingly attractive, as the active initiating species is known, unlike binary initiators.

In attempts to identify other options, our attention was drawn to Group 5 metals: vanadium, niobium and tantalum. Vanadium is prone to redox chemistry, and more commonly found in the +4 oxidation state, and therefore may present challenges in synthesizing the hexacoordinate anion. Both niobium and tantalum exhibit very similar chemistry, due to the lanthanide contraction. As a result of the large size, niobium and tantalum offer the opportunity for more bulky anions than those comprised of main group elements, including the use of more bulky ligands, and therefore should be more weakly coordinating.

Hexacoordinate niobium(V) WCAs with oxo-chelating ligands are not common, and only a few systems have been fully structurally characterized.^{113, 150, 157-163} Systems with a proton source as the cation that are attractive as possible initiators for cationic olefin polymerization are even more rare. Some examples are given in Figure 2.1. Binary initiators such as $\text{NbCl}_5/6\text{RLi}/\text{Ph}_3\text{CCl}$,¹⁶⁴ $\text{NbCl}_5/\text{ethylene glycol}$,¹⁶⁵ have been used to polymerize vinyl monomers via metal coordination polymerization, along with the $[\text{Nb}(\text{OC}_6\text{F}_5)]$ (**B**) anion for ethylene in combination with a bulky metallocene.^{113, 150} To the best of our knowledge, there are no Nb-O WCA systems that have been proven to be effective single component initiators for cationic olefin polymerization.

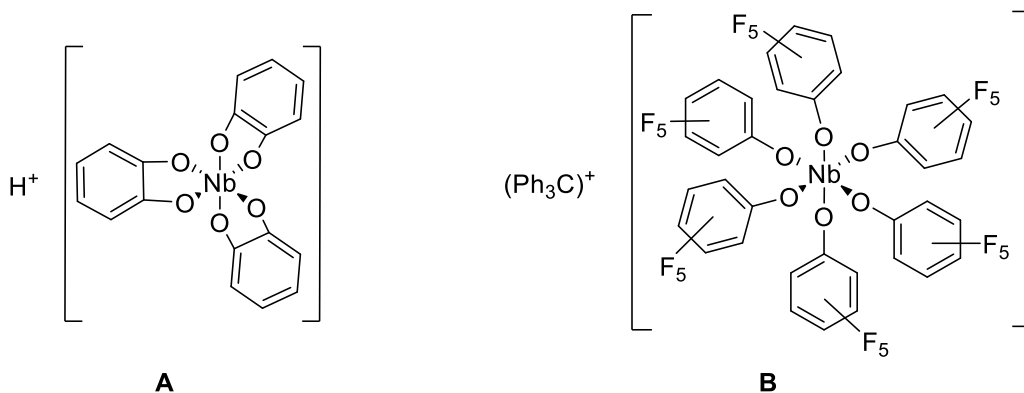


Figure 2.1 Examples of WCAs containing hexacoordinate Nb(V) anions.

Most recently, research in our group has discovered two solid Brønsted acids containing a Group 5 metal, $\text{H}(\text{OEt}_2)_2[\text{Ta}(\text{1,2-O}_2\text{C}_2\text{Cl}_4)_3]$ ($\text{H}(\text{OEt}_2)_2[\mathbf{Ta.1}]$) and $\text{H}(\text{OEt}_2)_2[\text{Ta}(\text{1,2-O}_2\text{C}_6\text{Cl}_4)_2(\text{1,2-OC}_6\text{Cl}_4\text{OH})_2]$ ($\text{H}(\text{OEt}_2)_2[\mathbf{Ta.2}]$). Interestingly, the tetrakis-substituted species was shown to have two bidentate tetrachlorocatechol ligands, and two monodentate ligands in a *cis* disposition. These Brønsted acids were shown to be highly efficient single component initiators for cationic olefin polymerization with a range of vinyl monomers: *n*-butyl vinyl ether, styrene, α -methylstyrene and isoprene.^{146, 147}

In this chapter, the syntheses and characterizations of two analogous Brønsted acids containing a niobium(V) centre, $\text{H}(\text{OEt}_2)_2[\mathbf{2.1}]$ and $\text{H}(\text{OEt}_2)_2[\mathbf{2.2}]$, are discussed. This chemistry is compared to the respective tantalum(V) derivatives. The use of $\text{H}(\text{OEt}_2)_2[\mathbf{2.1}]$ and $\text{H}(\text{OEt}_2)_2[\mathbf{2.2}]$ as single component initiators for cationic olefin polymerization is evaluated. Both Brønsted acids are effective initiators for the polymerization of *n*-butyl vinyl ether and styrene. Furthermore, $\text{H}(\text{OEt}_2)_2[\mathbf{2.2}]$ produced a high molecular weight syndiotactic-rich sample of poly(α -methylstyrene) at low temperatures, and oligoisoprene was successfully isolated.

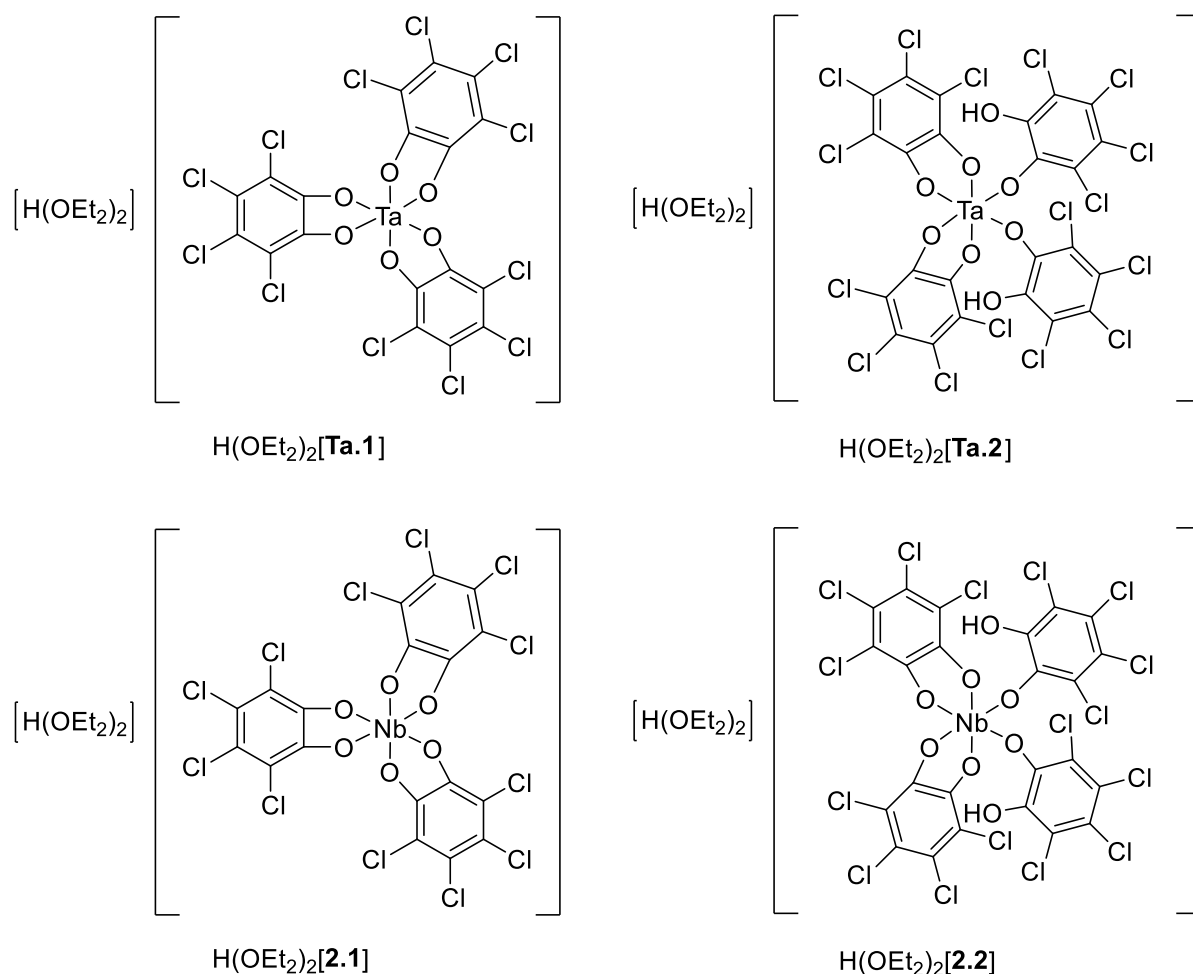


Figure 2.2 Previously reported Brønsted acids $\text{H}(\text{OEt}_2)_2[\mathbf{Ta.1}]$ and $\text{H}(\text{OEt}_2)_2[\mathbf{Ta.2}]$ and the Brønsted acids $\text{H}(\text{OEt}_2)_2[\mathbf{2.1}]$ and $\text{H}(\text{OEt}_2)_2[\mathbf{2.2}]$ pertaining to this thesis.

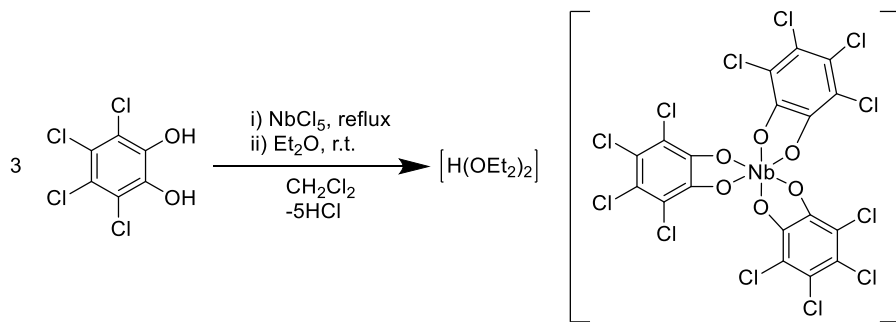
2.2 Results and discussion

2.2.1 Synthesis of $\text{H}(\text{OEt}_2)_2[\mathbf{2.1}]$

The synthesis of a Brønsted acid containing the TRISPHAT anion ($[\mathbf{1.17}]^-$, $\text{R} = \text{Cl}$) with an oxonium cation ($\text{L} = \text{Et}_2\text{O}$, THF, DMF) has previously been reported by our group.^{64, 65} These solid Brønsted acids are effective single component initiators for the cationic polymerization of *n*-butyl vinyl ether, styrene, α -methylstyrene and isoprene. The tantalum(V) analogue of the solid Brønsted acid ($\text{H}(\text{OEt}_2)_2[\mathbf{Ta.1}]$) has also been isolated, characterized and investigated as a cationic

initiator for vinyl monomers. It was shown to polymerize *n*-butyl vinyl ether and α -methylstyrene. A more sterically bulky species with four tetrachlorocatechol ligands ($\text{H}(\text{OEt}_2)_2[\mathbf{Ta.2}]$) was also isolated and used to polymerize a range of vinyl monomers.¹⁴⁶ Therefore, it is expected that the niobium(V) analogues should be accessible via the same synthetic pathway and these new acids may possess similar chemical behaviour.

Following the developed procedure for the Brønsted acids containing phosphorus(V) and tantalum(V) WCAs, the synthesis of a hexacoordinate niobium(V) anion with three chelating tetrachlorocatechol ligands was attempted. A warm solution of tetrachlorocatechol (3 equiv) in CH_2Cl_2 was added to a refluxing solution of niobium pentachloride in CH_2Cl_2 . The subsequent addition of excess diethyl ether at ambient temperature afforded an orange solid in moderate yield (41%).



Scheme 2.1 Synthesis of Brønsted acid $\text{H}(\text{OEt}_2)_2[\mathbf{2.1}]$.

The isolated solid was analyzed by ^1H NMR spectroscopy, and mass spectrometry. At 25 °C, the ^1H NMR spectrum shows two signals assigned to the diethyl ether molecules ($\delta = 3.76$ ppm, 8H, OCH_2CH_3 ; $\delta = 1.24$ ppm, 12H, OCH_2CH_3). At low temperature (-85 °C), a sharp signal attributed to the acidic proton was visible ($\delta = 16.69$ ppm, 1H, $[\text{H}(\text{OEt}_2)_2]^+$), with a downfield shift in the same region to the phosphorus(V) and tantalum(V) derivatives $\{\text{H}(\text{OEt}_2)_2[\text{P}(1,2\text{-C}_6\text{O}_2\text{Cl}_4)_3]$ ($T = -85$ °C, CD_2Cl_2 ; $\delta = 16.70$, H);⁶⁴ $\text{H}(\text{OEt}_2)_2[\mathbf{Ta.1}]$ ($T = -85$ °C, CD_2Cl_2 ; $\delta = 16.74$, H)¹⁴⁶. There was no broad peak between 9-10 ppm to indicate the presence of a hydroxyl proton of any

tetrachlorocatechols that are bound in a monodentate fashion. Due to the poor solubility of this Brønsted acid at $-85\text{ }^{\circ}\text{C}$, a $^{13}\text{C}\{^1\text{H}\}$ NMR spectrum of sufficient intensity could not be obtained. However, it was possible to perform an ESI-MS in negative ion mode. Importantly, the spectrum showed a major signal at $830.3\text{ }m/z$ consistent with the niobium(V) anion with three chelating tetrachlorocatechol moieties. Therefore, it is proposed that the isolated solid is the expected product $\text{H}(\text{OEt}_2)_2[\mathbf{2.1}]$. A signal with small intensity was observed at $1078.1\text{ }m/z$. This is consistent with the calculated molecular weight for a niobium(V) anion with four tetrachlorocatechol ligands. Like the tantalum(V) analogue, it may be possible to isolate the more sterically bulky Brønsted acid.

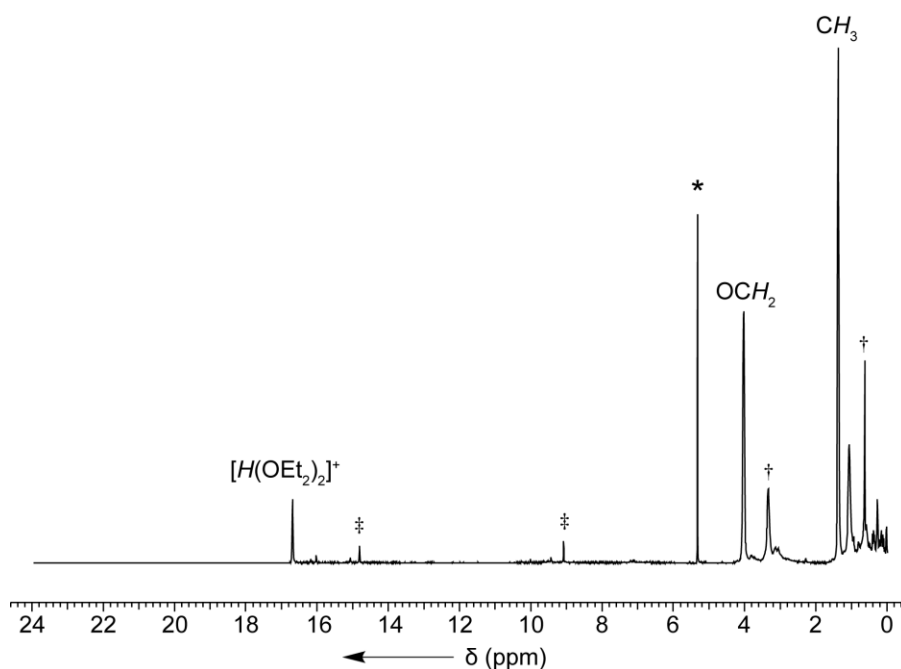


Figure 2.3 ^1H NMR (400 MHz, CD_2Cl_2 , $-85\text{ }^{\circ}\text{C}$) spectrum of $\text{H}(\text{OEt}_2)_2[\mathbf{2.1}]$. * indicates residual NMR solvent, † indicates free diethyl ether solvent, ‡ unassigned signal.

2.2.2 H(OEt₂)₂[**2.1**]-initiated polymerizations of *n*-butyl vinyl ether and styrene

Test polymerizations were carried out using crude H(OEt₂)₂[**2.1**] at -78 °C to initiate *n*-butyl vinyl ether and styrene. This data are shown in Table 2.1. These polymerizations resulted in polymer in moderate yield. The poly(*n*-butyl vinyl ether) produced was close to the expected molecular weight [M_n calc = 40 000 g mol⁻¹, M_n obsv = 32 780 g mol⁻¹, yield = 76%, \mathcal{D} = 1.39]. Single component initiators such as H(OEt₂)₂[**Ta.1**] have also shown similar data on polymerization with *n*-butyl vinyl ether [T = -78 °C, yield = 72%, M_n = 34 100 g mol⁻¹, \mathcal{D} = 1.45], whereas polymerizations with H(OEt₂)₂[P(1,2-O₂C₆Cl₄)₃] showed living character with *n*-butyl ether [T = -78 °C, yield = 88%, M_n = 41 600 g mol⁻¹, \mathcal{D} = 1.11].⁶⁴

Table 2.1 H(OEt₂)₂[**2.1**]-initiated polymerizations of *n*-butyl vinyl ether and styrene.

Entry	Monomer	Temp °C	[M]:[I] ^a	Yield %	M_n calc ^b g mol ⁻¹	M_n ^c g mol ⁻¹	\mathcal{D} ^d
1	<i>n</i> -butyl vinyl ether	-78	400	76	40 000	32 780	1.39
2	styrene	-78	400	70	41 700	10 380	4.41

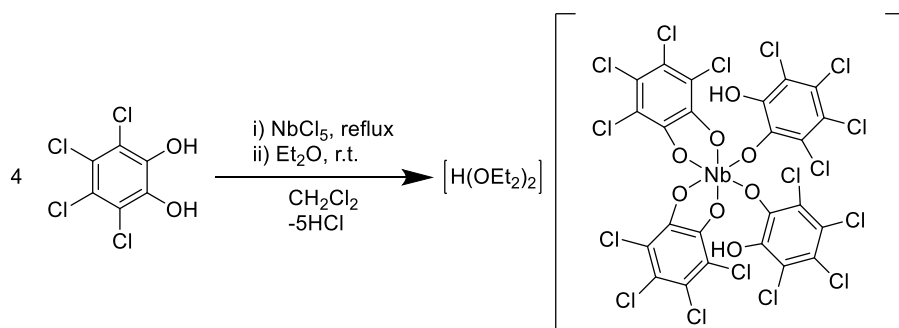
The polymerization was carried out in 2 mL CH₂Cl₂ using 0.015 mmol of Brønsted acid as initiator. ^a [monomer]/[initiator] ratio. ^b M_n calc = [M]:[I] x FW(monomer). The end group is not included in the calculation. ^c Absolute molecular weights were determined using laser light scattering gel permeation chromatography (GPC-LLS); differential refractive index (dn/dc) of poly(*n*-butyl vinyl ether) (dn/dc = 0.068 mL g⁻¹) in THF was calculated by assuming 100% mass recovery; (dn/dc) of polystyrene used is 0.185 mL g⁻¹. ^d Dispersity (\mathcal{D} = M_w/M_n), where M_w is the weight-average molar mass and M_n is the number average molar mass.

The polymerization of styrene initiated with H(OEt₂)₂[**2.1**] proved more challenging. Although the yield of polystyrene was promising, high molecular weight polymer was not obtained [M_n = 10 380 g mol⁻¹, yield = 70%, \mathcal{D} = 4.41] in comparison to the phosphorus(V) analogue, H(OEt₂)₂[P(1,2-O₂C₆Cl₄)₃] [T = -78 °C, yield = 7%, M_n = 163 000 g mol⁻¹, \mathcal{D} = 1.23],⁶⁴ therefore optimization of the anion system was necessary. As a peak for the more sterically bulky system was seen in the ESI-MS negative ion mode spectrum, synthesis of the tetrakis-substituted anion

was investigated further in attempt to isolate in high enough yield to assess the efficiency as a single component initiator for cationic olefin polymerization.

2.2.3 Synthesis of $\text{H}(\text{OEt}_2)_2[2.2]$

Interestingly, when tantalum was used in the place of phosphorus in the TRISPHAT anion, it was also possible to isolate a tetrakis-substituted tantalum(V) anion when reacted with four equivalents of tetrachlorocatechol.^{146, 147} Two of the tetrachlorocatechol ligands were bound in a bidentate fashion, and two were bound in a monodentate fashion. By employing NbCl_5 in place of TaCl_5 , isolation of an analogous Brønsted acid should be possible.



Scheme 2.2 Synthesis of Brønsted acid $\text{H}(\text{OEt}_2)_2[2.2]$.

A warm solution of tetrachlorocatechol (4 equiv) in CH_2Cl_2 was added to niobium pentachloride in refluxing CH_2Cl_2 . After cooling to ambient temperature excess Et_2O was added to afford the desired solid Brønsted acid as an orange powder in moderate yield (40%). The isolated product was analyzed by ^1H and $^{13}\text{C}\{^1\text{H}\}$ NMR spectroscopy and X-ray crystallography.

At ambient temperature, there were three resonances observed in the ^1H NMR spectrum in CD_2Cl_2 . Two signals were assigned to the two diethyl ether molecules ($\delta = 3.87$, 8H, OCH_2CH_3 ; 1.29, 12H, OCH_2CH_3), and a broad signal at 8.97 ppm. At -85°C , this signal shifted downfield to 9.42 ppm and significantly sharpened, and thus could be assigned to the hydroxyl proton of a tetrachlorocatechol bound in a monodentate fashion. An additional sharp resonance was visible at

16.61 ppm that was assigned to the acidic proton, $H(OEt_2)_2[2.2]$. In comparison, the acidic protons in the previously reported $H(OEt_2)_2[Ta.2]$ ($T = -85\text{ }^\circ\text{C}$, CD_2Cl_2 ; $\delta = 16.73$, H)¹⁴⁶ and $H(OEt_2)_2[P(1,2-C_6O_2Cl_4)_3]$ ($T = -85\text{ }^\circ\text{C}$, CD_2Cl_2 ; $\delta = 16.70$, H)⁶⁴ were within a similar region. Other protonated ether salts show a similar significant downfield shift. For example, $H(OEt_2)_2[P(C_2O_4)_3]$ ($\delta = 15.5$, $CDCl_3$)¹²⁸ and $H(OEt_2)_2[Al(OC(CF_3)_3)_4]$ ($\delta = 14.7$, C_6D_6)⁵⁹. The ratio of the acidic proton signal to the protons in the diethyl ether molecules is consistent with the proposed HL_2 stoichiometry of the cation.

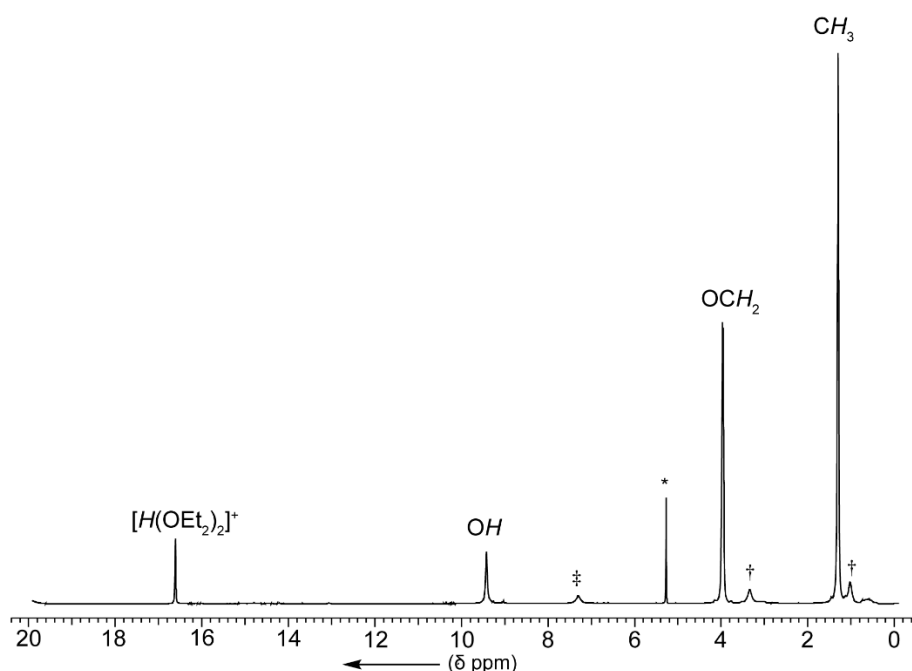


Figure 2.4 1H NMR (400 MHz, CD_2Cl_2 , $-85\text{ }^\circ\text{C}$) spectrum of $H(OEt_2)_2[2.2]$. * indicates residual NMR solvent, † indicates free diethyl ether solvent, ‡ unassigned signal.

Further evidence for the proposed structure was obtained from the $^{13}C\{^1H\}$ NMR spectrum ($T = -85\text{ }^\circ\text{C}$). Two signals were assigned to the diethyl ether molecules ($\delta = 70.5$, OCH_2CH_3 ; 13.5 , OCH_2CH_3). Nine further resonances between 150.7 and 115.6 ppm were assigned to the aryl carbons, three for the bidentate tetrachlorocatecholate moieties, and six for the monodentate bound tetrachlorocatecholate moieties (Appendix A.1).

Metrical Parameters Determined by Single Crystal X-ray Diffraction.

The Brønsted acid, $\text{H}(\text{OEt}_2)_2[\mathbf{2.2}]$, was crystallized at $-30\text{ }^\circ\text{C}$ from a concentrated solution of the crude product in CD_2Cl_2 , giving colourless crystals from the deep red solution. Upon analysis, the elucidated molecular structure is consistent with the proposed structure (Figure 2.5). There was a large amount of disorder in the cation, and unfortunately the acidic proton was not located.

The molecular structure exhibits a distorted octahedral geometry around the hexacoordinate niobium(V) centre. More saliently, the two monodentate tetrachlorocatechol ligands [Nb(1)-O(3), Nb(1)-O(7)] are coordinated in the *cis* position. The distortion from regular octahedral geometry is apparent from the consideration of the bond angles around the niobium(V) centre. The angles between the two monodentate ligands showed little deviation from octahedral geometry in the anion [O(3)-Nb(1)-O(7) = $94.7(4)^\circ$]. More divergence from regular octahedral geometry was observed with respect to the angles between the differently bound substituents [O(3)-Nb(1)-O(1) = $104.5(5)^\circ$; O(3)-Nb(1)-O(5) = $83.7(4)^\circ$; O(7)-Nb(1)-O(5) = $113.5(4)^\circ$; O(7)-Nb(1)-O(1) = $82.3(1)^\circ$]. This likely results from the steric repulsion of the two large tetrachlorocatecholate moieties in close proximity, or intramolecular forces, such as hydrogen bonding. The two chelated tetrachlorocatecholate moieties occupy the positions Nb(1)-O(1) and Nb(1)-O(2); Nb(1)-O(5) and Nb(1)-O(6). The internal angles of the five-membered chelate ring show a deviation from those expected for regular octahedral geometry [O(1)-Nb(1)-O(2) = $75.8(5)^\circ$; O(5)-Nb(1)-O(6) = $75.6(5)^\circ$] likely caused by the forced conformation. Both the steric repulsion from large ligands and the forced conformation from the five-membered rings will contribute to the deviation from a regular octahedral geometry.

The Nb-O distances in the anion range from 1.889(12) Å to 2.049(12) Å, with averages of avg. Nb-O_{eq} = 2.00(3) Å; and avg. Nb-O_{ax} = 1.94(2) Å. These distances are typical of previously reported values in similar Nb-O bonded systems {[Nb(C₆H₄O₂)₃py]} avg. = 2.049(5) Å¹⁶¹; [Ph₃C][Nb(OC₆F₅)₆] avg. = 1.955(1) Å¹¹³}; and other monodentate and bidentate systems with average bond lengths ranging from 1.86(2) Å to 2.14(2) Å.^{150, 162}

Intramolecular hydrogen bonding is observed between the hydroxyl proton on a monodentate tetrachlorocatechol and an oxygen atom of the chelated ligand in the anion [O(5)⋯H(4) = 1.872(12) Å; O(1)⋯H(8) = 2.293(11) Å]. This is within the van der Waals radii for oxygen and hydrogen [$r_{vdw} = 2.72\text{Å}$].¹⁶⁶ The tantalum(V) derivative H(OEt₂)₂[**Ta.2**] where the monodentate tetrachlorocatechol moieties are similarly bound in a *cis* fashion, also contains intramolecular hydrogen bonding of similar distances [O⋯H = 1.91(2) Å; O⋯H = 2.23(2)].¹⁴⁶

As a result of the disorder in the cations, the acidic proton is not detectable in the electron density map (only the major component is shown in Figure 2.5). It is hypothesized that the two diethyl ether molecules would not be orientated towards each other, if a proton was not present between them. Additionally, the distance between the two oxygens [O(9)⋯O(10) = 2.33(3) Å] is within the van der Waals radii of two oxygen atoms [$r_{vdw} = 3.04\text{Å}$].¹⁶⁶ Other [H(OEt₂)₂]⁺ cations have similar O⋯O distances in the cation. For example, H(OEt₂)₂H₂O[**Ta.2**] [O⋯O = 2.46(3) Å];¹⁴⁶ H(OEt₂)₂[(C₂H₃N₂)(B(C₆F₅)₃)₂] [O⋯O = 2.395(8) Å];¹⁶⁷ and H(OEt₂)₂[P(C₂O₄)₃] [avg. = 2.37(3) Å]¹²⁸.

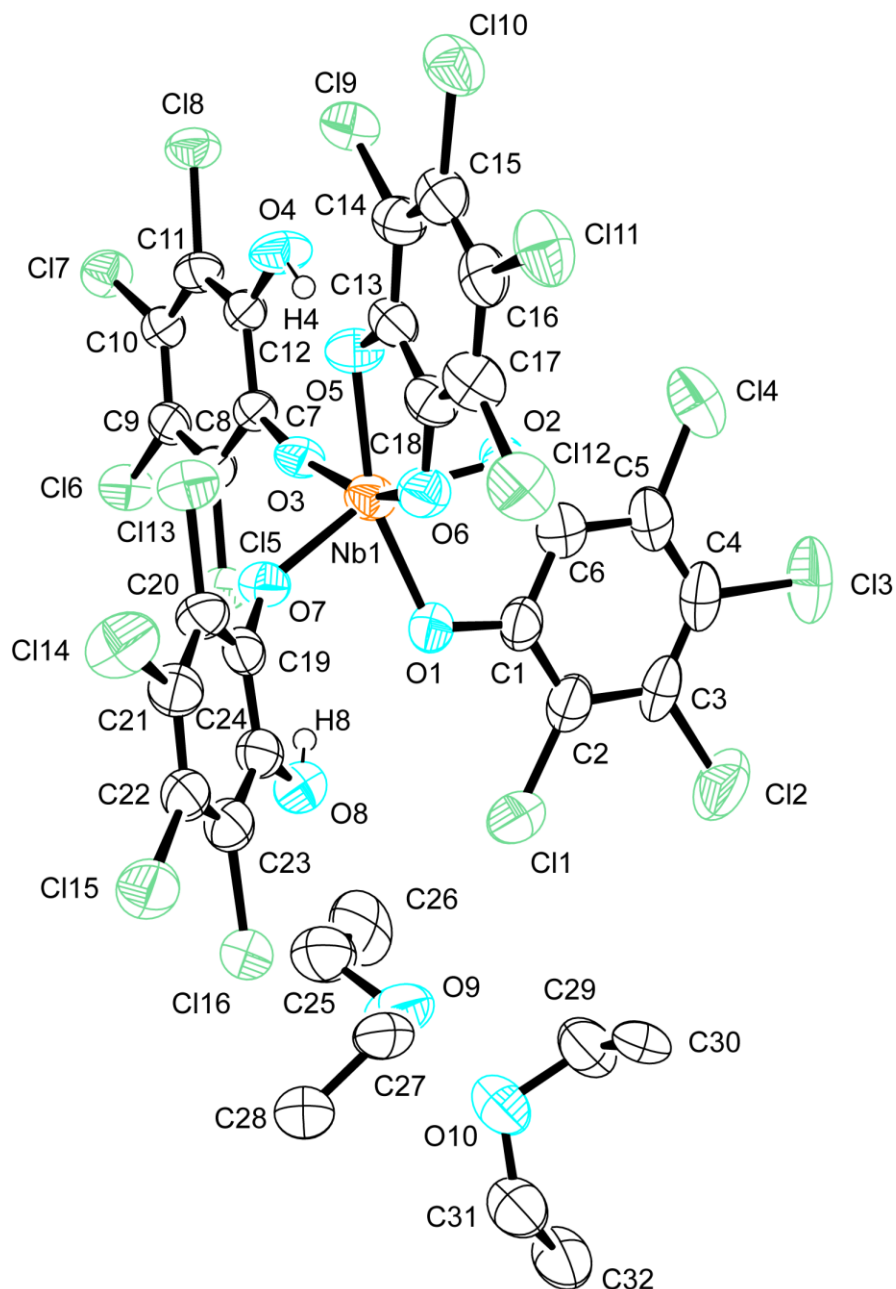
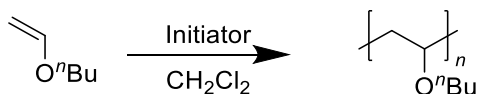


Figure 2.5 Molecular structure of $\text{H}(\text{OEt}_2)_2[2.2]$. Ellipsoids are drawn at the 50% probability level. Hydrogen atoms on the diethyl ether molecules in the cation are omitted for clarity. Selected bond lengths (\AA): $\text{Nb}(1)\text{-O}(1) = 2.014(11)$; $\text{Nb}(1)\text{-O}(2) = 1.998(11)$; $\text{Nb}(1)\text{-O}(3) = 1.897$; $\text{Nb}(1)\text{-O}(5) = 2.033(11)$; $\text{Nb}(1)\text{-O}(6) = 1.993(12)$; $\text{Nb}(1)\text{-O}(7) = 1.940(10)$; $\text{O}(4)\text{-C}(12) = 1.35(2)$; $\text{O}(8)\text{-C}(24) = 1.36(2)$; $\text{O}(9)\text{-C}(25) = 1.47(2)$; $\text{O}(9)\text{-C}(27) = 1.47(2)$; $\text{O}(10)\text{-C}(29) = 1.47(2)$; $\text{O}(10)\text{-C}(31) = 1.47(2)$. Selected bond angles ($^\circ$) = $\text{O}(1)\text{-Nb}(1)\text{-O}(2) = 75.8(5)$; $\text{O}(1)\text{-Nb}(1)\text{-O}(5) = 161.8(4)$; $\text{O}(2)\text{-Nb}(1)\text{-O}(7) = 157.4(5)$; $\text{O}(3)\text{-Nb}(1)\text{-O}(6) = 158.0(5)$; $\text{O}(5)\text{-Nb}(1)\text{-O}(6) = 75.6(4)$.

2.2.4 H(OEt₂)₂[2.2]-initiated polymerizations

To evaluate the efficiency of the isolated Brønsted acid as a single component initiator, it was reacted with a range of monomers (*n*-butyl vinyl ether, styrene, α -methylstyrene and isoprene) at a variety of temperatures (21 °C to -84 °C). The results are shown in Tables 2.2 and 2.3, and each data point is representative of two or more repeat runs. Each polymerization was carried out using freshly distilled solvents and monomers. H(OEt₂)₂[2.2] has been shown to successfully initiate the polymerization of *n*-butyl vinyl ether (Scheme 2.3), styrene (Scheme 2.4), α -methylstyrene (Scheme 2.5), and isoprene (Scheme 2.6).



Scheme 2.3 H(OEt₂)₂[2.2]-initiated cationic polymerization of *n*-butyl vinyl ether.

Vinyl ethers are readily polymerizable and often exhibit living polymerization. Because of this, they have commonly been used as a primary test monomer for cationic olefin polymerization. They exhibit an increased reactivity due to the resonance stabilized carbocationic intermediate compared to monomers without the electron donating ether functionality.¹⁹ H(OEt₂)₂[2.2] successfully polymerized *n*-butyl vinyl ether at both ambient and lower temperatures (entries 1-7, Table 2.2). At ambient temperature the polymerization resulted in a pale yellow, oily residue [yield = 52%, $M_n = 16\,250\text{ g mol}^{-1}$, $\bar{D} = 1.55$]. These results are equivalent to those with the tantalum(V) analogue, H(OEt₂)₂[Ta.2], of this single component initiator [yield = 33%, $M_n = 16\,300\text{ g mol}^{-1}$, $\bar{D} = 1.69$].¹⁴⁶ Upon polymerization at lower temperatures, the resulting polymer was colourless. The lack of colour in poly(*n*-butyl vinyl ether) has been previously reported to be caused by the absence of conjugated polyene moieties in the polymer. Chain transfer processes that result in the presence of polyene functionalities, are suppressed at lower temperatures.¹⁶⁸⁻¹⁷¹ Decreased polyene content at low temperature was corroborated by the ¹H NMR spectrum of the polymers

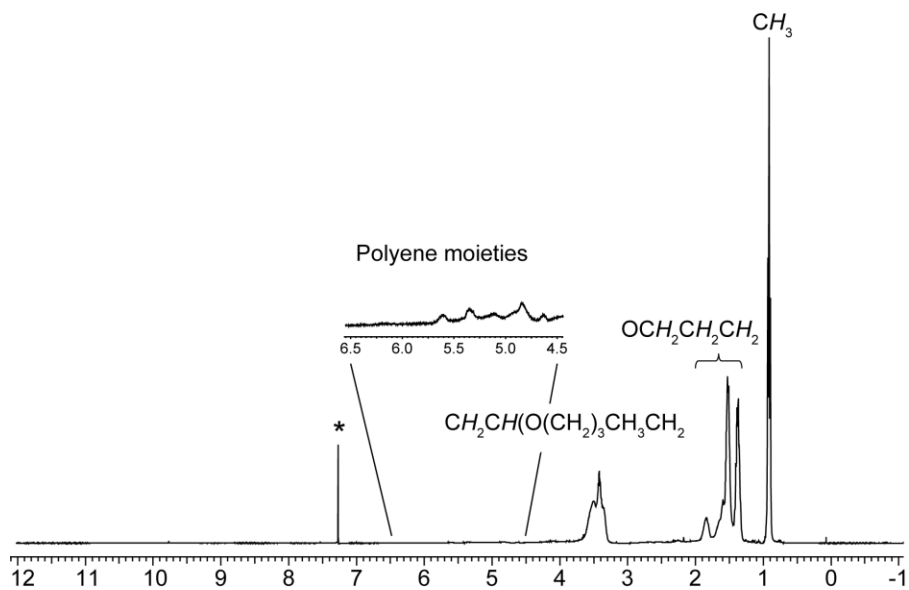
(Figure 2.4). The yellow-coloured polymers showed a multitude of broad signals between 4.5-5.5 ppm, whilst these were not present in the samples polymerized below -80 °C. However, the low abundance of the polyene moieties at higher temperatures with $\text{H}(\text{OEt}_2)_2[\mathbf{2.2}]$ suggests a polymerization performance superior to other single component initiators.

Table 2.2 Polymerization of *n*-butyl vinyl ether initiated with $\text{H}(\text{OEt}_2)_2[\mathbf{2.2}]$. The results shown are representative of multiple runs.

Entry	Monomer	Temp °C	[M]:[I] ^a	Yield %	M_n calc ^b g mol ⁻¹	M_n ^c g mol ⁻¹	\mathbf{D}^d
1	<i>n</i> -butyl vinyl ether	21	400	52	40 000	16 250	1.55
2	<i>n</i> -butyl vinyl ether	0	400	65	40 000	18 690	1.72
3	<i>n</i> -butyl vinyl ether	-15	400	53	40 000	17 900	1.52
4	<i>n</i> -butyl vinyl ether	-42	400	58	40 000	23 930	1.66
5	<i>n</i> -butyl vinyl ether	-50	400	49	40 000	22 160	1.70
6	<i>n</i> -butyl vinyl ether	-78	400	70	40 000	33 610	1.29
7	<i>n</i> -butyl vinyl ether	-84	400	94	40 000	52 700	1.62
8	<i>n</i> -butyl vinyl ether	-78	600	69	60 000	59 800	1.28

The polymerization was carried out in 2 mL CH_2Cl_2 using 0.015 mmol of Brønsted acid as initiator. ^a [monomer]/[initiator] ratio. ^b M_n calc = [M]:[I] x FW(monomer). The end group is not included in the calculation. ^c Absolute molecular weights were determined using laser light scattering gel permeation chromatography (GPC-LLS); differential refractive index (dn/dc) of poly(*n*-butyl vinyl ether) ($dn/dc = 0.068$ mL g⁻¹) in THF was calculated by assuming 100% mass recovery. ^d Dispersity ($\mathbf{D} = M_w/M_n$), where M_w is the weight-average molar mass and M_n is the number average molar mass.

a)



b)

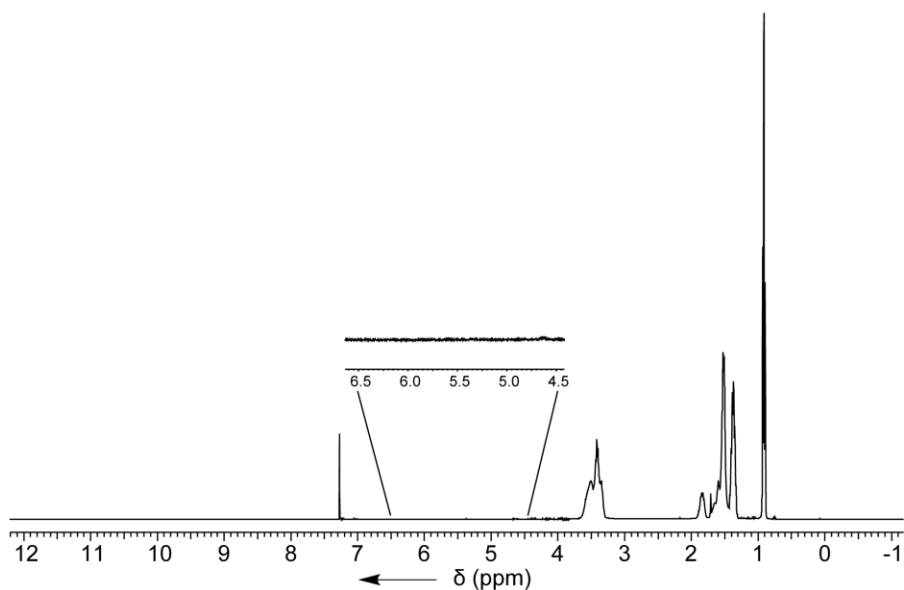


Figure 2.6 ^1H NMR spectrum (400 MHz, CDCl_3 , 25 °C) of poly(*n*-butyl vinyl ether) initiated with $\text{H}(\text{OEt})_2[2.2]$ at a) 21 °C and b) -84 °C. * indicates residual NMR solvent, † indicates residual CH_2Cl_2 .

While the isolated yields of poly(*n*-butyl vinyl ether) remained fairly consistent as the temperature lowered, the molecular weights of the polymer showed a larger difference. At lower

temperatures of polymerization, the molecular weights of the isolated polymers were higher, and close to the calculated mass [$T = -78\text{ }^{\circ}\text{C}$, $M_n\text{ calc} = 40\,000\text{ g mol}^{-1}$, $M_n\text{ obsv} = 33\,610\text{ g mol}^{-1}$, yield = 70%]. This polymerization data is closely comparable with $\text{H}(\text{OEt}_2)_2[\mathbf{2.1}]$ [$T = -78\text{ }^{\circ}\text{C}$, $M_n = 32\,780\text{ g mol}^{-1}$, yield = 76%, $\text{Đ} = 1.39$]. Single component initiators such as $\text{H}(\text{OEt}_2)_2[\text{P}(1,2\text{-O}_2\text{C}_6\text{Cl}_4)_3]$ have also shown similar data to polymerization with *n*-butyl vinyl ether [$T = -78\text{ }^{\circ}\text{C}$, yield = 88%, $M_n = 41\,600\text{ g mol}^{-1}$, $\text{Đ} = 1.11$],⁶⁴ as did the tantalum(V) derivative, $\text{H}(\text{OEt}_2)_2[\mathbf{Ta.2}]$ [$T = -78\text{ }^{\circ}\text{C}$, yield = 71%, $M_n = 32\,200\text{ g mol}^{-1}$, $\text{Đ} = 1.58$].¹⁴⁶ Cationic polymerization has been reported with binary initiating systems comprised of Lewis acids and a proton source, such as isobutyl vinyl ether (1-(isobutyoxy) ethyl acetate/ TiCl_4);¹⁷² (salphen/ ZrCl_4/HCl)¹⁷³ giving lower molecular weight and higher dispersity polymers than with this single component initiator.

It was also shown that when the monomer to initiator ratio was increased to [600]:[1], the observed molecular weight increased accordingly (entry 8, Table 2.2) [$T = -78\text{ }^{\circ}\text{C}$, $M_n\text{ calc} = 60\,000\text{ g mol}^{-1}$, $M_n\text{ obsv} = 59\,800\text{ g mol}^{-1}$]. However due to the broad dispersity obtained is not conclusive evidence of living polymerization behaviour.

The thermal properties of the polymers produced were assessed using differential scanning calorimetry (DSC) to determine the glass transition temperature (T_g). A wide variety of factors can influence the properties of polymers including, but not limited to: molecular weight, dispersity, tacticity, purity and thermal history. Poly(*n*-butyl vinyl ether) polymerized at $-84\text{ }^{\circ}\text{C}$ exhibited a second order transition temperature ($T_g\text{ mid} = -53\text{ }^{\circ}\text{C}$) in the same region as industry homopolymer standards ($T_g = -55\text{ }^{\circ}\text{C}$).¹⁷⁴ The DSC traces show the gradual shift in T_g towards higher temperatures as the temperature of polymerization increases. The lower molecular weight poly(*n*-butyl vinyl ether) polymerized at ambient temperature had a higher transition temperature ($T_g\text{ mid}$

= -47 °C), could be explained by the differing chemical structure of the polyene-containing polymer.

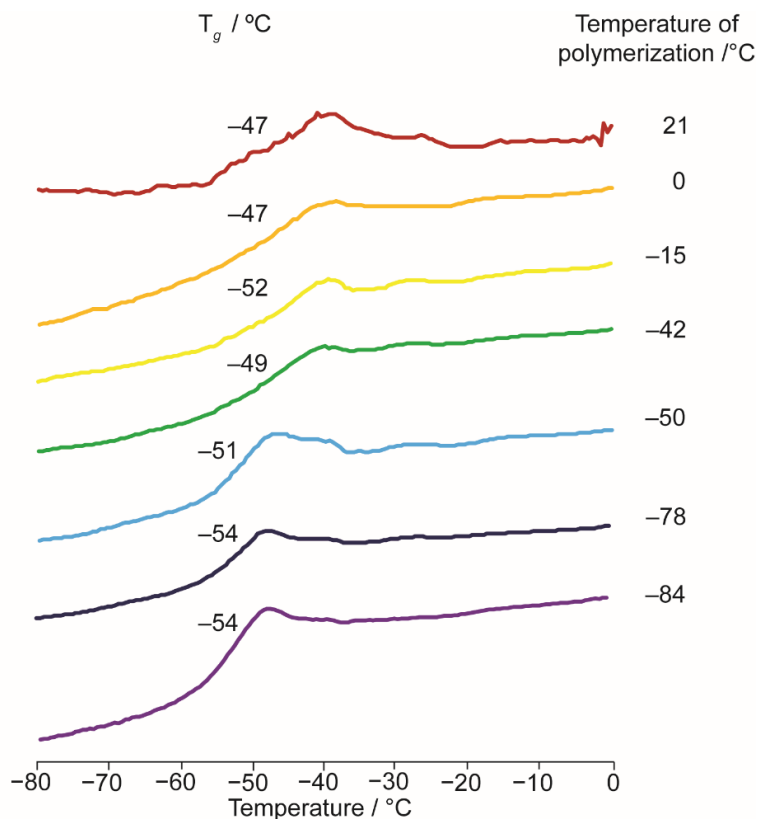
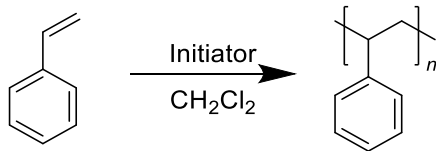


Figure 2.7 DSC traces of poly(*n*-butyl vinyl ether) initiated with H(OEt₂)₂[2.2] showing glass transition temperature (T_g) as a function of the temperature of polymerization.



Scheme 2.4 H(OEt₂)₂[2.2]-initiated cationic polymerization of styrene.

The propagating carbocation of styrene is not as stable as in the case of vinyl ethers, making it a significantly more challenging polymerization to control.^{175, 176} Uncontrolled polymerization has been observed to give lower molecular weight polymers with broader dispersities as a result of chain transfer processes when using binary initiating systems such as AlCl₃/CH₂Cl₂.¹⁵⁵ Styrene

was polymerized successfully by $\text{H}(\text{OEt}_2)_2[\mathbf{2.2}]$ at temperatures ranging from 21 °C to -78 °C (entries 1-4, Table 2.3).

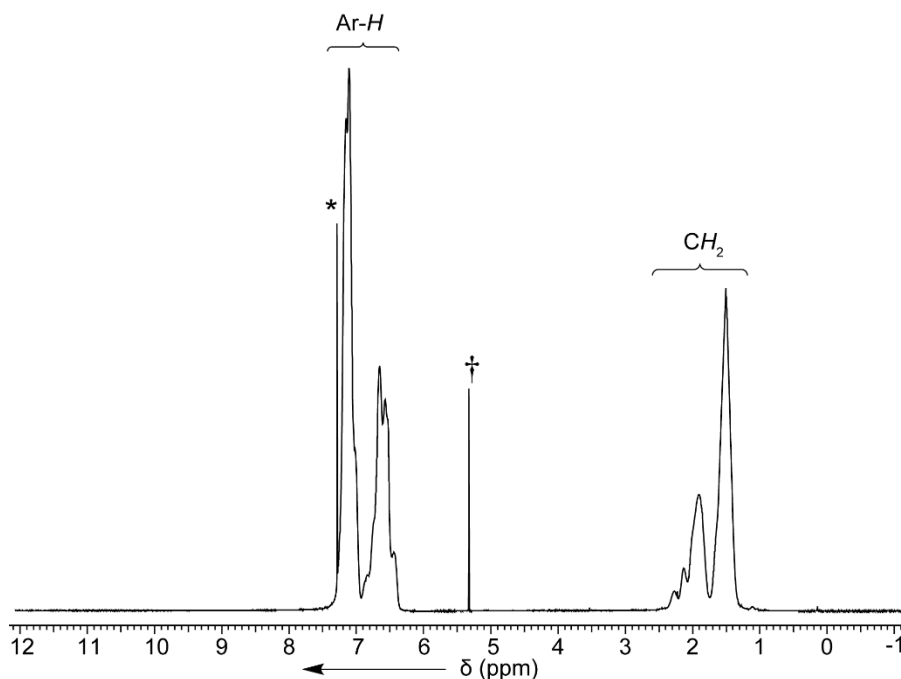
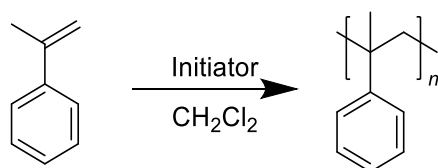


Figure 2.8 ^1H NMR spectrum (400 MHz, CDCl_3 , 25 °C) of polystyrene initiated with $\text{H}(\text{OEt}_2)_2[\mathbf{2.2}]$ at -50 °C.

* indicates residual NMR solvent, † indicates residual CH_2Cl_2 .

The ambient temperature polymerization of styrene gave a colourless polymer in high yield with low molecular weight [$T = 21$ °C, yield = 93%, $M_n = 10\,980$ g mol $^{-1}$, $\bar{D} = 2.40$]. As the temperature of polymerization is lowered, the molecular weights obtained from the isolated polymers significantly increased, and the dispersity narrows [$T = -50$ °C, yield = 43%, $M_n = 60\,050$ g mol $^{-1}$, $\bar{D} = 1.88$]. The trend observed here is typical of styrene polymerization, and has been seen with both $\text{H}(\text{OEt}_2)_2[\mathbf{Ta.2}]$ ($T = 18$ °C, $M_n = 6\,100$ g mol $^{-1}$, $\bar{D} = 2.16$, $[\text{M}]:[\text{I}] = 492$; $T = -50$ °C, $M_n = 37\,800$ g mol $^{-1}$, $\bar{D} = 1.43$, $[\text{M}]:[\text{I}] = 492$)¹⁴⁶ and $\text{H}(\text{OEt}_2)_2[\text{P}(1,2\text{-C}_6\text{O}_2\text{Cl}_4)_3]$ ($T = 17$ °C, $M_n = 5\,200$ g mol $^{-1}$, $\bar{D} = 2.36$, $[\text{M}]:[\text{I}] = 492$; $T = -50$ °C, $M_n = 147\,100$ g mol $^{-1}$, $\bar{D} = 1.88$, $[\text{M}]:[\text{I}] = 493$).⁶⁴ At temperatures below -50 °C the rate of polymerization becomes very low, and only minimal amounts of polymer are isolated.

DSC was used to determine the glass transition temperature of the polystyrene produced at $-50\text{ }^{\circ}\text{C}$. The dependence of T_g with respect to the molecular weight of the polystyrene has been studied in great detail ($M_n = 37\ 000\ \text{g mol}^{-1}$, $\mathcal{D} = 1.05$, $T_g = 105\text{ }^{\circ}\text{C}$; $M_n = 275\ 000\ \text{g mol}^{-1}$, $\mathcal{D} = 1.05$, $T_g = 106\text{ }^{\circ}\text{C}$).^{177, 178} Polystyrene produced at $-50\text{ }^{\circ}\text{C}$ has a slightly lower glass transition temperature, likely due to the broader dispersity index ($M_n = 37\ 000\ \text{g mol}^{-1}$, $\mathcal{D} = 1.88$, $T_g\ \text{mid} = 101\text{ }^{\circ}\text{C}$). Broader dispersities of polymers have been shown to lower the glass transition, in addition to molecular weight.^{179, 180} However, further investigation into the cause of the low glass transition temperature is needed.



Scheme 2.5 $\text{H}(\text{OEt}_2)_2[2.2]$ -initiated cationic polymerization of α -methylstyrene.

The successful polymerization of α -methylstyrene was also possible using $\text{H}(\text{OEt}_2)_2[2.2]$ at temperatures below $0\text{ }^{\circ}\text{C}$ (entries 5-7, Table 2.3) The rate of depolymerization of α -methylstyrene almost equals the rate of polymerization at ambient temperatures, which has been observed with other initiating systems.^{64, 146} Therefore temperatures above $0\text{ }^{\circ}\text{C}$ were not attempted.¹⁸¹ At $0\text{ }^{\circ}\text{C}$ to $-50\text{ }^{\circ}\text{C}$, a low molecular weight colourless solid was obtained [$T = 0\text{ }^{\circ}\text{C}$, $M_n = 3\ 140\ \text{g mol}^{-1}$; $T = -50\text{ }^{\circ}\text{C}$, $M_n = 6\ 030\ \text{g mol}^{-1}$]. At lower temperatures of polymerization, a significantly higher molecular weight polymer was isolated [$T = -78\text{ }^{\circ}\text{C}$, $M_n = 211\ 400\ \text{g mol}^{-1}$]. This is much higher than the calculated molecular weight, suggesting that branching or crosslinking occurred. There seems to be little dependence of the dispersity and yield on the temperature of polymerization.

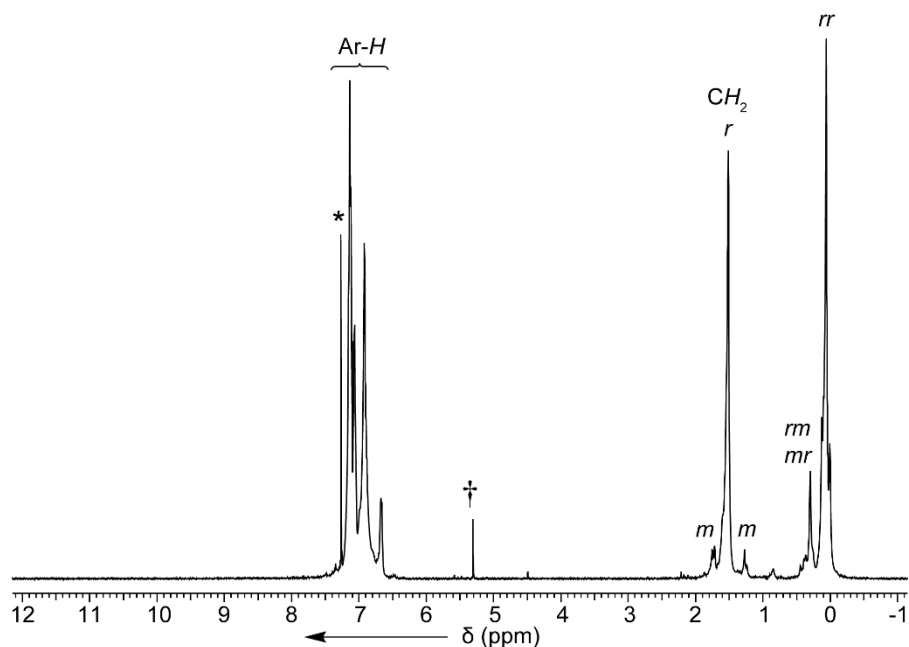
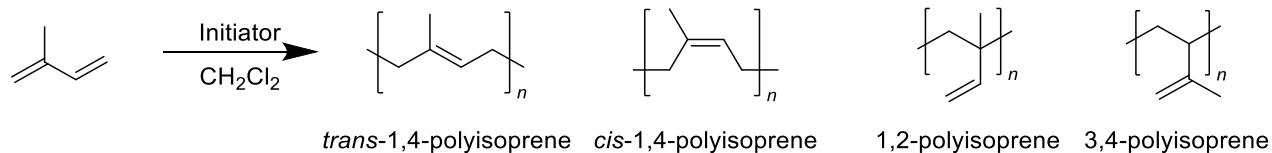


Figure 2.9 ^1H NMR spectrum (400 MHz, CDCl_3 , 25°C) of poly(α -methylstyrene) initiated with $\text{H}(\text{OEt}_2)_2[\mathbf{2.2}]$ at -78°C . * indicates residual NMR solvent, † indicates residual CH_2Cl_2 .

^1H NMR spectroscopy facilitated elucidation of the tacticity of poly(α -methylstyrene) produced at -78°C by integration of the triad signal (rr) (Figure 2.9).¹⁸² As with other reported single component initiator systems, $\text{H}(\text{OEt}_2)_2[\mathbf{2.2}]$ gave primarily syndiotactic-rich polymer (% rr = 83%). Syndiotactic-rich poly(α -methylstyrene) has also been observed for single component initiators ($\text{H}(\text{OEt}_2)_2[\mathbf{Ta.2}]$ % rr = 90 %; and $\text{H}(\text{OEt}_2)_2[\text{P}(1,2\text{-C}_6\text{O}_2\text{Cl}_4)_3]$ % rr = 87 %) ^{64, 146} and binary initiating systems [$\text{FeCl}_3/n\text{Bu}_4\text{NBr}$ % rr = 84 %; and other Lewis acids such as: SnCl_4 , SnBr_4 , ZnCl_2 % rr = > 90 %].^{183, 184}

Tacticity has also been shown to have an impact on the thermal properties of poly(α -methylstyrene), in addition to the molecular weight of the polymers.¹⁸³ Poly(α -methylstyrene) polymerized at -78°C [M_n = 211 400 g mol^{-1} , \bar{D} = 1.39, T_g mid = 182°C] compares to other syndiotactic-rich samples reported [M_n = 111 000 g mol^{-1} , T_g = 178°C ; M_n = 108 000, T_g = 171°C],^{185, 186} albeit higher. Significantly higher molecular weight than other polymers reported is believed to be the cause in the higher glass transition temperature.



Scheme 2.6 H(OEt₂)₂[2.2]-initiated cationic polymerization of isoprene.

The cationic polymerization of isoprene is very challenging, with many possible side reactions including, but not limited to: branching, cross-linking, cyclization, and chain transfer processes.^{187, 188} The reaction mechanism is not fully understood but deuterium labelling studies show that chain transfer processes prevent the formation of high molecular weight polymers.³⁴ At $-50\text{ }^\circ\text{C}$, low molecular weight polymers were obtained with a moderate dispersity (entry 8, Table 2.3) [$T = -50\text{ }^\circ\text{C}$, $M_n = 2\ 220\text{ g mol}^{-1}$, $\mathcal{D} = 1.80$]. At ambient temperature, the low yield of the polymer isolated meant GPC analysis could not be done (entry 9, Table 2.3). Other single component initiators with the same cation show similar initiation activity, such as H(OEt₂)₂[**Ta.2**] ($T = -50\text{ }^\circ\text{C}$, $M_n = 2\ 600\text{ g mol}^{-1}$, $\mathcal{D} = 1.73$)¹⁴⁶, and H(OEt₂)₂[P(1,2-O₂C₆Cl₄)₃] ($T = -35\text{ }^\circ\text{C}$, $M_n = 11\ 600\text{ g mol}^{-1}$).⁶⁴ At $-78\text{ }^\circ\text{C}$ this initiator was not active, indicating its limited initiating ability. Binary initiators, (e.g. TiCl₄/CF₃OOH³⁴ or ZnX₂/CCl₃COOD)¹⁸⁸ afford slightly higher molecular weight polymers, however with higher dispersity.

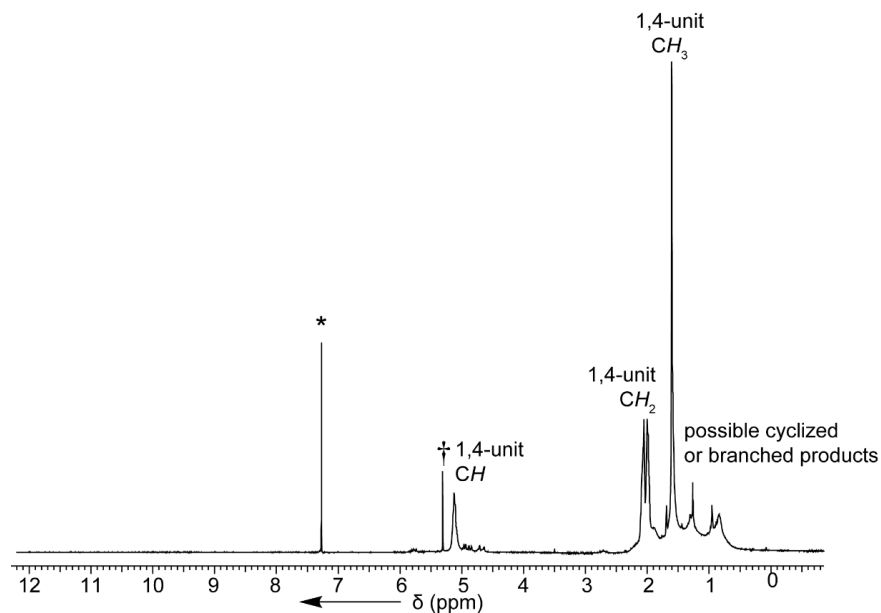


Figure 2.10 ¹H NMR spectrum (400 MHz, CDCl₃, 25 °C) of oligoisoprene initiated with H(OEt)₂[2.2] at -78 °C. * indicates residual NMR solvent, † indicates residual CH₂Cl₂.

Analysis of the ¹H NMR spectrum (Figure 2.10) showed predominantly resonances that can be assigned to the 1,4-microstructure. Weaker signals can be assigned to other microstructures of oligoisoprene [3,4-unit δ(CH₂) = 4.6-4.8 ppm; 1,2-unit δ(CH₂) = 4.8-5.0 ppm]. A broad signal between 0.7 and 1.2 ppm was assigned to cyclized or highly branched polymers that have been commonly seen before for cationically-initiated oligoisoprene. Further analysis of the microstructure was not possible due to the low yielding polymerizations.

Table 2.3 Cationic polymerization of styrene, α -methylstyrene, and isoprene initiated with H(OEt₂)₂[2.2]. The results shown are representative of multiple repeat runs.

Entry	Monomer	Temp °C	[M]:[I] ^a	Yield %	<i>M_n</i> calc ^b g mol ⁻¹	<i>M_n</i> ^c g mol ⁻¹	Đ ^d
1	styrene	21	400	93	41 700	10 980	2.40
2	styrene	0	400	88	41 700	19 480	2.11
3	styrene	-50	400	43	41 700	60 080	1.88
4	styrene	-78	400	10	41 700	119 800	1.44
5	α -methylstyrene	0	400	10	47 200	3 140	1.68
6	α -methylstyrene	-50	400	49	47 200	6 030	2.27
7	α -methylstyrene	-78	400	19	47 200	211 400	1.39
8	isoprene	21	400	1	27 200	n.d. ^e	n.d. ^e
9	isoprene	-50	400	2	27 200	2 220	1.80

The polymerization was carried out in 2 mL CH₂Cl₂ using 0.015 mmol of Brønsted acid as initiator. ^a [monomer]/[initiator] ratio. ^b *M_n* calc = [M]:[I] x FW(monomer). The end group is not included in the calculation. ^c Absolute molecular weights were determined using laser light scattering gel permeation chromatography (GPC-LLS); differential refractive index (*dn/dc*) of polystyrene used is 0.185 mL g⁻¹; (*dn/dc*) of poly(α -methylstyrene) used is 0.174 mL g⁻¹; (*dn/dc*) of polyisoprene used is 0.129 mL g⁻¹. ^d Dispersity (Đ = *M_w*/*M_n*), where *M_w* is the weight-average molar mass and *M_n* is the number average molar mass. ^e Not determined.

2.2.5 Summary

In this chapter, two solid Brønsted acids have been synthesized, characterized and evaluated as single component initiators for cationic olefin polymerization. By reacting NbCl₅ with different amounts of tetrachlorocatechol, two different hexacoordinate niobium(V) anions can be cleanly isolated: H(OEt₂)₂[2.1] and H(OEt₂)₂[2.2]. H(OEt₂)₂[2.1] was characterized by ¹H NMR spectroscopy and ESI-MS, and shown to initiate the cationic polymerization of *n*-butyl vinyl ether and styrene at low temperatures. However, the molecular weight of the isolated polystyrene was low. H(OEt₂)₂[2.2] was characterized by ¹H and ¹³C{¹H} NMR spectroscopy, mass spectrometry and X-ray crystallography. The molecular structure shows two bidentate ligands and two bound in a monodentate fashion with *cis* configuration. This solid Brønsted acid is a highly effective initiator for a range of olefin monomers (*n*-butyl vinyl ether, styrene, α -methylstyrene, and

isoprene). At low temperatures, H(OEt₂)₂[**2.2**] produced poly(*n*-butyl vinyl ether) with a molecular weight close to the calculated molecular weight, and low dispersity. Polystyrene was successfully polymerized using temperatures as low as -50 °C. At temperatures below this, high molecular weight polymers were isolated, but there was a significant reduction in yield. High molecular weight syndiotactic rich poly(α -methylstyrene) was also produced with low dispersities and moderate yields at low temperatures. Although only low molecular weight oligoisoprene was isolated upon initiation with H(OEt₂)₂[**2.2**], this is a success due to the challenging nature of cationic isoprene polymerization.

2.3 Experimental

2.3.1 General Procedures

All experiments were performed using standard Schlenk or glove box techniques under nitrogen atmosphere. CH₂Cl₂ and Et₂O were deoxygenated with nitrogen and dried by passing through a column containing activated alumina. CH₂Cl₂ (Sigma Aldrich), Et₂O (Fisher Scientific), *n*-butyl vinyl ether (Sigma Aldrich), styrene (Sigma Aldrich), α -methylstyrene (Sigma Aldrich) and isoprene (Sigma Aldrich) were dried over calcium hydride, distilled and freeze-pump-thaw (x3) degased prior to use. CH₂Cl₂ and Et₂O were stored over molecular sieves prior to use. Niobium pentachloride (Sigma Aldrich) was used without further purification. Tetrachlorocatechol was prepared following a literature procedure,¹²² azeotropically distilled and recrystallized from hot toluene prior to use.

NMR spectra, mass spectrometry, elemental analysis, X-ray crystallography, GPC analysis, and differential scanning calorimetry were all performed in the Chemistry Department Facilities. ¹H and ¹³C{¹H} NMR spectrum were recorded at ambient temperatures unless otherwise

stated on Bruker Avance 400 MHz and referenced to deuterated solvents. Different cooling baths were used to cool the polymerizations (0°C = ice/ H_2O ; -15°C = ethylene glycol/ CO_2 ; -42°C = acetonitrile/ N_2 ; -50°C = $\text{CaCl}_{2(\text{aq})}$ / N_2 ; -78°C = acetone/ CO_2 ; -84°C = ethyl acetate/ N_2). Triple detection gel permeation chromatography (GPC-LLS) was used to determine the molecular weights of the polymers. An Agilent 1260 Series standard autosampler, an Agilent 1260 series isocratic pump, Phenomenex Phenogel 5 μm narrowbore columns (4.6 x 300 mm) 10^4 Å (5000-500,000), 500 Å (1,000-15,000) and 10^3 Å (1,000-75,000) Wyatt Optilab rEx differential refractometer ($\lambda = 658$ nm, 25°C), Wyatt tristar miniDAWN (laser light scattering detector ($\lambda = 690$ nm)), and a Wyatt ViscoStar viscometer were utilized. Samples were dissolved in THF (*ca.* 2 mg mL^{-1}) and a flow rate of 0.5 mL min^{-1} was applied. The differential refractive index of poly(*n*-butyl vinyl ether) was previously calculated ($dn/dc = 0.068$ mL g^{-1}) using Wyatt ASTRA software 6.1 assuming 100% mass recovery.¹⁴⁶ The differential refractive indices of polystyrene ($dn/dc = 0.185$ mL g^{-1}), poly(α -methylstyrene) ($dn/dc = 0.174$ mL g^{-1})¹⁸⁹, and polyisoprene ($dn/dc = 0.129$ mL g^{-1})¹⁹⁰ have been reported.

2.3.2 X-ray Structure Determination

X-ray crystallography data were collected on a Bruker X8 APEX II diffractometer with graphite-monochromated Mo $K\alpha$ radiation. A single crystal was immersed in oil and mounted on a glass fibre. Data were collected and integrated using the Bruker SAINT software package and corrected for absorption effect using SADABS.^{191, 192} All structures were solved by direct methods and subsequent Fourier difference techniques. All non-hydrogen atoms were refined anisotropically. All C–H hydrogen atoms were placed in calculated positions. All O–H hydrogens

were placed in calculated positions. All refinements were performed using the SHELXL-2015 via the Olex2 interface.^{193, 194}

Table 2.4 Crystallographic parameters for H(OEt)₂[2.2].

Empirical formula	C₃₂H₂₂Cl₁₆NbO₁₀
Formula weight	1226.60
Temperature/K	100(2)
Crystal system	Monoclinic
Space group	P2 ₁ /c
a/Å	10.2408(12)
b/Å	29.229(3)
c/Å	15.6110(16)
α/°	90
β/°	108.806(3)
γ/°	90
Volume/Å³	4423.4(9)
Z	4
ρ_{calc} g/cm³	1.842
μ/mm⁻¹	1.292
F(000)	2428.0
Crystal size/mm³	0.26 × 0.12 × 0.1
Radiation	MoKα (λ = 0.71073)
2θ range for data collection/°	2.786 to 45.592
Reflections collected	5705
Independent reflections	5705 [R _{int} = 0.106, R _{sigma} = 0.0784]
Data/restraints/parameters	5705/1103/634
Goodness-of-fit on F²	1.082
Final R indexes [I ≥ 2σ (I)]	R ₁ = 0.1205, wR ₂ = 0.2629
Final R indexes [all data]	R ₁ = 0.1640, wR ₂ = 0.2792

2.3.3 Differential Scanning Calorimetry

The glass transition temperatures (T_g) of samples were measured on a Netzsch DSC 214 *Polyma* at a heating rate of 10K/min. The T_g of samples was recorded after the second cycle of heating to remove the previous thermal history of the sample. The DSC instrument was calibrated at heating rates of 5, 10 and 20 K min⁻¹ using: adamantane, indium, tin, bismuth and caesium chloride.

2.3.4 Synthesis of H(OEt₂)₂[2.1]

NbCl₅ (0.254 g, 0.940 mmol) was stirred in anhydrous CH₂Cl₂ (8 mL) and the yellow suspension was slowly heated to reflux under N₂ atmosphere. In another Schlenk flask, tetrachlorocatechol (0.767 g, 3.09 mmol) was prepared in warm anhydrous CH₂Cl₂ (6 mL) and the bright orange-red solution was added via cannula to the refluxing NbCl₅ suspension to afford a dark red reaction mixture. The reaction mixture was refluxed for 100 minutes and cooled to ambient temperature. Upon addition of Et₂O (20 mL), a dark red clear solution formed. The solvent was removed under a reduced pressure at 0 °C. The solid was collected by filtration, washed with CH₂Cl₂ (2 mL) and dried *in vacuo*. Yield = (0.419 g, 0.428 mmol, 41%) ¹H NMR (400 MHz, CD₂Cl₂, 25 °C): δ = 3.76 (broad, 8H, CH₂CH₃), 1.24 ppm (broad, 12H, CH₂CH₃). ¹H NMR (400 MHz, CD₂Cl₂, -80 °C): δ = 16.73 (s, 1H, H(Et₂O)₂), 4.08 (³J_{HH} = 4.87, q, 4H, CH₂CH₃), 1.44 ppm (³J_{HH} = 6.59, t, 6H, CH₂CH₃). ESI-MS(-ve) = 830.3, 1078.1 *m/z*.

2.3.5 Representative procedure for H(OEt₂)₂[2.1]-initiated polymerization of *n*-butyl vinyl ether

In a glovebox, freshly distilled, degassed CH₂Cl₂ (2 mL) was added to H(OEt₂)₂[2.1] (0.015 g, 0.015 mmol) in a Schlenk flask. The flask was removed from the glovebox and cooled to -78 °C. Freshly distilled, *n*-butyl vinyl ether (0.61 g, 6.1 mmol) was prepared in a syringe, removed from the glovebox and added rapidly to the initiator solution. After 15 min, the reaction was quenched with a solution of NH₄OH in MeOH (0.2 mL, 10 vol%), and all volatiles were removed *in vacuo*. The crude product was dissolved in CH₂Cl₂ (2 mL) and added one drop at a time to stirred MeOH (40 mL) to precipitate a colourless oily

residue. The polymer was collected by centrifugation and dried *in vacuo*. The isolated material was analyzed by GPC. Yield = (0.47 g, 76%).

2.3.6 Representative procedure for H(OEt₂)₂[2.1]-initiated polymerization of styrene

In a glovebox, freshly distilled, degassed CH₂Cl₂ (2 mL) was added to H(OEt₂)₂[2.1] (0.015 g, 0.015 mmol) in a Schlenk flask. The flask was removed from the glovebox and cooled to -78 °C. Freshly distilled, styrene (0.64 g, 6.1 mmol) was prepared in a syringe, removed from the glovebox and added rapidly to the initiator solution. After 15 min, the reaction was quenched with a solution of NH₄OH in MeOH (0.2 mL, 10 vol%), and all volatiles were removed *in vacuo*. The crude product was dissolved in CH₂Cl₂ (2 mL) and added one drop at a time to stirred MeOH (40 mL) to precipitate a white solid residue. The polymer was collected by centrifugation and dried *in vacuo*. The isolated material was analyzed by GPC. Yield = (0.45 g, 71%).

2.3.7 Synthesis of H(OEt₂)₂[2.2]

NbCl₅ (0.134 g, 0.496 mmol) was stirred in anhydrous CH₂Cl₂ (6 mL) and the yellow suspension was slowly heated to reflux under N₂ atmosphere. In another Schlenk flask, tetrachlorocatechol (0.531 g, 2.14 mmol, 4.3 equivalents) was prepared in warm anhydrous CH₂Cl₂ (6 mL) and the bright orange-red solution was added via cannula to the refluxing NbCl₅ solution to afford a dark red reaction mixture. The reaction mixture was refluxed for 100 min and cooled to ambient temperature. Upon addition of excess Et₂O (20 mL), a dark red clear solution formed. The solution was cooled in an ice bath, and concentrated by half, which afforded an off-white precipitate. The solid was collected by filtration, washed with CH₂Cl₂ (2 mL) and dried *in vacuo*.

Yield = (0.246 g, 0.200 mmol, 40%). ^1H NMR (400 MHz, CD_2Cl_2 , 25 °C): δ = 8.97 (broad, 1H, OH), 3.87 ($^3J_{\text{HH}}$ = 6.71 Hz, q, 8H, CH_2CH_3), 1.29 ppm ($^3J_{\text{HH}}$ = 6.71 Hz, t, 12H, CH_2CH_3). ^1H NMR (400 MHz, CD_2Cl_2 , -80 °C): δ = 16.61 (s, 1H, $\text{H}(\text{Et}_2\text{O})_2$), 9.42 (s, 1H, OH), 3.97 ($^3J_{\text{HH}}$ = 7.38, q, 8H, CH_2CH_3), 1.29 ppm ($^3J_{\text{HH}}$ = 6.72, t, 12H, CH_2CH_3). ^{13}C NMR (101 MHz, CD_2Cl_2 , 25 °C): δ = 150.7 (s, Ar-C), 147.2 (s, Ar-C), 144.7 (s, Ar-C), 140.1 (s, Ar-C), 125.6 (s, Ar-C), 123.2 (s, Ar-C), 121.4 (s, Ar-C), 119 (s, Ar-C), 115.6 (s, Ar-C), 70.5 (s, OCH_2), 13.5 (s, CH_3). A concentrated solution of $\text{H}(\text{OEt}_2)_2[2.2]$ in CD_2Cl_2 (-30°C) afforded a colourless crystal suitable for diffraction. A single crystal was removed for single crystal X-ray diffraction without drying.

2.3.8 Representative procedure for $\text{H}(\text{OEt}_2)_2[2.2]$ -initiated polymerization of *n*-butyl vinyl ether

In a glovebox, freshly distilled, degassed CH_2Cl_2 (2 mL) was added to $\text{H}(\text{OEt}_2)_2[2.2]$ (0.013 g, 0.011 mmol) in a Schlenk flask. The flask was removed from the glovebox and cooled to -78 °C. Freshly distilled, *n*-butyl vinyl ether (0.42 g, 4.3 mmol) was prepared in a syringe, removed from the glovebox and added rapidly to the initiator solution. After 15 min, the reaction was quenched with a solution of NH_4OH in MeOH (0.2 mL, 10 vol%), and all volatiles were removed *in vacuo*. The crude product was dissolved in CH_2Cl_2 (2 mL) and added one drop at a time to stirred MeOH (40 mL) to precipitate a colourless oily residue. The polymer was collected by centrifugation and dried *in vacuo*. The isolated material was analyzed by ^1H NMR spectroscopy (400 MHz, CDCl_3 , 25 °C): δ = 3.67-3.31 (br, $\text{CH}_2\text{CH}(\text{O}(\text{CH}_2)_3\text{CH}_3)\text{CH}_2$), 1.92-1.31 (br, $\text{OCH}_2\text{CH}_2\text{CH}_2$), 0.94 (t, CH_3), DSC and GPC. Yield = (0.35 g, 94%).

2.3.9 Representative procedure for H(OEt₂)₂[2.2]-initiated polymerization of styrene

In a glovebox, freshly distilled, degassed CH₂Cl₂ (2 mL) was added to H(OEt₂)₂[2.2] (0.010 g, 0.0081 mmol) in a Schlenk flask. The flask was removed from the glovebox and cooled to -50 °C. Freshly distilled, styrene (0.33 g, 3.3 mmol) was prepared in a syringe, removed from the glovebox and added rapidly to the initiator solution. After 15 min, the reaction was quenched with a solution of NH₄OH in MeOH (0.2 mL, 10 vol%), and all volatiles were removed *in vacuo*. The crude product was dissolved in CH₂Cl₂ (2 mL) and added one drop at a time to stirred MeOH (40 mL) to precipitate a white solid residue. The polymer was collected by centrifugation and dried *in vacuo*. The isolated material was analyzed by ¹H NMR spectroscopy (400 MHz, CDCl₃, 25 °C): δ = 7.23-6.31 (br, Ar-*H*), 2.14-1.72 (br, CH), 1.66-1.31(br, CH₂), DSC and GPC. Yield = (0.02 g, 6%).

2.3.10 Representative procedure for H(OEt₂)₂[2.2]-initiated polymerization of α-methylstyrene

In a glovebox, freshly distilled, degassed CH₂Cl₂ (2 mL) was added to H(OEt₂)₂[2.2] (0.009 g, 0.007 mmol) in a Schlenk flask. The flask was removed from the glovebox and cooled to -78 °C. Freshly distilled, α-methylstyrene (0.35 g, 3.0 mmol) was prepared in a syringe, removed from the glovebox and added rapidly to the initiator solution. After 15 min, the reaction was quenched with a solution of NH₄OH in MeOH (0.2 mL, 10 vol%), and all volatiles were removed *in vacuo*. The crude product was dissolved in CH₂Cl₂ (2 mL) and added one drop at a time to stirred MeOH (40 mL) to precipitate a white solid residue. The polymer was collected by centrifugation and dried *in vacuo*. The isolated material was analyzed by ¹H NMR spectroscopy (400 MHz, CDCl₃, 25 °C): δ = 7.30-6.81

(br, Ar-H), 1.89-1.40 (br, $\text{CH}_2\text{CH}_2\text{CH}(\text{Ar-H})\text{CH}_3$), 0.26-0.14 (br, $\text{CH}_3\text{CH}(\text{Ar-H})\text{CH}_2\text{CH}_2$), DSC and GPC. Yield = (0.068 g, 19%).

2.3.11 Representative procedure for $\text{H}(\text{OEt}_2)_2[2.2]$ -initiated polymerization of isoprene

In a glovebox, freshly distilled, degassed CH_2Cl_2 (2 mL) was added to $\text{H}(\text{OEt}_2)_2[2.2]$ (0.010 g, 0.0081 mmol) in a Schlenk flask. The flask was removed from the glovebox and cooled to -50°C . Freshly distilled, isoprene (0.22 g, 3.3 mmol) was prepared in a syringe, removed from the glovebox and added rapidly to the initiator solution. After 15 min, the reaction was quenched with a solution of NH_4OH in MeOH (0.2 mL, 10 vol%), and all volatiles were removed *in vacuo*. The crude product was dissolved in CH_2Cl_2 (2 mL) and added one drop at a time to stirred MeOH (40 mL) to precipitate a white solid residue. The polymer was collected by centrifugation and dried *in vacuo*. The isolated material was analysed by ^1H NMR spectroscopy (400 MHz, CDCl_3 , 25°C): $\delta = 5.13$ (br, 1,4-unit CH), 5.0-4.8 (br, 1,2-unit CH_2), 4.8-4.6 (br, 3,4-unit CH_2), 2.1-1.9 (br, 1,4-unit CH_2), 1.61 (br, 1,4-unit CH_3), and GPC. Yield = (0.006 g, 3%).

Chapter 3: Hexacoordinate Perfluorinated Weakly Coordinating Anions

Using Group 5 Metals as Solid Brønsted Acids as Cationic Initiators for Olefin Polymerization

3.1 Introduction

The optimal Coulombic interaction between the cation and anion of a solid Brønsted acid allows the isolation of a highly effective single component initiator for cationic olefin polymerization. If the interaction between the cation and anion is too strong, termination will occur resulting in low molecular weight polymers and oligomers. Conversely, if the interaction is too weak, side reactions such as chain transfer processes will occur, resulting in broader dispersities and ultimately premature termination. Weakly coordinating anions (WCAs) are commonly used as counterions, allowing access to high molecular weight polymers, with low dispersity.

A key feature in the development WCAs is the incorporation of electron-withdrawing substituents, like halogens. These functionalities distribute electron density over the entire anion, reducing the electrostatic interaction between the cation and anion. Classical WCAs, for example $[\text{BF}_4]^-$ and $[\text{PF}_6]^-$, demonstrate this ideology.⁶⁹ Progression of WCAs in the search for the least coordinating anion has led to a higher proportion of halogens in an anion, and greater steric bulk as a beneficial side effect. Of particular note, is $[\text{B}(\text{Ar}_\text{F})_4]^-$, e.g. $[\text{B}\{3,5\text{-(CF}_3)_2\text{C}_6\text{H}_3\}_4]^-$,⁶⁸ which has been used to stabilize a number of highly reactive cations including $[\text{H}(\text{OEt}_2)_2]^+$.¹⁴⁰ To be an active initiator for the cationic polymerization of olefins, a protic moiety like $[\text{H}(\text{OEt}_2)_2]^+$ is necessary.^{63, 140} Similar Brønsted acids have been previously studied for the cationic polymerization of vinyl monomers, and shown to be efficient single component initiators.^{63, 140, 141,}

Traditionally WCAs contain a Group 13 element, however this group form solely four-coordinate anions. By replacing the Group 13 element with a main group element that can bind six substituents, an anion with greater steric bulk can be isolated. Hexacoordinate phosphorus(V) anions based on $[\text{PF}_6]^-$ exhibit a weakly coordinating nature, with strong Brønsted acids isolated and shown to initiate cationic olefin polymerization.^{64, 65, 67, 143} To increase steric bulk further, Group 5 metals have been investigated to a lesser extent. Additionally, stronger M-O bonds can be formed,¹³³ to improve anion stability. There are few examples of Group 5 metals with highly fluorinated ligands as WCAs, most notably $[\text{M}(\text{OC}(\text{CF}_3)_2\text{H})_6]^-$ (M = Nb, Ta) by Krossing et al. (Figure 3.1).^{136, 196} However, the corresponding Brønsted acids have not been isolated, nor investigated as initiators for polymerization. Non-fluorinated Group 5 WCAs have been isolated, but investigation into the single component initiator behaviour is rare.^{113, 150, 157-163} $\text{NbCl}_4(1,2\text{-O}_2\text{C}_3\text{H}_6)/\text{MAO}$ has been reported as a binary initiator for ethylene polymerization, which follows a metal-mediated polymerization mechanism.¹⁹⁷ To the best of our knowledge, the only Group 5 containing complex studied as a single component initiator is $[\text{Ph}_3\text{C}][\text{TaF}_6]$.¹³⁷

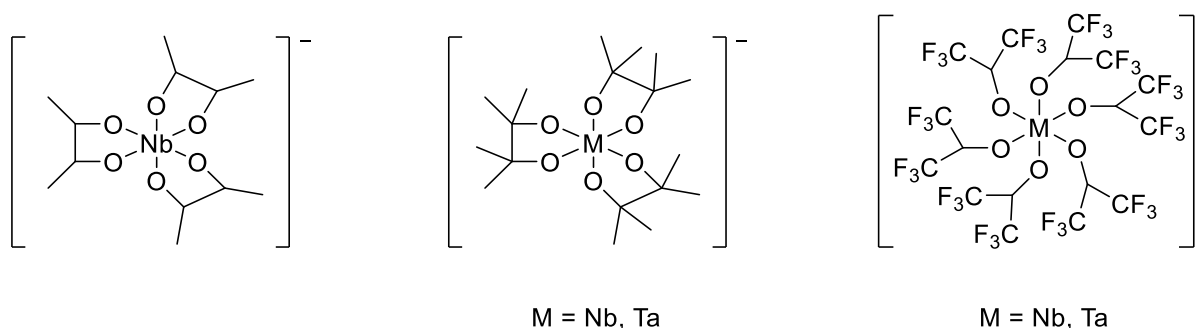


Figure 3.1 Examples of Group 5 WCAs.

We wanted to develop a Brønsted acid using the successful diethyl ether cation,^{63, 64, 140} with a perfluorinated anion, containing a Group 5 metal. The desire to have highly fluorinated chelating ligands brought one compound to forefront. First synthesized at Dupont in the 1960s, perfluoropinacol is a fully fluorinated diol, and has been shown to successfully coordinate in a

bidentate fashion to a variety of metals in mixed ligand complexes (Ni^{2+} , Pd^{2+} , Pt^{2+} , Cu^{2+}), although these have not been structurally characterized.¹⁹⁸⁻²⁰⁰

The attempts to synthesize two Brønsted acids by reaction of perfluoropinacol with niobium(V) and tantalum(V) are discussed. Upon isolation, the reaction with various olefin monomers has been studied: *n*-butyl vinyl ether; styrene; α -methylstyrene; and isoprene. Both Brønsted acids initiate the aforementioned monomers to give polymers. When *n*-butyl vinyl ether is polymerized at low temperatures, the polymer is isolated in high yields with high molecular weights and narrow dispersities. Polystyrene and poly(α -methylstyrene) are both collected with high molecular weights in moderate yields. Isoprene was successfully polymerized and isolated with low molecular weights.

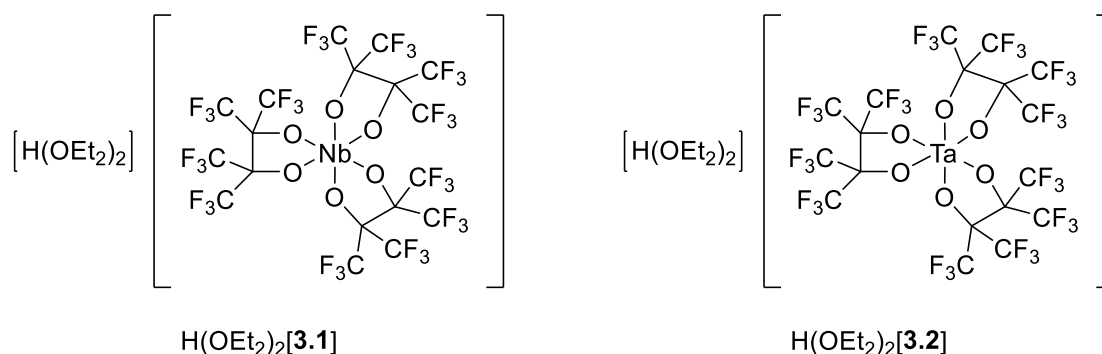


Figure 3.2 Brønsted acids $\text{H}(\text{OEt}_2)_2[3.1]$ and $\text{H}(\text{OEt}_2)_2[3.2]$.

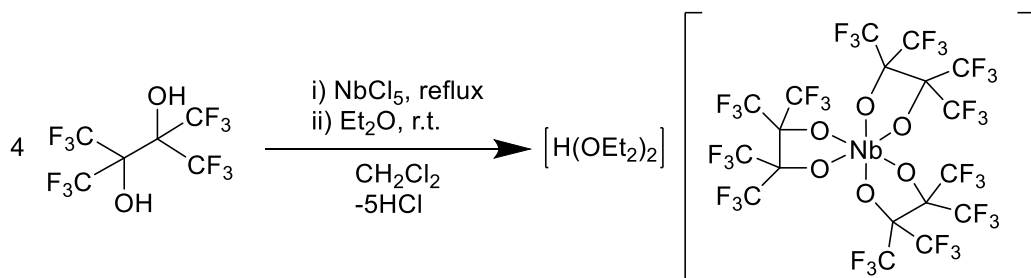
3.2 Results and discussion

3.2.1 Synthesis of $\text{H}(\text{OEt}_2)_2[3.1]$

The reaction of perfluoropinacol, with two Group 5 metal chlorides was investigated. Niobium pentachloride and tantalum pentachloride were selected as suitable reagents, since they have been shown to work in similar syntheses. Vanadium is prone to redox chemistry and may pose a greater synthetic challenge, and therefore was not attempted. Extreme care must be taken

when handling perfluoropinacol and products; it has been reported that the compound is highly toxic.²⁰¹⁻²⁰³

A solution of perfluoropinacol (4 equivs) in CH₂Cl₂ was added to refluxing niobium pentachloride in CH₂Cl₂, before the addition of excess diethyl ether after cooling to ambient temperature. An off-white precipitate was isolated in moderate yield (50%) and characterized. Four equivalents were added to ensure full reaction.



Scheme 3.1 Synthesis of Brønsted acid H(OEt₂)₂[**3.1**].

The isolated solid was characterized by ¹H and ¹⁹F{¹H} NMR spectroscopy and mass spectrometry. At ambient temperature, the ¹H NMR spectrum showed two signals corresponding to two diethyl ether molecules ($\delta = 4.03$, 8H, OCH₂CH₃; 1.41, 12H, OCH₂CH₃). At lower temperatures (-85 °C), a downfield shifted resonance was observed at 16.68 ppm. This is diagnostic of an acidic proton in the proposed cation, [H(OEt₂)₂]⁺. Other similar systems with the same cation have shown resonances in a similar region [H(OEt₂)₂[Nb(1,2-C₆O₂Cl₄)₃] {H(OEt₂)₂[**2.1**], Chapter 2} (T = -85 °C, CD₂Cl₂; $\delta = 16.69$ ppm, H); H(OEt₂)₂[Ta(1,2-C₆O₂Cl₄)₃] (T = -85 °C, CD₂Cl₂; $\delta = 16.74$ ppm, H);¹⁴⁶ and H(OEt₂)₂[P(1,2-C₆O₂Cl₄)₃] (T = -85 °C, CD₂Cl₂; $\delta = 16.70$ ppm, H).⁶⁴ Although four equivalents of perfluoropinacol were added, no pendant OH protons were observed. The formation of H(OEt₂)₂[**3.1**] was consistent with the spectrum obtained by ESI-MS in negative ion mode which showed a single signal at 1088.6 *m/z*. No signals were observed at 1422.80 *m/z*, the calculated mass of a niobium(V) anion with four ligands. Due to the

perfluorinated groups on the ligand, it is expected that the diol protons are highly acidic. The steric bulk of the perfluoropinacol ligands, with consideration of the acidity of the ligands, are hypothesized to be reasons it is not possible to form a more substituted anion.

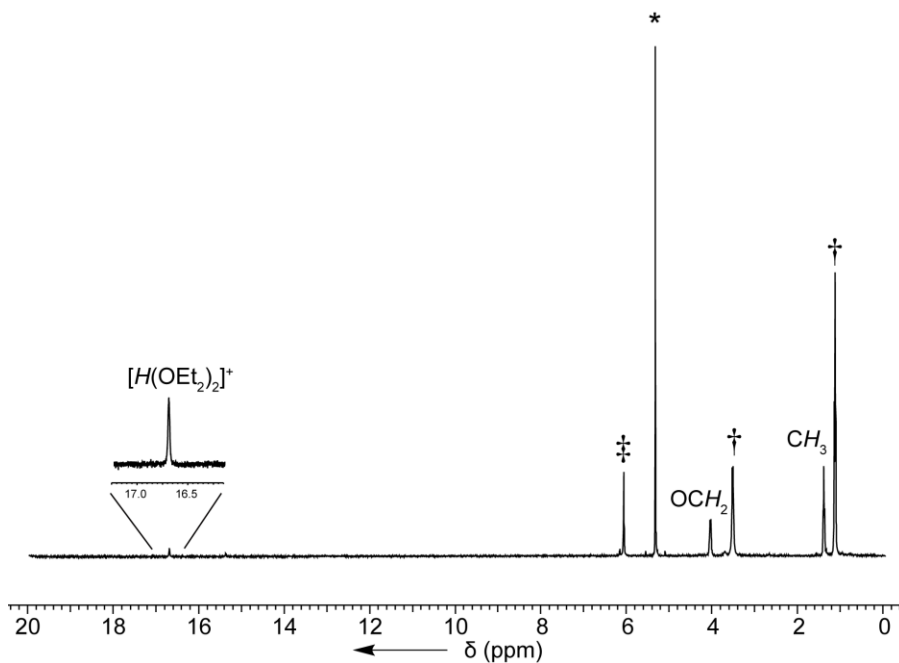


Figure 3.3 ^1H NMR (400 MHz, CD_2Cl_2 , $-85\text{ }^\circ\text{C}$) spectrum of $\text{H}(\text{OEt}_2)_2[3.1]$. * indicates residual NMR solvent, † indicates free diethyl ether solvent, ‡ unassigned signal.

At ambient temperature the $^{19}\text{F}\{^1\text{H}\}$ NMR spectrum shows three signals between -67 and -71 ppm. After cooling, the two small peaks broaden and split and the large sharp peak [$T = 25\text{ }^\circ\text{C}$, $\delta = -70.23$ ppm; $T = -85\text{ }^\circ\text{C}$, $\delta = -70.23$ ppm] remains. Although no internal standard was used, this could be mistaken for leftover starting material, perfluoropinacol [$T = 25\text{ }^\circ\text{C}$, $\delta = -70.69$ ppm]. However, no OH signal that would also be present from the unbound diol is observed in the ^1H NMR spectrum. It is possible the anion is switching between conformations, or other fluxional process such as disassociation and re-coordination of the ligand in the solution state. It therefore requires further investigation into the cause of these inequivalent fluorine atoms.

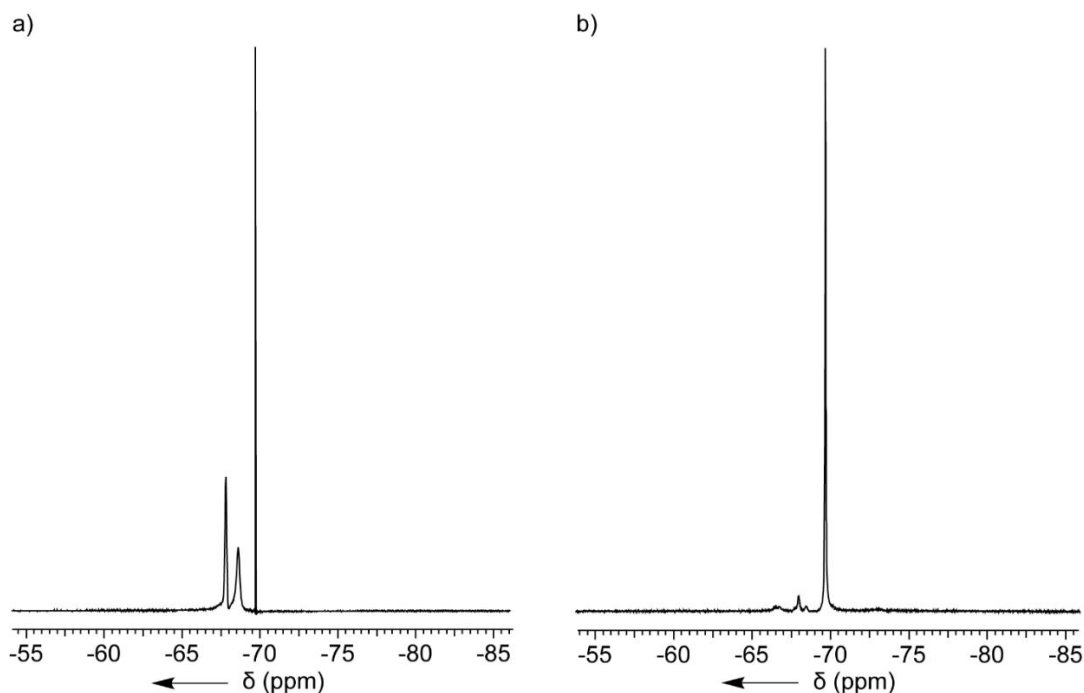
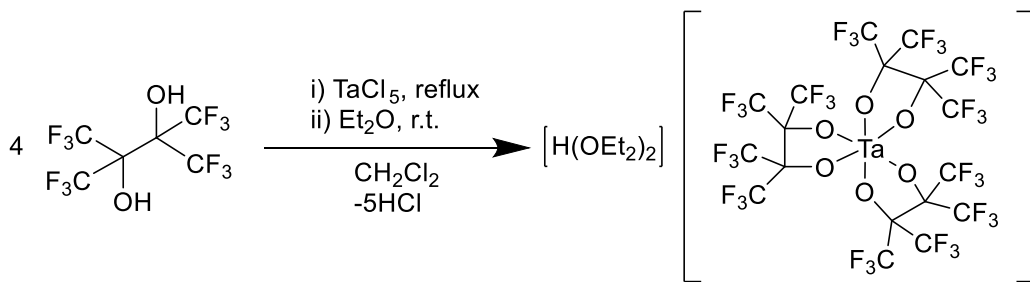


Figure 3.4 $^{19}\text{F}\{^1\text{H}\}$ NMR (376 MHz, CD_2Cl_2) spectrum of $\text{H}(\text{OEt}_2)_2[3.1]$ at a) 25 °C, and b) -85 °C.

3.2.2 Synthesis of $\text{H}(\text{OEt}_2)_2[3.2]$

Following the successful synthesis of the hexacoordinate niobium(V) anion with perfluoropinacol, the same reaction pathway was followed to attempt the equivalent tantalum(V) anion. A solution of perfluoropinacol (4 equivs) in CH_2Cl_2 was added to a solution of tantalum pentachloride in CH_2Cl_2 at reflux. Upon cooling to ambient temperature, excess diethyl ether was added, leading to a precipitation and isolation of a white solid in a moderate yield (50%).



Scheme 3.2 Synthesis of $\text{H}(\text{OEt}_2)_2[3.2]$.

Upon analysis of the ^1H NMR spectrum at ambient temperature, two resonances were observed corresponding to the two diethyl ether molecules present in the cation [$\delta = 4.00, 8\text{H}, \text{OCH}_2\text{CH}_3; 1.40, 12\text{H}, \text{OCH}_2\text{CH}_3$]. No broad peaks that could be assigned to OH signals were observed, as with $\text{H}(\text{OEt}_2)_2[\mathbf{3.1}]$. After cooling to $-85\text{ }^\circ\text{C}$, the signal intensity versus residual solvent decreased, due to the poor solubility of $\text{H}(\text{OEt}_2)_2[\mathbf{3.2}]$; there was a large amount of precipitation present afterwards. Despite this, a sharp signal at 16.71 ppm can be assigned to the acidic proton present in the cation moiety, $[\text{H}(\text{OEt}_2)_2]^+$. Other oxonium cations with diethyl ether show a resonance for the acidic proton in a similar range.^{63, 64, 77, 140, 146} As a result of the poor solubility of the Brønsted acid in a deuterated solvent at a sufficiently low temperature for clear elucidation of peaks, it was not possible to obtain a $^{13}\text{C}\{^1\text{H}\}$ NMR spectrum. However, an ESI-MS spectrum in negative ion mode was obtained. The spectrum showed a clear signal 1176.6 m/z , clearly indicating a tantalum(V) centre with three perfluoropinacol ligands.

$\text{H}(\text{OEt}_2)_2[\mathbf{3.2}]$ gave a similar $^{19}\text{F}\{^1\text{H}\}$ NMR spectrum (Figure 3.6) as $\text{H}(\text{OEt}_2)_2[\mathbf{3.1}]$, providing further evidence that there is some fluxional process occurring that is affecting the equivalencies of the fluorine atoms in the perfluoropinacol ligand. This requires further investigation.

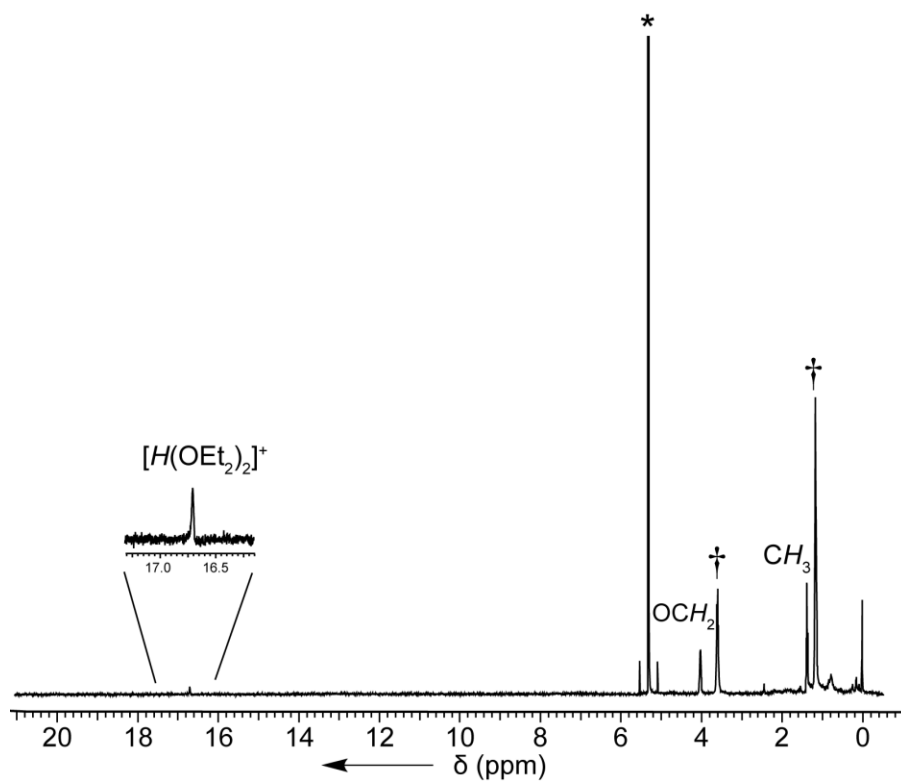


Figure 3.5 ^1H NMR (400 MHz, CD_2Cl_2 , $-85\text{ }^\circ\text{C}$) spectrum of $\text{H}(\text{OEt}_2)_2[3.2]$. * indicates residual NMR solvent,

† indicates free diethyl ether solvent.

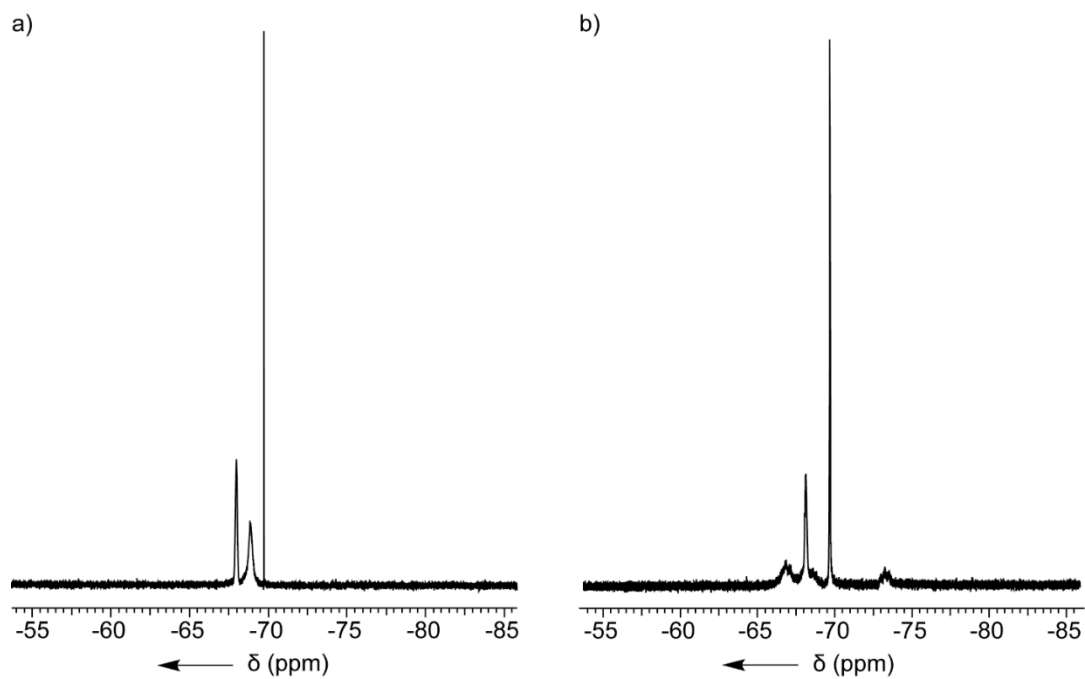


Figure 3.6 $^{19}\text{F}\{^1\text{H}\}$ NMR (376 MHz, CD_2Cl_2) spectrum of $\text{H}(\text{OEt}_2)_2[3.2]$ at a) $25\text{ }^\circ\text{C}$, and b) $-85\text{ }^\circ\text{C}$.

Metrical Parameters of H(OEt₂)₂[**3.2**]

A single crystal suitable for X-ray diffraction was obtained from a concentrated solution of crude H(OEt₂)₂[**3.2**] in 1,2-difluorobenzene under nitrogen atmosphere at -30°C. The molecular structure is consistent with NMR spectroscopy and mass spectrometry and shows a *tris*-perfluoropinacolate complex (Figure 3.5).

Surprisingly, the molecular structure of H(OEt₂)₂[**3.2**] exhibits a distorted trigonal prismatic geometry indicated by the bond angles between the chelating ligands [O(1)-Ta(1)-O(2) = 75.75(7)°; O(3)-Ta(1)-O(4) = 76.01(7)°; O(5)-Ta(1)-O(6) = 75.87(7)°]. The group of Donat reported a tantalum(V) pinacolate anion with trigonal prismatic geometry.¹³⁵ Trigonal prismatic geometry is most commonly a result of a chelating ligand with a small bite angle.²⁰⁴ Additionally, ligand-ligand interactions such as sulfur-sulfur bonds in [M(S₂C₂R₂)₃] complexes,²⁰⁵⁻²⁰⁸ or very small σ -donor ligands in complexes like [Zr(CH₃)₆]²⁻²⁰⁹ can force a trigonal prismatic geometry. It is highly likely that the chelating ring is the cause of the distorted trigonal prismatic geometry in this anion, as the equivalent anion with monodentate ligands reported by Krossing has a distorted octahedral geometry.¹³⁶ Tantalum(V) has been found to be trigonal prismatic in [TaPh₆]⁻ and [Ta(CH₃)₆]⁻.²¹⁰ Only H(OEt₂)₂ Λ -[**3.2**] was seen, however as only one single crystal was taken for analysis, the Δ -isomer will also be present.

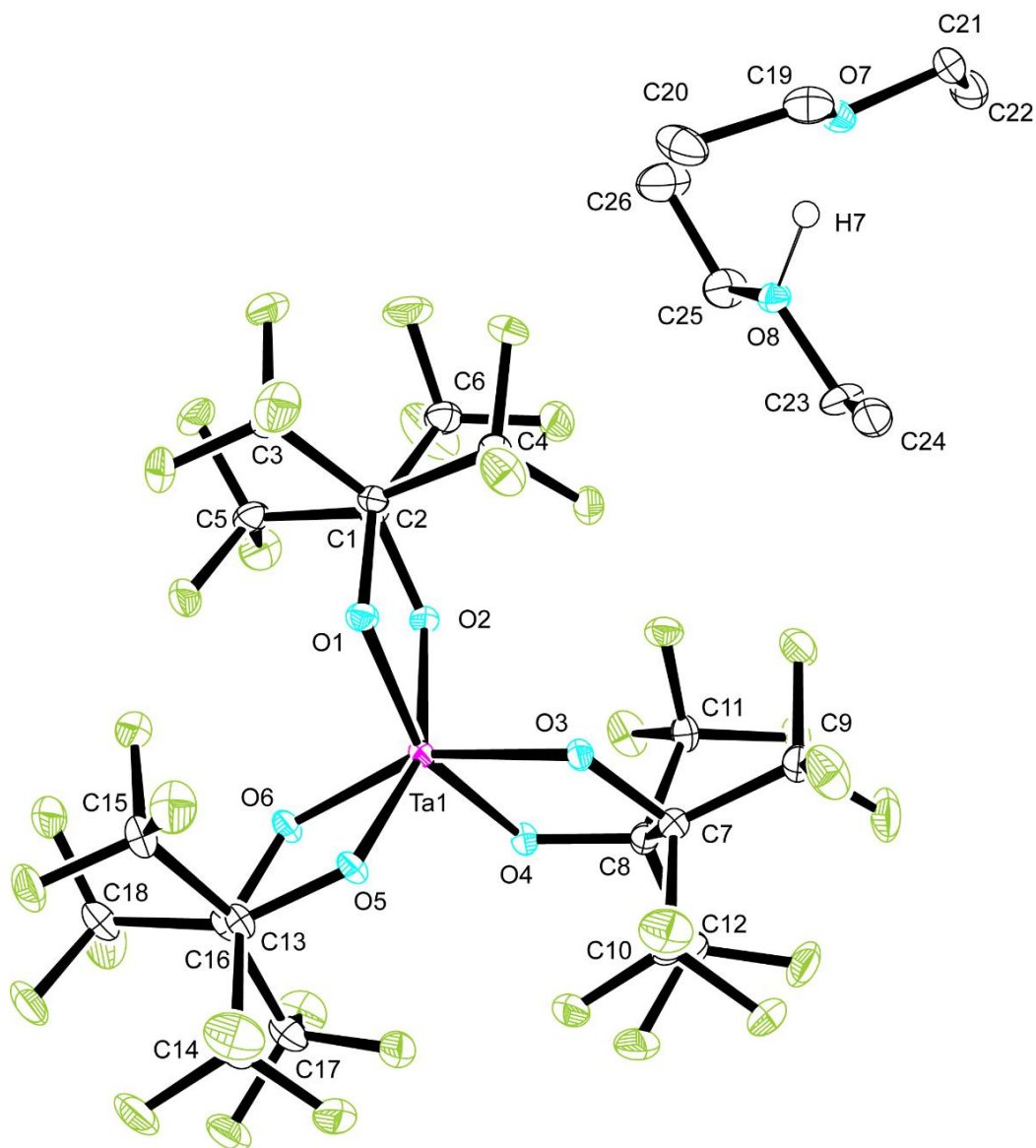


Figure 3.7 Molecular structure of $\text{H}(\text{OEt}_2)_2 \Lambda\text{-}[3.2]$. Ellipsoids are drawn at the 50% probability level.

Hydrogen atoms on the diethyl ether solvent molecules in the cation are omitted for clarity. Selected bond lengths (Å): Ta(1)-O(1) = 1.975(2); Ta(1)-O(2) = 1.974(2); Ta(1)-O(3) = 1.979(2); Ta(1)-O(4) = 1.975(2); Ta(1)-O(5) = 1.975(2); Ta(1)-O(6) = 1.978(2); O(7)-C(19) = 1.471(3); O(7)-C(21) = 1.461(3); O(8)-C(23) = 1.450(3); O(8)-C(25) = 1.456(3). Selected bond angles (°): O(1)-Ta(1)-O(2) = 75.75(7); O(1)-Ta(1)-O(4) = 157.72(7); O(2)-Ta(1)-O(5) = 156.88(7); O(3)-Ta(1)-O(4) = 76.01(7); O(3)-Ta(1)-O(6) = 154.76(7); O(5)-Ta(1)-O(6) = 75.87(7).

The Ta-O bond lengths in the anion range from 1.974(2) Å to 1.979(2) Å. The average Ta-O bond [avg. Ta-O = 1.976(4) Å] lies in between the average for Donat's unhalogenated analogue [avg. Ta-O = 1.94(2) Å]¹³⁵ and Krossing's complex featuring the monodentate hexafluoroisopropanol [avg. Ta-O_(2-coordinate) = 1.918 Å, avg. Ta-O_(3-coordinate) = 2.037 Å, avg. Ta-O = 2.005 Å]. Strong cation-anion interactions between the Li⁺ and oxygens in the anion were observed lengthening the Ta-O bonds.¹³⁶

The acidic proton in the cation moiety was located in the electron density map and refined isotropically. The proton is coordinated asymmetrically between the two diethyl ether oxygen atoms [O(8)⋯H(7) = 1.15(5) Å; O(7)⋯H(7) = 1.30(5) Å]. Both of the distances between the acidic proton and the ether molecules are within the van der Waals radii for oxygen and hydrogen [$r_{vdw} = 2.72\text{Å}$], as is the O⋯O distance [O(8)⋯O(7) = 2.444(3) Å; $r_{vdw} = 3.04\text{ Å}$].¹⁶⁶ Asymmetric coordination has been observed before with H(OEt₂)₂[P(1,2-O₂C₆Cl₄)₃]⁶⁴ and H(OEt₂)₂[Al{OC(CF₃)₃}]₄.⁵⁹ Deviations in the C–C bond lengths in the diethyl ether molecules in the cation can be seen as a result, this is demonstrated below.

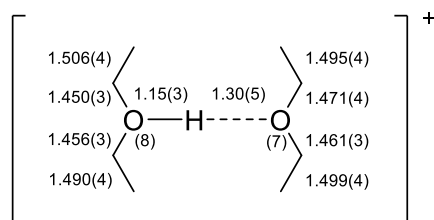


Figure 3.8 Metrical parameters [Å] for the cation in H(OEt₂)₂[3.2].

3.2.3 H(OEt₂)₂[3.1] and H(OEt₂)₂[3.2]-initiated polymerizations

The isolated Brønsted acids were tested with a range of monomers (*n*-butyl vinyl ether, styrene, α -methylstyrene and isoprene) to investigate their viability as single component initiators for cationic olefin polymerization. The results are shown in Tables 3.1 and 3.2. Both H(OEt₂)₂[3.1] and H(OEt₂)₂[3.2] were shown to be effective initiators for *n*-butyl vinyl ether, styrene, and α -methylstyrene, giving high molecular weight polymers. The polymerization with isoprene did not afford a high molecular weight polymer, but an oligomeric material.

Table 3.1 H(OEt₂)₂[3.1]-initiated polymerization of *n*-butyl vinyl ether, styrene, α -methylstyrene and isoprene. The results shown are representative of multiple runs.

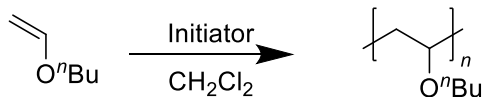
Entry	Monomer	Temp °C	[M]:[I] ^a	Yield %	<i>M_n</i> calc ^b g mol ⁻¹	<i>M_n</i> ^c g mol ⁻¹	Đ ^d
1	<i>n</i> -butyl vinyl ether	21	400	35	40 000	16 900	1.52
2	<i>n</i> -butyl vinyl ether	-78	400	70	40 000	35 600	1.21
3	<i>n</i> -butyl vinyl ether	-84	400	89	40 000	46 880	1.41
4	styrene	21	400	87	41 700	6 150	2.49
5	styrene	-50	400	75	41 700	7 880	2.90
6	styrene	-78	400	3	41 700	97 620	1.56
7	α -methylstyrene	0	400	3	47 200	3 450	1.47
8	α -methylstyrene	-50	400	44	47 200	6 130	2.42
9	α -methylstyrene	-78	400	35	47 200	231 400	1.46
10	isoprene	21	400	58	27 200	3 570	3.38
11	isoprene	-50	400	< 1	27 200	3 748	2.54

The polymerization was carried out in 2 mL CH₂Cl₂ using 0.015 mmol of Brønsted acid as initiator. ^a [monomer]/[initiator] ratio. ^b *M_n* calc = [M]:[I] x FW(monomer). The end group is not included in the calculation. ^c Absolute molecular weights were determined using laser light scattering gel permeation chromatography (GPC-LLS); differential refractive index (*dn/dc*) of poly(*n*-butyl vinyl ether) (*dn/dc* = 0.068 mL g⁻¹) in THF was calculated by assuming 100% mass recovery; (*dn/dc*) of polystyrene used is 0.185 mL g⁻¹; (*dn/dc*) of poly(α -methylstyrene) used is 0.174 mL g⁻¹; (*dn/dc*) of polyisoprene used is 0.129 mL g⁻¹. ^d Dispersity (Đ = *M_w*/*M_n*), where *M_w* is the weight-average molar mass and *M_n* is the number average molar mass.

Table 3.2 H(OEt)₂[3.2]-initiated polymerization of *n*-butyl vinyl ether, styrene, α -methylstyrene and isoprene. The results shown are representative of multiple runs.

Entry	Monomer	Temp °C	[M]:[I] ^a	Yield %	<i>M</i> _n calc ^b g mol ⁻¹	<i>M</i> _n c g mol ⁻¹	Đ ^d
1	<i>n</i> -butyl vinyl ether	21	348	44	34 800	17 010	1.62
2	<i>n</i> -butyl vinyl ether	0	353	33	35 300	19 550	1.63
3	<i>n</i> -butyl vinyl ether	-15	353	38	35 300	22 940	1.80
4	<i>n</i> -butyl vinyl ether	-42	348	32	34 800	26 000	1.47
5	<i>n</i> -butyl vinyl ether	-78	400	93	32 100	21 040	1.25
6	<i>n</i> -butyl vinyl ether	-84	400	96	40 000	46 630	1.29
7	<i>n</i> -butyl vinyl ether	-78	600	67	60 000	69 510	1.49
8	styrene	21	400	69	41 700	5 700	1.97
9	styrene	-50	400	68	41 700	84 560	1.51
10	styrene	-78	400	3	41 700	124 900	1.58
11	α -methylstyrene	21	400	0	47 200	n.d. ^e	n.d. ^e
12	α -methylstyrene	-50	400	41	47 200	6 992	2.25
13	α -methylstyrene	-78	400	19	47 200	169 000	1.46
14	isoprene	21	400	71	27 200	3 730	2.34
15	isoprene	-50	400	3	27 200	3 180	1.44
16	isoprene	-78	400	0	27 200	n.d. ^e	n.d. ^e

The polymerization was carried out in 2 mL CH₂Cl₂ using 0.015 mmol of Brønsted acid as initiator. ^a [monomer]/[initiator] ratio. ^b *M*_n calc = [M]:[I] x FW(monomer). The end group is not included in the calculation. Absolute molecular weights were determined using laser light scattering gel permeation chromatography (GPC-LLS); differential refractive index (*dn/dc*) of poly(*n*-butyl vinyl ether) (*dn/dc* = 0.068 mL g⁻¹) in THF was calculated by assuming 100% mass recovery; (*dn/dc*) of polystyrene used is 0.185 mL g⁻¹; (*dn/dc*) of poly(α -methylstyrene) used is 0.174 mL g⁻¹; (*dn/dc*) of polyisoprene used is 0.129 mL g⁻¹. ^d Dispersity (Đ = *M*_w/*M*_n), where *M*_w is the weight-average molar mass and *M*_n is the number average molar mass. ^e Not determined.



Scheme 3.3 H(OEt₂)₂[**3.1**] and H(OEt₂)₂[**3.2**]-initiated cationic polymerization of *n*-butyl vinyl ether.

Due to the resonance stabilized carbocationic intermediate of vinyl ethers, they are readily polymerizable.¹⁹ Both H(OEt₂)₂[**3.1**] and H(OEt₂)₂[**3.2**]-initiated polymerizations of *n*-butyl vinyl ether gave polymer upon initiation (entries 1-3, Table 3.1; entries 1-7, Table 2.3 respectively). Oily, brown residues of moderate molecular weight were isolated at ambient temperatures [H(OEt₂)₂[**3.1**], $M_n = 16\,900\text{ g mol}^{-1}$, $\mathcal{D} = 1.52$; H(OEt₂)₂[**3.2**], $M_n = 17\,010\text{ g mol}^{-1}$, $\mathcal{D} = 1.62$]. When polymerized at lower temperatures the molecular weight of the isolated colourless polymer was close to the calculated molecular weight, with high yields and low dispersities [H(OEt₂)₂[**3.1**], $T = -84\text{ }^\circ\text{C}$, yield = 89%, $M_n\text{ calc} = 40\,000\text{ g mol}^{-1}$, $M_n = 46\,880\text{ g mol}^{-1}$, $\mathcal{D} = 1.41$; H(OEt₂)₂[**3.2**], $T = -84\text{ }^\circ\text{C}$, yield = 96%, $M_n\text{ calc} = 40\,000\text{ g mol}^{-1}$, $M_n = 46\,630\text{ g mol}^{-1}$, $\mathcal{D} = 1.29$]. The polymerization data are consistent with that seen with H(OEt₂)₂[**2.2**] [$T = -84\text{ }^\circ\text{C}$, yield = 94%, $M_n\text{ calc} = 40\,000\text{ g mol}^{-1}$, $M_n = 52\,700\text{ g mol}^{-1}$, $\mathcal{D} = 1.62$] and other Brønsted acid initiating systems with *n*-butyl vinyl ether [H(OEt₂)₂[Ta(1,2-O₂C₆Cl₄)₂(1,2-OC₆Cl₄OH)₂], yield = 57 %, $M_n = 39\,100\text{ g mol}^{-1}$, $\mathcal{D} = 1.12$]; H(OEt₂)₂[P(1,2-O₂C₆Cl₄)₃], $T = -78\text{ }^\circ\text{C}$, yield = 88%, $M_n = 41\,600\text{ g mol}^{-1}$, $\mathcal{D} = 1.11$].^{64, 146} As with H(OEt₂)₂[**3.2**] as the monomer to initiator ratio is increased to [600]:[1], the molecular weight of the polymer increased accordingly (entry 7, Table 3.2) [$M_n\text{ calc} = 60\,000\text{ g mol}^{-1}$, $M_n = 69\,510\text{ g mol}^{-1}$]. However due to the broad dispersity obtained it is not conclusive of living polymerization, whereas H(OEt₂)₂[P(1,2-O₂C₆Cl₄)₃] has been demonstrated to show living polymerization [$T = -78\text{ }^\circ\text{C}$, yield = 88%, $M_n = 41\,600\text{ g mol}^{-1}$, $\mathcal{D} = 1.11$].⁶⁴

The change in the colour of the poly(*n*-butyl vinyl ether) was elucidated from analysis of the ¹H NMR spectrum. Analysis of the spectrum obtained from the brown-coloured poly(*n*-butyl vinyl ether) isolated upon initiation by either H(OEt₂)₂[**3.1**] or H(OEt₂)₂[**3.2**] gave rise to a number

of broad resonances between 4.5-6.5 ppm. In the spectra of the polymers produced below $-80\text{ }^{\circ}\text{C}$ there were no signals observed in this region. These signals were attributed to the CH_2 functionalities from polyene moieties as a result of chain transfer processes. A reduction in the temperature suppresses the rate of chain transfer processes and allows higher molecular weight polymers with lower dispersities to be isolated.¹⁶⁸⁻¹⁷¹ Similar polyene functionalities have also been observed in brown coloured polymers initiated with similar Brønsted acids.^{64, 65, 146} In the aforementioned systems, there were little to no polyene functionalities observed with lower temperatures of polymerization.

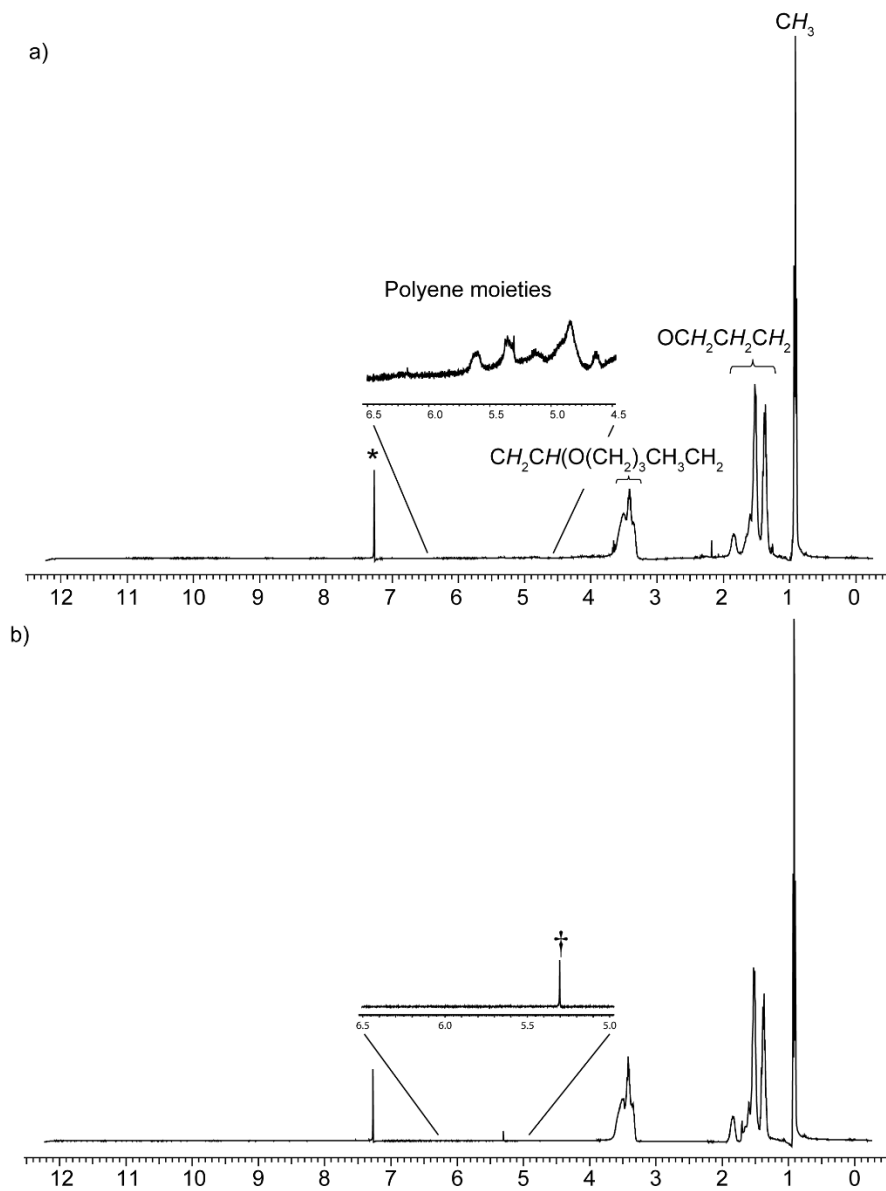


Figure 3.9 1H NMR spectrum (400 MHz, $CDCl_3$, 25 °C) of poly(*n*-butyl vinyl ether) initiated with: a) $H(OEt_2)_2[3.1]$ at 21 °C and b) $H(OEt_2)_2[3.1]$ at -84 °C. * indicates residual NMR solvent, † indicates CH_2Cl_2 .

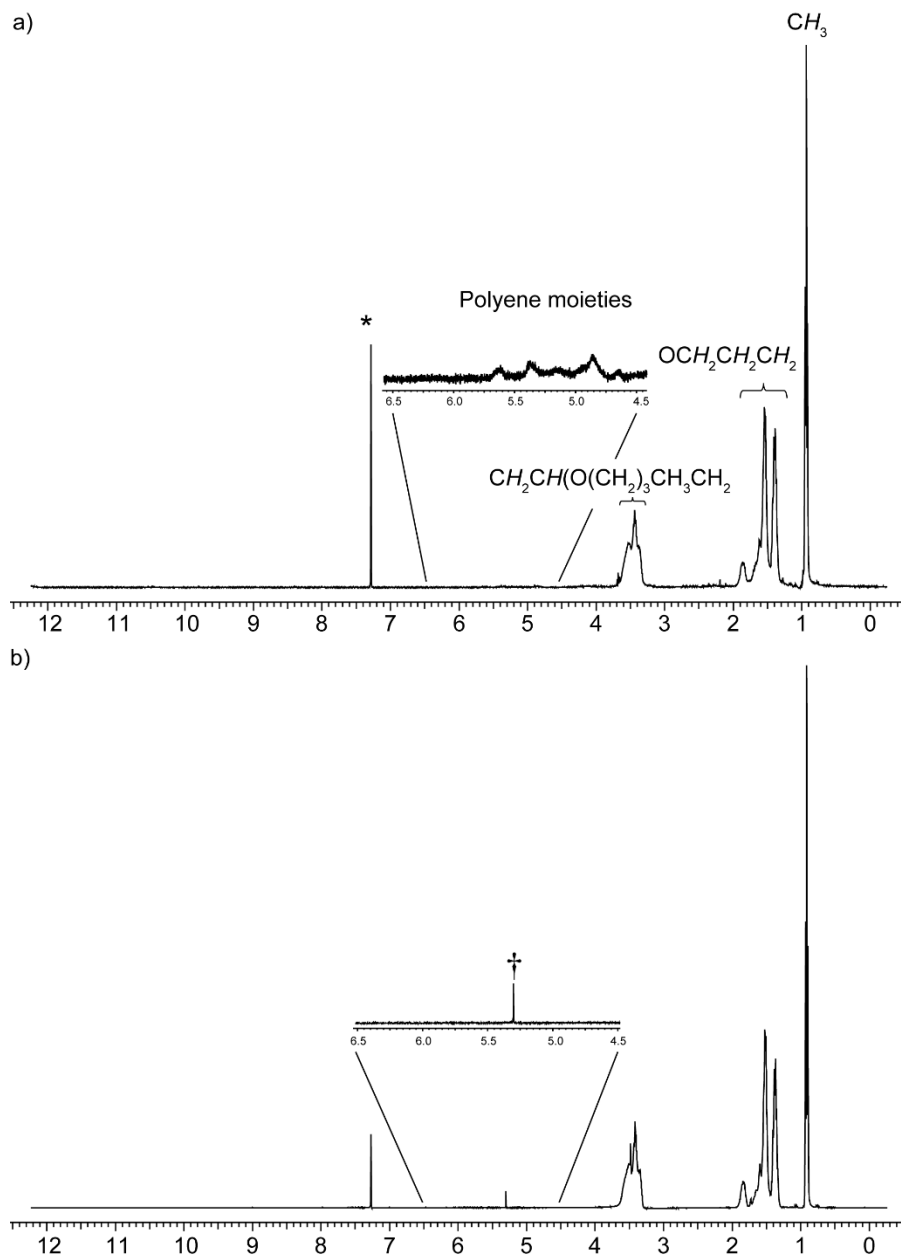


Figure 3.10 ^1H NMR spectrum (400 MHz, CDCl_3 , 25 °C) of poly(*n*-butyl vinyl ether) initiated with: a) $\text{H}(\text{OEt}_2)_2[\mathbf{3.2}]$ at 21 °C and b) $\text{H}(\text{OEt}_2)_2[\mathbf{3.2}]$ at -84 °C. * indicates residual NMR solvent, † indicates CH_2Cl_2 .

Differential scanning calorimetry (DSC) of the isolated poly(*n*-butyl vinyl ether) polymers was recorded to investigate if there was an influence of $\text{H}(\text{OEt}_2)_2[\mathbf{3.2}]$ on the resulting polymer. A clear shift of the glass transition temperature (T_g) to a more negative value was seen, as the

temperature of polymerization decreased ($T = 21\text{ }^{\circ}\text{C}$, $T_g \text{ mid} = -45\text{ }^{\circ}\text{C}$; $T = -84\text{ }^{\circ}\text{C}$, $T_g \text{ mid} = -60\text{ }^{\circ}\text{C}$). These glass transition temperatures are within the range of industrially reported values for poly(*n*-butyl vinyl ether) ($T_g = -55\text{ }^{\circ}\text{C}$),¹⁷⁴ and poly(*n*-butyl vinyl ether) produced upon initiation with $\text{H}(\text{OEt}_2)_2[2.2]$ ($T_g = -53\text{ }^{\circ}\text{C}$). However, other factors can influence the T_g of a polymer, for example: tacticity, purity, molecular weight and dispersity. Therefore, more studies to investigate these variables need to be done before conclusions can be drawn from this behaviour.

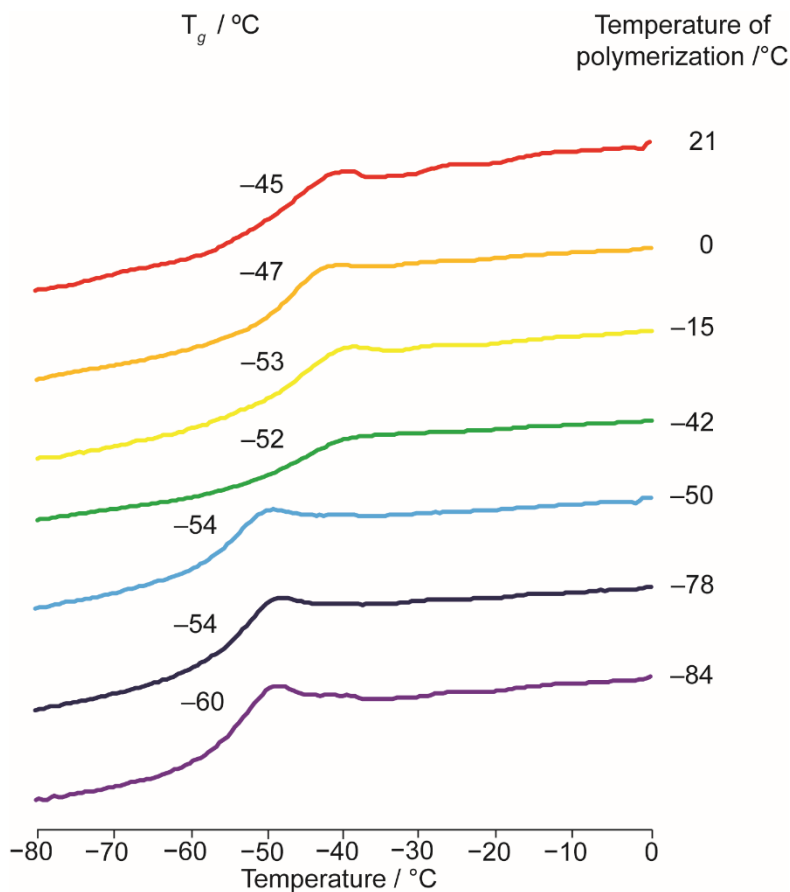
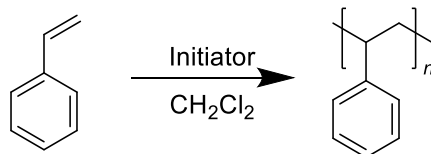


Figure 3.11 DSC traces of poly(*n*-butyl vinyl ether) initiated with $\text{H}(\text{OEt}_2)_2[3.2]$ showing glass transition temperature (T_g) as a function of the temperature of polymerization.



Scheme 3.4 H(OEt₂)₂[**3.1**] and H(OEt₂)₂[**3.2**]-initiated cationic polymerization of styrene.

The cationic polymerization of styrene is less controlled than with respect to vinyl ethers, due to the instability of the propagating carbocation.^{175, 176} No resonance forms of the carbocationic intermediate are possible. This commonly results in low molecular weight polymers with binary initiating systems, such as AlCl₃/CH₂Cl₂,¹⁵⁵ as chain transfer processes and termination reactions are likely to occur.

The single component initiators H(OEt₂)₂[**3.1**] and H(OEt₂)₂[**3.2**] successfully polymerized styrene (entries 4-6, Table 3.1; entries 8-10, Table 3.2). The polystyrene produced at ambient temperatures is of low molecular weight and broad dispersity [H(OEt₂)₂[**3.1**], T = 21 °C; $M_n = 6\,150\text{ g mol}^{-1}$, yield = 87%, $\mathcal{D} = 2.49$; H(OEt₂)₂[**3.2**], T = 21 °C; $M_n = 5\,700\text{ g mol}^{-1}$, yield = 67%, $\mathcal{D} = 1.97$). As the temperature of polymerization is lowered high molecular weight polymers, with a moderate dispersity can be isolated, albeit with a significantly decreased yield [H(OEt₂)₂[**3.1**], T = -78 °C; $M_n = 97\,620\text{ g mol}^{-1}$, yield = 3%, $\mathcal{D} = 1.56$; H(OEt₂)₂[**3.2**], T = -78 °C; $M_n = 124\,900\text{ g mol}^{-1}$, yield = 3%, $\mathcal{D} = 1.58$]. This behaviour has been observed before with H(OEt₂)₂[**2.2**], H(OEt₂)₂[Ta(1,2-O₂C₆Cl₄)₂(1,2-OC₆Cl₄OH)₂],¹⁴⁶ and H(OEt₂)₂[P(1,2-O₂C₆Cl₄)₃].⁶⁴ At temperatures below -50 °C the rate of propagation becomes very slow, and only minimal amounts of polymer are isolated.

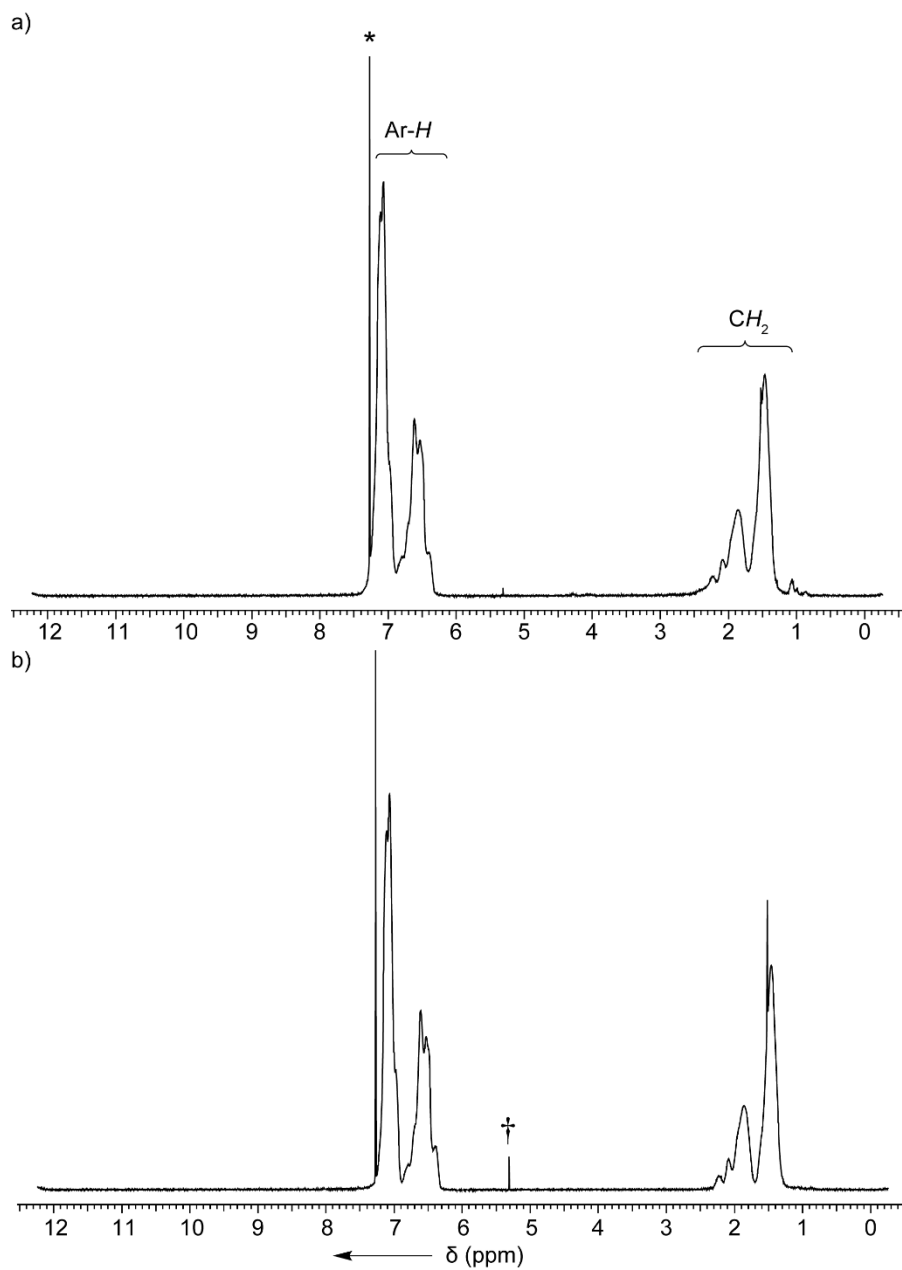
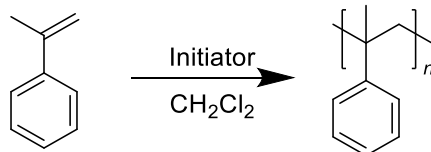


Figure 3.12 ¹H NMR spectrum (400 MHz, CDCl₃, 25 °C) of polystyrene initiated with a) H(OEt)₂[3.1] and b) H(OEt)₂[3.2]. * indicates residual NMR solvent, † indicates residual CH₂Cl₂.



Scheme 3.5 H(OEt₂)₂[**3.1**] and H(OEt₂)₂[**3.2**]-initiated cationic polymerization of α -methylstyrene.

Poly(α -methylstyrene) was successfully isolated at low temperatures using both isolated Brønsted acids with very high molecular weight and low dispersities (entries 7-9, Table 3.1; entries 11-13, Table 3.2) [H(OEt₂)₂[**3.1**], T = -78 °C, M_n = 231 400 g mol⁻¹; H(OEt₂)₂[**3.2**], T = -78 °C, M_n = 169 000 g mol⁻¹), due to branching and crosslinking. High molecular weight polymers have been observed on initiation of α -methylstyrene with other Brønsted acids: H(OEt₂)₂[**2.2**] (M_n = 211 400 g mol⁻¹), and H(OEt₂)₂[Ta(1,2-C₆O₂Cl₄)₂(1,2-C₆OCl₄OH)₂] (M_n = 279 500 g mol⁻¹),¹⁴⁶ give similarly very high molecular weight polymers when the reaction mixture was cooled to -78 °C. H(OEt₂)₂[P(1,2-C₆O₂Cl₄)₃] gave significantly lower molecular weight polymers at low temperatures [M_n = 67 600 g mol⁻¹].⁶⁴ The high molecular weight of the polymers initiated by H(OEt₂)₂[**3.1**] and H(OEt₂)₂[**3.2**] is likely as a result of branching and crosslinking reactions, commonly seen with aryl monomers.¹⁹ As expected the attempted polymerization at 21 °C using H(OEt₂)₂[**3.2**] was unsuccessful, this is above the ceiling temperature of α -methylstyrene.¹⁸¹

The ¹H NMR spectrum of poly(α -methylstyrene) with low temperatures of polymerization show a syndiotactic-rich polymer (H(OEt₂)₂[**3.1**] %*rr* = 87%; H(OEt₂)₂[**3.2**] %*rr* = 92%). Previously reported similar single component Brønsted acid initiating systems also give syndiotactic-rich polymers {H(OEt₂)₂[**2.2**] %*rr* = 83%; [H(OEt₂)₂[Ta(1,2-C₆O₂Cl₄)₂(1,2-C₆OCl₄OH)₂] %*rr* = 90%; and H(OEt₂)₂[P(1,2-C₆O₂Cl₄)₃] %*rr* = 87%}.⁶⁴
¹⁴⁶ Binary initiating systems are also prone to producing syndiotactic-rich polymers

[FeCl₃/*n*Bu₄NBr %*rr* = 84%; and other Lewis acids such as: SnCl₄, SnBr₄, ZnCl₂ %*rr* = > 90%].^{183, 184}

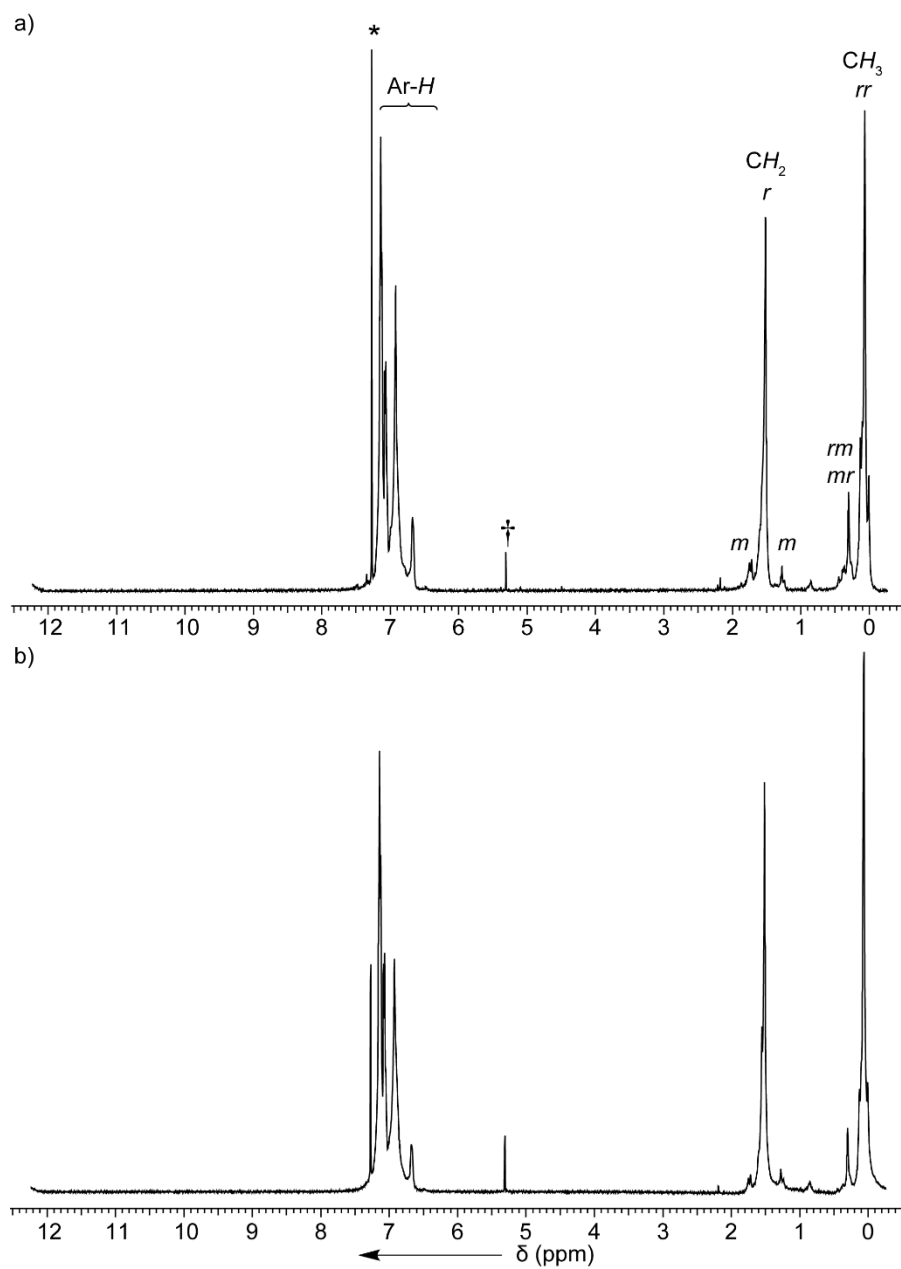
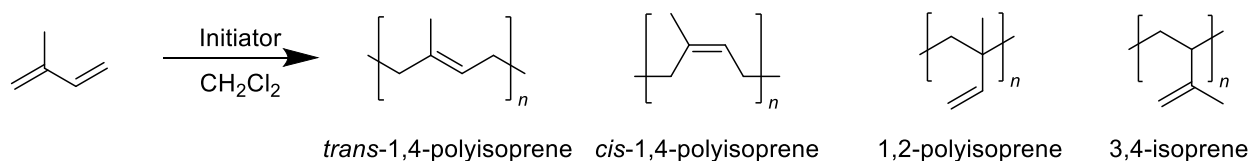


Figure 3.13 ¹H NMR spectrum (400 MHz, CDCl₃, 25 °C) of poly(*α*-methylstyrene) initiated with a) H(OEt₂)₂[3.1] and b) H(OEt₂)₂[3.2]. * indicates residual NMR solvent, † indicates residual CH₂Cl₂.



Scheme 3.6 H(OEt₂)₂[3.1**] and H(OEt₂)₂[**3.2**]-initiated cationic polymerization of isoprene.**

The H(OEt₂)₂[**3.1**] and H(OEt₂)₂[**3.2**]-initiated polymerizations of isoprene did not yield high molecular weight polymers, instead oligomers were isolated (entries 10 and 11, Table 3.1; entries 14-16, Table 3.2 respectively) [H(OEt₂)₂[**3.1**], T = 21 °C, $M_n = 3\,570\text{ g mol}^{-1}$, yield = 58%, $\bar{D} = 3.38$; H(OEt₂)₂[**3.1**], T = -50 °C, $M_n = 3\,750\text{ g mol}^{-1}$, yield = < 1%, $\bar{D} = 2.54$; H(OEt₂)₂[**3.2**], T = 21 °C, $M_n = 3\,730\text{ g mol}^{-1}$, yield = 71%, $\bar{D} = 2.34$; H(OEt₂)₂[**3.2**], T = -50 °C, $M_n = 3\,180\text{ g mol}^{-1}$, yield = 3%, $\bar{D} = 1.44$]. The reaction of solid Brønsted acids with isoprene commonly results in oligomeric isoprene, as opposed to high molecular weight polymers. For example, H(OEt₂)₂[**2.2**] [T = -50°C, $M_n = 2\,220\text{ g mol}^{-1}$, $\bar{D} = 1.80$], H(OEt₂)₂[Ta(1,2-C₆O₂Cl₄)₂(1,2-C₆OCl₄OH)₂] [T = -50°C, $M_n = 2\,600\text{ g mol}^{-1}$, $\bar{D} = 1.73$],¹⁴⁶ and H(OEt₂)₂[P(1,2-O₂C₆Cl₄)₃] [T = -35°C, $M_n = 11\,600\text{ g mol}^{-1}$].⁶⁴ Isoprene can be very challenging to polymerize as a result of the number of side reactions that can occur.^{187, 188} When the polymerizations are carried out at lower temperatures, these side reactions are suppressed along with the rate of propagation contributing to the low yield, and no polymer was isolated when initiated at -78 °C with H(OEt₂)₂[**3.2**].

There are multiple microstructures of oligoisoprene (Scheme 3.6). Upon analysis of the ¹H NMR spectrum predominately the 1,4-microstructure is present. The additional resonances observed are consistent with traces of 1,2-isoprene, and 3,4-isoprene. Due to the low yield, no further investigation of the microstructure was possible.

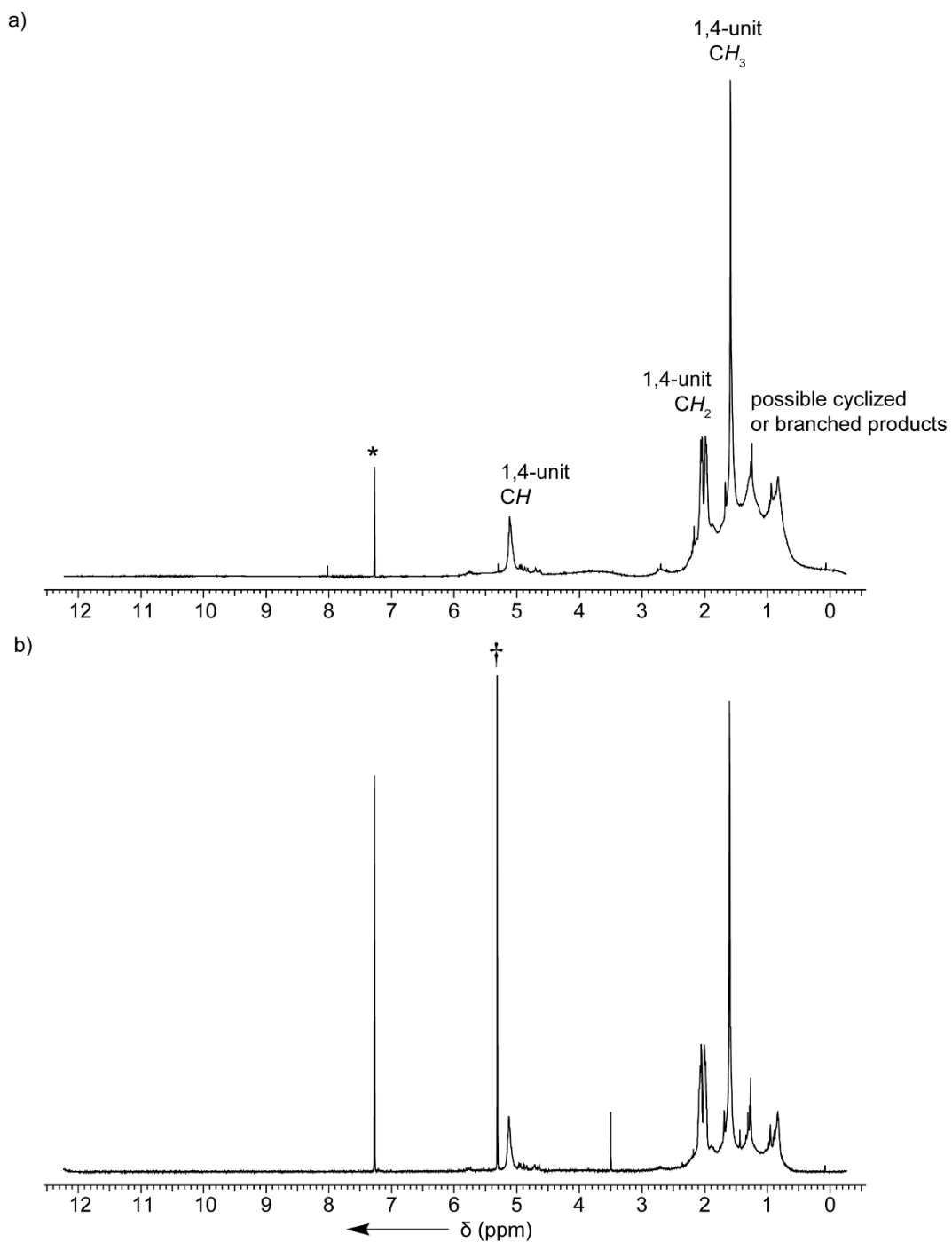


Figure 3.14 ^1H NMR spectrum (400 MHz, CDCl_3 , 25 °C) of oligoisoprene initiated with a) $\text{H}(\text{OEt}_2)_2[3.1]$ and b) $\text{H}(\text{OEt}_2)_2[3.2]$. * indicates residual NMR solvent, † indicates residual CH_2Cl_2 .

3.3 Summary

In this chapter, two perfluorinated Brønsted acids, $\text{H}(\text{OEt}_2)_2[\mathbf{3.1}]$ and $\text{H}(\text{OEt}_2)_2[\mathbf{3.2}]$, were synthesized. Both solids were characterized by ^1H and $^{19}\text{F}\{^1\text{H}\}$ NMR spectroscopy and mass spectrometry. The molecular structure of $\text{H}(\text{OEt}_2)_2[\mathbf{3.2}]$ obtained by X-ray crystallography was shown to have a distorted trigonal prismatic geometry. The viability of $\text{H}(\text{OEt}_2)_2[\mathbf{3.1}]$ and $\text{H}(\text{OEt}_2)_2[\mathbf{3.2}]$ as single component initiators for cationic olefin polymerization was investigated with different vinyl monomers. There is little difference in reactivity between the niobium(V) and tantalum(V) derivatives of perfluorinated Brønsted acid. At low temperatures, both initiators gave high molecular weight poly(*n*-butyl vinyl ether) that was close to the expected molecular weight. Polystyrene was produced with high molecular weights and moderate dispersities in high yields above -50 °C. High molecular weight, syndiotactic-rich poly(α -methylstyrene) was obtained with initiators $\text{H}(\text{OEt}_2)_2[\mathbf{3.1}]$ and $\text{H}(\text{OEt}_2)_2[\mathbf{3.2}]$. Finally, both solid single component Brønsted acids successfully oligomerized isoprene at ambient temperatures.

3.4 Experimental

3.4.1 General procedures

All experiments were performed using standard Schlenk or glove box techniques under nitrogen atmosphere. CH_2Cl_2 (Sigma Aldrich) and Et_2O (Fisher Scientific) were deoxygenated with nitrogen and dried by passing through a column containing activated alumina. CH_2Cl_2 and Et_2O were dried over calcium hydride, distilled and freeze-pump-thawed (x3) before storing over molecular sieves prior to use. *n*-Butyl vinyl ether, styrene, α -methylstyrene and isoprene were dried over calcium hydride, distilled and freeze-pump-

thawed (x3) degassed prior to use. Tantalum pentachloride (Strem Chemicals) and niobium pentachloride (Sigma Aldrich) were used without further purification. Hexafluoro-2,3-bis(trifluoromethyl)-2,3-butanediol (perfluoropinacol) (Oakwood Chemicals) was dried over calcium hydride, distilled and freeze-pump-thaw (x3) degassed prior to use. CAUTION: perfluoropinacol has been reported to be extremely toxic.²⁰¹⁻²⁰³ Due care should be taken when handling this compound and products.

NMR spectra, mass spectrometry, X-ray crystallography, GPC analysis, and differential scanning calorimetry were all performed in the Chemistry Department Facilities. ¹H and ¹⁹F{¹H} NMR spectrum were recorded at ambient temperatures unless otherwise stated on Bruker Avance 400 MHz and referenced to deuterated solvents. Different cooling baths were used to cool the polymerizations (0°C = ice/H₂O; -15°C = ethylene glycol/CO₂; -42°C = acetonitrile/N₂; -50°C = CaCl_{2(aq)}/N₂; -78°C = acetone/CO₂; -84°C = ethyl acetate/N₂). Triple detection gel permeation chromatography (GPC-LLS) was used to determine the molecular weights of the polymers. An Agilent 1260 Series standard autosampler, an Agilent 1260 series isocratic pump, Phenomenex Phenogel 5 μm narrowbore columns (4.6 x 300 mm) 10⁴ Å (5000-500,000), 500 Å (1,000-15,000) and 10³ Å (1,000-75,000) Wyatt Optilab rEx differential refractometer (λ = 658 nm, 25°C), Wyatt tristar miniDAWN (laser light scattering detector (λ = 690 nm)), and a Wyatt ViscoStar viscometer were utilized. Samples were dissolved in THF (*ca.* 2 mg mL⁻¹) and a flow rate of 0.5 mL min⁻¹ was applied. The differential refractive index of poly(*n*-butyl vinyl ether was previously calculated ($dn/dc = 0.068 \text{ mL g}^{-1}$) using Wyatt ASTRA software 6.1 assuming 100% mass recovery.¹⁴⁶ The differential refractive indices of polystyrene (dn/dc

= 0.185 mL g⁻¹), poly(α -methylstyrene) ($dn/dc = 0.174$ mL g⁻¹)¹⁸⁹, and polyisoprene ($dn/dc = 0.129$ mL g⁻¹)¹⁹⁰ have been reported.

3.4.2 X-ray structure determination

X-ray crystallography data were collected on a Bruker X8 APEX II diffractometer with graphite-monochromated Mo K α radiation. A single crystal was immersed in oil and mounted on a glass fibre. Data were collected and integrated using the Bruker SAINT software package and corrected for absorption effect using SADABS.^{191, 192} All structures were solved by direct methods and subsequent Fourier difference techniques. All non-hydrogen atoms were refined anisotropically. All C–H hydrogen atoms were placed in calculated positions. A hydrogen atom situated between two diethyl ether molecules was located in a difference map and refined isotropically. All other O–H hydrogens were placed in calculated positions. All refinements were performed using the SHELXL-2015 via the Olex2 interface.^{193, 194}

Table 3.3 Crystallographic parameters for H(OEt₂)₂[3.2].

Empirical formula	C₂₆H₂₁F₃₆O₈Ta
Formula weight	1326.38
Temperature/K	100(2)
Crystal system	Monoclinic
Space group	I2/a
a/Å	18.4903(17)
b/Å	15.9101(16)
c/Å	26.745(3)
α/°	90
β/°	94.215(2)
γ/°	90
Volume/Å³	7846.7(15)
Z	8
ρ_{calc}/cm³	2.246
μ/mm⁻¹	3.020
F(000)	5104.0
Crystal size/mm³	0.38 × 0.21 × 0.09
Radiation	MoKα (λ = 0.71073)
2θ range for data collection/°	2.98 to 61.192
Index ranges	-26 ≤ h ≤ 26, -22 ≤ k ≤ 22, -38 ≤ l ≤ 38
Reflections collected	87567
Independent reflections	12047 [R _{int} = 0.0869, R _{sigma} = 0.0503]
Data/restraints/parameters	12047/0/648
Goodness-of-fit on F²	1.018
Final R indexes [I ≥ 2σ (I)]	R ₁ = 0.0288, wR ₂ = 0.0544
Final R indexes [all data]	R ₁ = 0.0423, wR ₂ = 0.0589

3.4.3 Differential Scanning Calorimetry

The glass transition temperatures (T_g) of samples were measured on a Netzsch DSC 214 *Polyma* at a heating rate of 10K/min. The T_g of samples was recorded after the second cycle of heating to remove the previous thermal history of the sample. The DSC instrument was calibrated at heating rates of 5, 10 and 20 K min⁻¹ using: adamantane, indium, tin, bismuth and caesium chloride.

3.4.4 Synthesis of H(OEt₂)₂[3.1]

NbCl₅ (0.242 g, 0.895 mmol) was stirred in anhydrous CH₂Cl₂ (6 mL) and the pale-yellow suspension was slowly heated to reflux under N₂ atmosphere. In a separate Schlenk flask, perfluoropinacol (1.31 g, 3.93 mmol) was dissolved in warm anhydrous CH₂Cl₂ (6 mL) and the solution was added via cannula to the refluxing NbCl₅ solution to afford an off-white mixture. The reaction mixture was refluxed for 100 min and cooled to ambient temperature. Upon addition of Et₂O (18 mL), a brown clear solution formed. The solution was cooled in an ice bath to afford an off-white precipitate within 30 min. The solid was collected by filtration, washed with CH₂Cl₂ (2 mL) and dried *in vacuo*. Yield = (0.553 g, 0.447 mmol, 50%). ¹H NMR (400 MHz, CD₂Cl₂, 25 °C): δ = 4.01 (³J_{HH} = 6.51 Hz, q, 8H, CH₂CH₃), 1.41 ppm (³J_{HH} = 6.83 Hz, t, 12H, CH₂CH₃). ¹H NMR (400 MHz, CD₂Cl₂, -80 °C): δ = 6.68 (s, 1H, H(OEt₂)₂), 4.04 (³J_{HH} = 6.54 Hz, q, 8H, CH₂CH₃), 1.38 ppm (³J_{HH} = 6.88 Hz, t, 12H, CH₂CH₃). ¹⁹F NMR (376 MHz, CD₂Cl₂, 25°C): δ = -68.31 (br), -69.11 (br), -70.23 ppm (s). ¹⁹F NMR (376 MHz, CD₂Cl₂, -80 °C): δ = -67.09 (d), -68.47 (br), -68.92 (br), -70.17 ppm (s). ESI-MS(-ve) = 1088.6 *m/z*.

3.4.5 Synthesis of H(OEt₂)₂[3.2]

TaCl₅ (0.242 g, 0.895 mmol) was stirred in anhydrous CH₂Cl₂ (8 mL) and the white suspension was slowly heated to reflux under N₂ atmosphere. In a separate Schlenk flask, perfluoropinacol (1.312 g, 3.927 mmol) was dissolved in warm anhydrous CH₂Cl₂ (10 mL) and the solution was added via cannula to the refluxing TaCl₅ solution to afford a brown mixture. The reaction mixture was refluxed for 100 min and cooled to ambient temperature. Upon addition of Et₂O (20 mL), a brown clear solution formed. The solution was cooled in

an ice bath to afford an off-white precipitate within 30 min. The solid was collected by filtration, washed with CH₂Cl₂ (2 mL) and dried *in vacuo*. Yield = (0.553 g, 0.447 mmol, 50%). ¹H NMR (400 MHz, CD₂Cl₂, 25 °C): δ = 4.00 (³J_{HH} = 7.20 Hz, q, 8H, CH₂CH₃), 1.41 ppm (³J_{HH} = 7.12 Hz, t, 12H, CH₂CH₃). ¹H NMR (400 MHz, CD₂Cl₂, -80 °C): δ = 16.71 (s, 1H, H(OEt₂)₂), 4.03 (³J_{HH} = 7.02 Hz, q, 8H, CH₂CH₃), 1.38 ppm (³J_{HH} = 6.88 Hz, t, 12H, CH₂CH₃). ¹⁹F NMR (376 MHz, CD₂Cl₂, 25 °C): δ = -68.48 (br), -69.34 (br), -70.22 ppm (s). ¹⁹F NMR (376 MHz, CD₂Cl₂, -80 °C): δ = -67.29 (br), -68.65 (br), -70.18 (s), -73.75 ppm (br). ESI-MS(-ve) = 1176.6 *m/z*.

3.4.6 Representative procedure for H(OEt₂)₂[3.1]-initiated polymerization of *n*-butyl vinyl ether

In a glovebox, freshly distilled, degassed CH₂Cl₂ (2 mL) was added to H(OEt₂)₂[3.1] (0.010 g, 0.008 mmol) in a Schlenk flask. The flask was removed from the glovebox and cooled to -78 °C. Freshly distilled, *n*-butyl vinyl ether (0.33 g, 3.25 mmol) was prepared in a syringe, removed from the glovebox and added rapidly to the initiator solution. After 15 min, the reaction was quenched with a solution of NH₄OH in MeOH (0.2 mL, 10 vol%), and all volatiles were removed *in vacuo*. The crude product was dissolved in CH₂Cl₂ (2 mL) and added one drop at a time to stirred MeOH (40 mL) to precipitate a colourless oily residue. The polymer was collected by centrifugation and dried *in vacuo*. The isolated material was analyzed by ¹H NMR spectroscopy (400 MHz, CDCl₃, 25 °C): δ = 3.68-3.30 (br, CH₂CH(O(CH₂)₃CH₃)CH₂), 1.88-1.28 (br, OCH₂CH₂CH₂), 0.91 (t, CH₃), GPC and DSC. Yield = (0.23 g, 70%).

3.4.7 Representative procedure for H(OEt₂)₂[3.1]-initiated polymerization of styrene

In a glovebox, freshly distilled, degassed CH₂Cl₂ (2 mL) was added to H(OEt₂)₂[3.1] (0.010 g, 0.008 mmol) in a Schlenk flask. The flask was removed from the glovebox and cooled to -50 °C. Freshly distilled, styrene (0.34 g, 3.23 mmol) was prepared in a syringe, removed from the glovebox and added rapidly to the initiator solution. After 15 min, the reaction was quenched with a solution of NH₄OH in MeOH (0.2 mL, 10 vol%), and all volatiles were removed *in vacuo*. The crude product was dissolved in CH₂Cl₂ (2 mL) and added one drop at a time to stirred MeOH (40 mL) to precipitate a white solid residue. The polymer was collected by centrifugation and dried *in vacuo*. The isolated material was analyzed by ¹H NMR spectroscopy (400 MHz, CDCl₃, 25 °C): δ = 7.32-6.35 (br, Ar-H), 2.12-1.71 (br, CH), 1.68-1.09 (br, CH₂), and GPC. Yield = (0.25 g, 75%).

3.4.8 Representative procedure for H(OEt₂)₂[3.1]-initiated polymerization of α-methylstyrene

In a glovebox, freshly distilled, degassed CH₂Cl₂ (2 mL) was added to H(OEt₂)₂[3.1] (0.010 g, 0.008 mmol) in a Schlenk flask. The flask was removed from the glovebox and cooled to -78 °C. Freshly distilled, α-methylstyrene (0.38 g, 3.23 mmol) was prepared in a syringe, removed from the glovebox and added rapidly to the initiator solution. After 15 min, the reaction was quenched with a solution of NH₄OH in MeOH (0.2 mL, 10 vol%), and all volatiles were removed *in vacuo*. The crude product was dissolved in CH₂Cl₂ (2 mL) and added one drop at a time to stirred MeOH (40 mL) to precipitate a colourless oily residue. The polymer was collected by centrifugation and dried *in vacuo*. The isolated material was analyzed by ¹H NMR spectroscopy (400 MHz, CDCl₃, 25 °C): δ = 7.49-6.60

(br, Ar-H), 1.79-1.23 (br, $\text{CH}_2\text{CH}_2\text{CH}(\text{Ar-H})\text{CH}_3$), 0.40-0.01 (br, $\text{CH}_3\text{CH}(\text{Ar-H})\text{CH}_2\text{CH}_2$) and GPC. Yield = (0.14 g, 35%).

3.4.9 Representative procedure for $\text{H}(\text{OEt}_2)_2[3.1]$ -initiated polymerization of isoprene

In a glovebox, freshly distilled, degassed CH_2Cl_2 (2 mL) was added to $\text{H}(\text{OEt}_2)_2[3.1]$ (0.010 g, 0.008 mmol) in a Schlenk flask. The flask was removed from the glovebox and cooled to $-50\text{ }^\circ\text{C}$. Freshly distilled, isoprene (0.22 g, 3.23 mmol) was prepared in a syringe, removed from the glovebox and added rapidly to the initiator solution. After 15 min, the reaction was quenched with a solution of NH_4OH in MeOH (0.2 mL, 10 vol%), and all volatiles were removed *in vacuo*. The crude product was dissolved in CH_2Cl_2 (2 mL) and added one drop at a time to stirred MeOH (40 mL) to precipitate a colourless solid. The polymer was collected by centrifugation and dried *in vacuo*. The isolated material was analyzed by ^1H NMR spectroscopy (400 MHz, CDCl_3 , $25\text{ }^\circ\text{C}$): $\delta = 5.10$ (br, 1,4-unit CH), 5.0-4.8 (br, 1,2-unit CH_2), 4.8-4.6 (br, 3,4-unit CH_2), 2.1-1.9 (br, 1,4-unit CH_2), 1.60 (br, 1,4-unit CH_3), and GPC. Yield = (0.13 g, 58%).

3.4.10 Representative procedure for $\text{H}(\text{OEt}_2)_2[3.2]$ -initiated polymerization of *n*-butyl vinyl ether

In a glovebox, freshly distilled, degassed CH_2Cl_2 (2 mL) was added to $\text{H}(\text{OEt}_2)_2[3.2]$ (0.010 g, 0.008 mmol) in a Schlenk flask. The flask was removed from the glovebox and cooled to $-78\text{ }^\circ\text{C}$. Freshly distilled, *n*-butyl vinyl ether (0.30 g, 3.01 mmol) was prepared in a syringe, removed from the glovebox and added rapidly to the initiator solution. After 15 min, the reaction was quenched with a solution of NH_4OH in MeOH (0.2 mL, 10 vol%),

and all volatiles were removed *in vacuo*. The crude product was dissolved in CH₂Cl₂ (2 mL) and added one drop at a time to stirred MeOH (40 mL) to precipitate a colourless oily residue. The polymer was collected by centrifugation and dried *in vacuo*. The isolated material was analyzed by ¹H NMR spectroscopy (400 MHz, CDCl₃, 25 °C): δ = 3.65-3.28 (br, CH₂CH(O(CH₂)₃CH₃)CH₂), 1.94-1.28 (br, OCH₂CH₂CH₂), 0.92 (t, CH₃), GPC and DSC. Yield = (0.12 g, 33%).

3.4.11 Representative procedure for H(OEt)₂[3.2]-initiated polymerization of styrene

In a glovebox, freshly distilled, degassed CH₂Cl₂ (2 mL) was added to H(OEt)₂[3.2] (0.010 g, 0.007 mmol) in a Schlenk flask. The flask was removed from the glovebox and cooled to -50 °C. Freshly distilled, styrene (0.32 g, 3.1 mmol) was prepared in a syringe, removed from the glovebox and added rapidly to the initiator solution. After 15 min, the reaction was quenched with a solution of NH₄OH in MeOH (0.2 mL, 10 vol%), and all volatiles were removed *in vacuo*. The crude product was dissolved in CH₂Cl₂ (2 mL) and added one drop at a time to stirred MeOH (40 mL) to precipitate a white solid residue. The polymer was collected by centrifugation and dried *in vacuo*. The isolated material was analyzed by ¹H NMR spectroscopy (400 MHz, CDCl₃, 25 °C): δ = 7.35-6.32 (br, Ar-H), 2.23-1.73 (br, CH), 1.68-1.12 (br, CH₂), and GPC. Yield = (0.21 g, 67%).

3.4.12 Representative procedure for H(OEt)₂[3.2]-initiated polymerization of *α*-methylstyrene

In a glovebox, freshly distilled, degassed CH₂Cl₂ (2 mL) was added to H(OEt)₂[3.2] (0.010 g, 0.007 mmol) in a Schlenk flask. The flask was removed from the glovebox and

cooled to $-78\text{ }^{\circ}\text{C}$. Freshly distilled, α -methylstyrene (0.35 g, 3.00 mmol) was prepared in a syringe, removed from the glovebox and added rapidly to the initiator solution. After 15 min, the reaction was quenched with a solution of NH_4OH in MeOH (0.2 mL, 10 vol%), and all volatiles were removed *in vacuo*. The crude product was dissolved in CH_2Cl_2 (2 mL) and added one drop at a time to stirred MeOH (40 mL) to precipitate a colourless solid. The polymer was collected by centrifugation and dried *in vacuo*. The isolated material was analyzed by ^1H NMR spectroscopy (400 MHz, CDCl_3 , $25\text{ }^{\circ}\text{C}$): $\delta = 7.31\text{-}6.66$ (br, Ar-H), $1.78\text{-}1.20$ (br, $\text{CH}_2\text{CH}_2\text{CH}(\text{Ar-H})\text{CH}_3$), $0.31\text{-}0.01$ (br, $\text{CH}_3\text{CH}(\text{Ar-H})\text{CH}_2\text{CH}_2$) and GPC. Yield = (0.066 g, 19%).

3.4.13 Representative procedure for $\text{H}(\text{OEt}_2)_2[3.2]$ -initiated polymerization of isoprene

In a glovebox, freshly distilled, degassed CH_2Cl_2 (2 mL) was added to $\text{H}(\text{OEt}_2)_2[3.2]$ (0.009 g, 0.007 mmol) in a Schlenk flask. The flask was removed from the glovebox and cooled to $-50\text{ }^{\circ}\text{C}$. Freshly distilled, isoprene (0.15 g, 2.20 mmol) was prepared in a syringe, removed from the glovebox and added rapidly to the initiator solution. After 15 min, the reaction was quenched with a solution of NH_4OH in MeOH (0.2 mL, 10 vol%), and all volatiles were removed *in vacuo*. The crude product was dissolved in CH_2Cl_2 (2 mL) and added one drop at a time to stirred MeOH (40 mL) to precipitate a white solid residue. The polymer was collected by centrifugation and dried *in vacuo*. The isolated material was analyzed by ^1H NMR spectroscopy (400 MHz, CDCl_3 , $25\text{ }^{\circ}\text{C}$): $\delta = 5.12$ (br, 1,4-unit CH), $5.0\text{-}4.8$ (br, 1,2-unit CH_2), $4.8\text{-}4.6$ (br, 3,4-unit CH_2), $2.1\text{-}1.9$ (br, 1,4-unit CH_2), 1.61 (br, 1,4-unit CH_3), and GPC. Yield = (0.007 g, 5%).

Chapter 4: Conclusion

4.1 Introduction

Weakly coordinating anions (WCAs) have been a focus for chemists for many years. The goal of this work was to develop a WCA to stabilize a HL_2^+ cation and isolate a solid Brønsted acid. The efficiency of this Brønsted acid as a single component initiator for the cationic polymerization of olefins was then investigated. The interaction between the anion and cation must be balanced to allow for high molecular weight polymers, at temperatures higher than -100°C during the polymerization. Both an interaction too weak or strong will lead to premature termination of the polymerization. Although WCAs containing main group elements, such as boron, aluminium and phosphorus,^{59, 67, 151} have dominated the design of anions, few Group 5 metal-containing WCAs are known.^{66, 110, 113, 136, 150, 157-163, 196, 211, 212} We hypothesized that by utilizing a WCA with a Group 5 metal, adding steric bulk and strong M-O bonds,¹³³ a solid Brønsted acid could be isolated that would give high molecular weight polymers upon reaction of olefin monomers.

4.2 Group 5 Hexacoordinate WCAs

Described in Chapter 2 is the synthesis of two solid Brønsted acids, $H(\text{OEt}_2)_2[\mathbf{2.1}]$ and $H(\text{OEt}_2)_2[\mathbf{2.2}]$. Interestingly by controlling the equivalents of tetrachlorocatechol in the reaction, different substitution patterns on the niobium(V) centre can be obtained: either a tris-substituted tetrachlorocatecholate niobium(V) anion; or a more substituted anion with 4 tetrachlorocatecholate ligands. These Brønsted acids were investigated as single component initiators for cationic polymerization of a range of olefins (*n*-butyl vinyl ether, styrene, α -methylstyrene and isoprene).

Both H(OEt₂)₂[**2.1**] and H(OEt₂)₂[**2.2**] produced poly(*n*-butyl vinyl ether) close to the expected molecular weight at -84 °C, with narrow dispersities. The DSC of the polymers initiated with H(OEt₂)₂[**2.2**] showed that the T_g was decreasing accordingly with the temperature of polymerization. Polystyrene was isolated with high molecular weights, by both H(OEt₂)₂[**2.1**] and H(OEt₂)₂[**2.2**]. On initiation of α -methylstyrene with H(OEt₂)₂[**2.2**] syndiotactic-rich poly(α -methylstyrene) was isolated. Additionally, oligomeric isoprene was obtained at a range of temperatures of polymerization in low yields. Further work on this system could entail a more thorough polymerization study, investigating whether living behaviour can be exhibited by H(OEt₂)₂[**2.2**] when reacted with *n*-butyl vinyl ether. A more focused temperature study on the polymerization of styrene and α -methylstyrene to determine the point at which the molecular weight of polymers isolated significantly increases could also be pertinent.

Chapter 3 outlines the investigation to reaction of a perfluorinated ligand with niobium(V) and tantalum(V) to isolate solid Brønsted acids, H(OEt₂)₂[**3.1**] and H(OEt₂)₂[**3.2**]. There is little difference between the polymers produced by both solid single component initiators. Poly(*n*-butyl vinyl ether) was isolated in moderate yields with high molecular weights. The T_g of the resulting polymers was comparable to literature values and showed a similar trend versus temperature of polymerization when compared to the polymers produced with Brønsted acid H(OEt₂)₂[**2.2**] from Chapter 2. High molecular weight polymers of polystyrene and poly(α -methylstyrene) were isolated upon initiation with H(OEt₂)₂[**3.1**] and H(OEt₂)₂[**3.2**]. Isoprene proved more challenging and only oligomeric material was obtained in low yields. Further work needs to be done on this anion. In particular there needs to be investigation relating to the inequivalence of the fluorine atoms. It would be helpful to use a different cation to isolate the salt, which may prove to be more stable, and easier to handle than the acid containing the HL₂⁺ cation. Computational studies may

help elucidate the electronic distribution over the anion. Finally, examining the stability of these anions to air, moisture and temperature would provide an insightful summary.

References

- (1) The Editors of Encyclopaedia Britannica, Rubber Tree, <https://www.britannica.com/plant/rubber-tree> (Accessed 17 September 2018).
- (2) Langenheim, J.H. Introduction to Rubber Usage among the Maya, https://www.maya-archaeology.org/Mayan_anthropology_ethnography_archaeology_art_history_iconography_epigraphy_ethnobotany/rubber_hule_Castilla_elastica_incense_idols_ball_game_balls_Guatemala_Chiapas_Mexico_Belize_Hevea_brasiliensis.php (Accessed 9 August 2018).
- (3) AZoM Natural Rubber - History and Developments in the Natural Rubber Industry, <https://www.azom.com/article.aspx?ArticleID=2101> (Accessed 9 August 2018).
- (4) Mackintosh <https://mackintosh.com/ca/brand-story> (Accessed 9 August 2018).
- (5) Lichtman, J. Z.; Chatten, C. K. *Anal. Chem.* **1952**, *24*, 812-818.
- (6) The Editors of Encyclopaedia Britannica, Vulcanization, <https://www.britannica.com/technology/vulcanization> (Accessed 18 September 2018).
- (7) Goodyear, C. Improvement in India-Rubber Fabrics, US3633, June 15, 1844
- (8) Thomas, R. M.; Sparks, W. J.; Frolich, P. K. *J. Am. Chem. Soc.* **1940**, *62*, 276-280.
- (9) Thomas, R. M.; Lightbrown, I. E.; Sparks, W. J.; Frolich, P. K.; Murphree, E. V. *Ind. Eng. Chem.* **1940**, *32*, 1283-1292.
- (10) Thomas, R.M.; Sparks, R.W. Standard Oil Development Company, US2,356,128, 1944
- (11) Grand View Research, Inc. Available <https://www.grandviewresearch.com/industry-analysis/butyl-rubber-iir-market> (accessed on 8 August 2018)
- (12) Industrial Rubber Goods - Butyl Rubber Applications, <http://www.industrialrubbergoods.com/articles/butyl-rubber-applications.html> (Accessed 14 September 2018).
- (13) Association of Natural Rubber Producing Countries <http://www.anrpc.org/> (Accessed 26 September 2018).
- (14) Warren-Thomas, E.; Dolman, P. M.; Edwards, D. P. *Conserv. Lett.* **2015**, *8*, 230-241.
- (15) van Beilen, J. B.; Poirier, Y. *Plant J.* **2008**, *54*, 684-701.
- (16) Roy, S. G.; Banerjee, S.; De, P., Cationic Polymerization of Nonpolar Vinyl Monomers for Producing High Performance Polymers. In *Reference Module in Materials Science and Materials Engineering*, Elsevier: 2016.
- (17) Matyjaszewski, K. *Cationic Polymerizations: Mechanisms, Synthesis, & Applications*, CRC Press, 1996.
- (18) Odian, G. *Principles of Polymerization*. Fourth ed. Wiley and Sons, 2004.
- (19) Su, W.-F., Ionic Chain Polymerization. In *Principles of Polymer Design and Synthesis*, Springer Berlin Heidelberg: Berlin, Heidelberg, 2013; pp 185-218.
- (20) Matyjaszewski, K., 41 - Carbocationic Polymerization: Styrene and Substituted Styrenes. In *Comprehensive Polymer Science and Supplements*, Allen, G.; Bevington, J. C., Eds. Pergamon: Amsterdam, 1989; pp 639-671.
- (21) Pitsikalis, M., Ionic Polymerization. In *Reference Module in Chemistry, Molecular Sciences and Chemical Engineering*, Elsevier: 2013.
- (22) Kostjuk, S.V. *RSC Adv.* **2015**, *5*, 13125-13144.
- (23) Farkas, A.; Farkas, L. *Ind. Eng. Chem.* **1942**, *34*, 716-721.
- (24) Cho, C. G.; Feit, B. A.; Webster, O. W. *Macromolecules* **1992**, *25*, 2081-2085.

- (25) Hayes, M. J.; Pepper, D. C. *Proc. R. Soc. A* **1961**, 263, 63-74.
- (26) Clayden, J.; Greeves, N.; Warren, S. *Organic Chemistry*, Second ed., Oxford University Press, UK, 2001.
- (27) Ward, I.M. in *Polymers: Chemistry and Physics of Modern Materials*, Cowie, J.M.G; Arrighi, V. Third Ed., Taylor and Francis, 2009.
- (28) Aoshima, S.; Kanaoka, S. *Chem. Rev.* **2009**, 109, 5245-5287.
- (29) IUPAC. *Compendium of Chemical Terminology*, 2nd ed. (the "Gold Book"). McNaught, A. D.; Wilkinson, A. Ed. Blackwell Scientific Publications, Oxford, 1997.
- (30) Plesch, P. H.; Austin, J. C. *J. Polym. Sci., Part A: Polym. Chem.* **2008**, 46, 4265-4284.
- (31) Kanoh, N.; Ikeda, K.; Gotoh, A.; Higashimura, T.; Okamura, S. *Makromol. Chem.* **1965**, 86, 200-216.
- (32) Overberger, C. G.; Kamath, V. G. *J. Am. Chem. Soc.* **1959**, 81, 2910-2911.
- (33) Overberger, C. G.; Kamath, V. G. *J. Am. Chem. Soc.* **1963**, 85, 446-449.
- (34) Rozentsvet, V. A.; Kozlov, V. G.; Stotskaya, O. A.; Sablina, N. A.; Peruch, F.; Kostjuk, S. V. *Eur. Polym. J.* **2018**, 103, 11-20.
- (35) Stevens, M.P. *Polymer Chemistry - An Introduction*. Third Ed., Oxford University Press, 1999.
- (36) Gyor, M.; Wang, H.-C.; Faust, R. *J. Macromol. Sci., Part A: Pure Appl.Chem.* **1992**, 29, 639-653.
- (37) Kennedy, J. P. *J. Macromol. Sci., Part A: Pure Appl.Chem.* **1982**, 18, 1-1.
- (38) Mayo, F. R. *J. Am. Chem. Soc.* **1943**, 65, 2324-2329.
- (39) Han, L.; Wu, Y.-b.; Dan, Y.; Wang, H.; Zhang, X.-q.; Wei, X.-l.; Guo, W.-l.; Li, S.-x. *RSC Adv.* **2016**, 6, 105322-105330.
- (40) Burnett, G. M.; Cameron, G. G., Branching and Crosslinking in Styrene-Butadiene Polymerizations. In *Polymerization Kinetics and Technology*, American Chemical Society, 1973, Vol. 128, pp 102-109.
- (41) *Proc. R. Soc. A* **1954**, 221, 453-462.
- (42) Shamiri, A.; Chakrabarti, M. H.; Jahan, S.; Hussain, M. A.; Kaminsky, W.; Aravind, P. V.; Yehye, W. A. *Materials* **2014**, 7, 5069-5108.
- (43) Ziegler-Natta Catalysts. In *Kirk-Othmer Encyclopedia of Chemical Technology*.
- (44) Chen, E. Y.-X.; Marks, T. J. *Chem. Rev.* **2000**, 100, 1391-1434.
- (45) Su, W.-F., Coordination Polymerization. In *Principles of Polymer Design and Synthesis*, Springer Berlin Heidelberg: Berlin, Heidelberg, 2013; pp 219-232.
- (46) Danusso, F.; Sianesi, D.; Calcagno, B., 84 - Stereospecific Polymerization of Styrene. Note III: Kinetics with Catalysts From $\text{Al}(\text{C}_2\text{H}_5)_3$ and TiCl_4 . In *Stereoregular Polymers and Stereospecific Polymerizations*, Natta, G.; Danusso, F., Eds. Pergamon: 1967; p 470.
- (47) Natta, G.; Danusso, F.; Sianesi, D., 98 - Stereospecific Polymerization and Isotactic Polymers of Vinyl Aromatic Monomers. In *Stereoregular Polymers and Stereospecific Polymerizations*, Natta, G.; Danusso, F., Eds. Pergamon: 1967; pp 569-578.
- (48) Natta, G.; Porri, L.; Mazzei, A., 108 - Stereospecific Polymerizations of Conjugated Diolefins. In *Stereoregular Polymers and Stereospecific Polymerizations*, Natta, G.; Danusso, F., Eds. Pergamon: 1967; pp 595-596.
- (49) Hoff, R.; Mathers, R.T. *Handbook of Transition Metal Polymerization Catalysts*. John Wiley & Sons, USA, 2009.

- (50) Nowlin, T.E.; Mink, R.I.; Kissin, Y.V. Supported Magnesium/Titanium-Based Ziegler Catalysts for Production of Polyethylene. In *Handbook of Transition Metal Polymerization Catalysts*, Hoff, R.; Mathers, R.T. Eds., John Wiley & Sons, USA, 2009.
- (51) Natta, G.; Corradini, P., 137 - Structure and Properties of Isotactic Polypropylene. In *Stereoregular Polymers and Stereospecific Polymerizations*, Natta, G.; Danusso, F., Eds. Pergamon: 1967; pp 743-746.
- (52) Yang, X.; Stern, C. L.; Marks, T. J. *J. Am. Chem. Soc.* **1991**, *113*, 3623-3625.
- (53) Kamigaito, M.; Maeda, Y.; Sawamoto, M.; Higashimura, T. *Macromolecules* **1993**, *26*, 1643-1649.
- (54) Kojima, K.; Sawamoto, M.; Higashimura, T. *Macromolecules* **1989**, *22*, 1552-1557.
- (55) Kamigaito, M.; Sawamoto, M.; Higashimura, T. *Macromolecules* **1991**, *24*, 3988-3992.
- (56) Kostjuk, S. V.; Ganachaud, F. *Macromolecules* **2006**, *39*, 3110-3113.
- (57) Storey, R. F.; Choate, K. R. *Macromolecules* **1997**, *30*, 4799-4806.
- (58) Barsan, F.; Karam, A. R.; Parent, M. A.; Baird, M. C. *Macromolecules* **1998**, *31*, 8439-8447.
- (59) Huber, M.; Kuerk, A.; Krossing, I.; Muelhaupt, R.; Schoeckel, H. *Z. Anorg. Allg. Chem.* **2009**, *635*, 1787-1793.
- (60) Garratt, S.; Carr, A. G.; Langstein, G.; Bochmann, M. *Macromolecules* **2003**, *36*, 4276-4287.
- (61) Nuyken, O.; Vierle, M. *Designed Monomers and Polymers*, **2005**, *8*, 91-105.
- (62) Lichtenthaler, M. R.; Higelin, A.; Kraft, A.; Hughes, S.; Steffani, A.; Plattner, D. A.; Slattery, J. M.; Krossing, I. *Organometallics* **2013**, *32*, 6725-6735.
- (63) Rudolph, T.; Kempe, K.; Crotty, S.; Paulus, R. M.; Schubert, U. S.; Krossing, I.; Schacher, F. H. *Polym. Chem.* **2013**, *4*, 495-505.
- (64) Siu, P. W.; Hazin, K.; Gates, D. P. *Chem. - Eur. J.* **2013**, *19*, 9005-9014.
- (65) Hazin, K.; Serin, S. C.; Patrick, B. O.; Ezhova, M. B.; Gates, D. P. *Dalton Trans.* **2017**, *46*, 5901-5910.
- (66) Strauss, S. H. *Chem. Rev.* **1993**, *93*, 927-942.
- (67) Krossing, I.; Raabe, I. *Angew. Chem., Int. Ed.* **2004**, *43*, 2066-2090.
- (68) Nishida, H.; Takada, N.; Yoshimura, M.; Sonoda, T.; Kobayashi, H. *B. Chem. Soc. Jpn.* **1984**, *57*, 2600-2604.
- (69) Honeychuck, R. V.; Hersh, W. H. *Inorg. Chem.* **1989**, *28*, 2869-2886.
- (70) Yakelis, N. A.; Bergman, R. G. *Organometallics* **2005**, *24*, 3579-3581.
- (71) Chen, E.; Lancaster, S. in *Comprehensive Inorganic Chemistry II*, Ed. J Poeppelemeier, Elsevier, 2013, 707-754.
- (72) Massey, A. G.; Park, A. J. *J. Organomet. Chem.* **1964**, *2*, 245-250.
- (73) Xu, K.; Zhang, S. S.; Jow, T. R.; Xu, W.; Angell, C. A. *Electrochem. Solid-State Lett.* **2002**, *5*, A26-A29.
- (74) Finze, M.; Bernhardt, E.; Willner, H. *Angew. Chem., Int. Ed.* **2007**, *46*, 9180-9196.
- (75) Bernhardt, E.; Brauer, D. J.; Finze, M.; Willner, H. *Angew. Chem., Int. Ed.* **2006**, *45*, 6383-6386.
- (76) Bernhardt, E.; Henkel, G.; Willner, H.; Pawelke, G.; Burger, H. *Chem. - Eur. J.* **2001**, *7*, 4696-4705.
- (77) Jutzi, P.; Müller, C.; Stammli, A.; Stammli, H.-G. *Organometallics* **2000**, *19*, 1442-1444.
- (78) Chien, J. C. W.; Tsai, W. M.; Rausch, M. D. *J. Am. Chem. Soc.* **1991**, *113*, 8570-8571.

- (79) Chien, J. C. W.; Song, W.; Rausch, M. D. *Macromolecules* **1993**, *26*, 3239-3240.
- (80) Rupp, A. B. A.; Krossing, I. *Acc. Chem. Res.* **2015**, *48*, 2537-2546.
- (81) Bulut, S.; Klose, P.; Krossing, I. *Dalton Trans.* **2011**, *40*, 8114-8124.
- (82) Rupp, A. B. A.; Klose, P.; Scherer, H.; Krossing, I. *ChemPhysChem* **2014**, *15*, 3729-3731.
- (83) Rupp, A. B. A.; Welle, S.; Klose, P.; Scherer, H.; Krossing, I. *ChemPhysChem* **2015**, *16*, 1940-1947.
- (84) Bawn, C. E. H.; Ledwith, A.; Matthies, P. *Journal of Polymer Science* **1959**, *34*, 93-108.
- (85) Allan, M.; Janzen, A. F.; Willis, C. J. *Can. J. Chem.* **1968**, *46*, 3671-&.
- (86) Xu, W.; Shusterman, A. J.; Videa, M.; Velikov, V.; Marzke, R.; Angell, C. A. *J. Electrochem. Soc.* **2003**, *150*, E74-E80.
- (87) Freudenmann, D.; Wolf, S.; Wolff, M.; Feldmann, C. *Angew. Chem., Int. Ed.* **2011**, *50*, 11050-11060.
- (88) Younesi, R.; Veith, G. M.; Johansson, P.; Edström, K.; Vegge, T. *Energy Environ. Sci.* **2015**, *8*, 1905-1922.
- (89) LaPointe, R. E.; Roof, G. R.; Abboud, K. A.; Klosin, J. *J. Am. Chem. Soc.* **2000**, *122*, 9560-9561.
- (90) Lancaster, S. J.; Rodriguez, A.; Lara-Sanchez, A.; Hannant, M. D.; Walker, D. A.; Hughes, D. H.; Bochmann, M. *Organometallics* **2002**, *21*, 451-453.
- (91) McInenly, P. J.; Drewitt, M. J.; Baird, M. C. *Macromol. Chem. Phys.* **2004**, *205*, 1707-1712.
- (92) Tse, C. K. W.; Penciu, A.; McInenly, P. J.; Kumar, K. R.; Drewitt, M. J.; Baird, M. C. *Eur. Polym. J.* **2004**, *40*, 2653-2657.
- (93) Reed, C. A. *Acc. Chem. Res.* **1998**, *31*, 133-139.
- (94) Shelly, K.; Reed, C.A.; Lee, Y.J.; Scheidt, J. *J. Am. Chem. Soc.* **1986**, *108*, 3117.
- (95) Knapp, C. in *Comprehensive Inorganic Chemistry II*, Elsevier, **2013**, 651.
- (96) Körbe, S.; Schreiber, P. J.; Michl, J. *Chem. Rev.* **2006**, *106*, 5208-5249.
- (97) Crowther, D. J.; Borkowsky, S. L.; Swenson, D.; Meyer, T. Y.; Jordan, R. F. *Organometallics* **1993**, *12*, 2897-2903.
- (98) Reed, C. A. *Chem. Commun.* **2005**, 1669-1677.
- (99) Reed, C. A. *Acc. Chem. Res.* **2010**, *43*, 121-128.
- (100) Cummings, S.; Hratchian, H. P.; Reed, C. A. *Angew. Chem., Int. Ed.* **2016**, *55*, 1382-1386.
- (101) Nava, M.; Stoyanova, I.; Cummings, S.; Stoyanov, E.; Reed, C.A. *Angew. Chem.* **2014**, *126*, 1149.
- (102) Lipping, L.; Leito, I.; Koppel, I.; Krossing, I.; Himmel, D.; Koppel, I. A. *J. Phys. Chem. A* **2015**, *119*, 735-743.
- (103) Olah, G. A.; Prakash, G. K. S.; Sommer, J. *Science* **1979**, *206*, 13-20.
- (104) Himmel, D.; Radtke, V.; Butschke, B.; Krossing, I. *Angew. Chem., Int. Ed.* **2018**, *57*, 4386-4411.
- (105) Körbe, S.; Schreiber, P. J.; Michl, J. *Chem. Rev.* **2006**, *106*, 5208-5249.
- (106) Chen, Y.-X.; Stern, C. L.; Marks, T. J. *J. Am. Chem. Soc.* **1997**, *119*, 2582-2583.
- (107) Chen, Y.-X.; Metz, M. V.; Li, L.; Stern, C. L.; Marks, T. J. *J. Am. Chem. Soc.* **1998**, *120*, 6287-6305.
- (108) Barbarich, T. J.; Handy, S. T.; Miller, S. M.; Anderson, O. P.; Grieco, P. A.; Strauss, S. H. *Organometallics* **1996**, *15*, 3776-3778.

- (109) Ivanova, S. M.; Nolan, B. G.; Kobayashi, Y.; Miller, S. M.; Anderson, O. P.; Strauss, S. H. *Chem. - Eur. J.* **2001**, *7*, 503-510.
- (110) Strauss, S. H. *Abstr. Pap. Am. Chem. Soc.* **1998**, *216*, U828-U828.
- (111) Krossing, I. *Chem. - Eur. J.* **2001**, *7*, 490-502.
- (112) Tsujioka, S.; Nolan, B. G.; Takase, H.; Fauber, B. P.; Strauss, S. H. *J. Electrochem. Soc.* **2004**, *151*, A1418-A1423.
- (113) Sun, Y. M.; Metz, M. V.; Stern, C. L.; Marks, T. J. *Organometallics* **2000**, *19*, 1625-1627.
- (114) Moganty, S.; Sinicropi, J.; Torres, G.; Abbate, L.; Wu, Y. Modified Ionic Liquids Containing Phosphorus. US2017/0288269 A1, 5 October, 2017.
- (115) Carrow, B. P.; Zhang, W. Transition Metal Catalysts for Olefin Polymerization, US2017/0137549 A1, 18 May, 2017.
- (116) Schmitz, L. A.; McCollum, A. M.; Rheingold, A. L.; Green, D. B.; Fritsch, J. M. *Polyhedron* **2018**, *147*, 94-105.
- (117) Goodenough, J. B.; Kim, Y. *Chem. Mater.* **2010**, *22*, 587-603.
- (118) M. Gordon, C.; D. Holbrey, J.; R. Kennedy, A.; R. Seddon, K. *J. Mater. Chem.* **1998**, *8*, 2627-2636.
- (119) Constant, S.C.; Lacour, J. New Trends in Hexacoordinated Phosphorus Chemistry. In *New Aspects Phosphorus Chemistry V*, Majoral, J.P-. Ed. Springer: Berlin, 2005.
- (120) Hellwinkel, D. *Angew. Chem.* **1965**, *77*, 378-379.
- (121) Hellwinkel, D.; Wilfinger, H.-J. *Chem. Ber.* **1970**, *103*, 1056-1064.
- (122) Lacour, J.; Ginglinger, C.; Grivet C.; Bernardinelli, G. *Angew. Chem. Int. Ed. Engl.* **1997**, *36*, 608.
- (123) Bas, D.; Bürgi, T.; Lacour, J.; Vachon, J.; Weber, J. *Chirality* **2005**, *17*, S143-S148.
- (124) Jodry, J. J.; Frantz, R.; Lacour, J. *Inorg. Chem.* **2004**, *43*, 3329-3331.
- (125) Lacour, J.; Vial, L.; Bernardinelli, G. *Org. Lett.* **2002**, *4*, 2309-2312.
- (126) Eberwein, M.; Schmid, A.; Schmidt, M.; Zabel, M.; Burgemeister, T.; Barthel, J.; Kunz, W.; Gores, H. J. *J. Electrochem. Soc.* **2003**, *150*, A994-A999.
- (127) Handa, M.; Suzuki, M.; Suzuki, J.; Kanematsu, H.; Sasaki, Y. *Electrochem. Solid-State Lett.* **1999**, *2*, 60-62.
- (128) Weitelmann, U.; Bonrath, W.; Netscher, T.; Nöth, H.; Panitz, J.-C.; Wohlfart-Mehrens, M. *Chem. Eur. J.* **2004**, *10*, 2451.
- (129) Takahashi, M.; Morinaka, T.; Shinmen, Y.; Kawabata, W.; Kubo, M.; Matasuzaki, H.; Yamamoto, K. Method for the preparation of difluoro ionic complex. WO2016/052092, 7 April, 2016.
- (130) Koenig, M.; Klaébé, A.; Munoz, A.; Wolf, R. *J. Chem. Soc., Perkin Trans. 2* **1976**, 955-958.
- (131) Klaébé, A.; Koenig, M.; Wolf, R.; Ahlberg, P. *J. Chem. Soc., Dalton Trans.* **1977**, 570-574.
- (132) Koenig, M.; Klaebe, A.; Munoz, A.; Wolf, R. *J. Chem. Soc., Perkin Trans. 2* **1979**, 40-44.
- (133) Luo, Y. R., *Comprehensive Handbook of Chemical Bond Energies*, CRC Press, Boca Raton, FL, 2007.
- (134)
- (135) Donat, M.; Seisenbaeva, G. A.; Kessler, V. G. *J. Sol-Gel Sci. Technol.* **2008**, *48*, 61-65.

- (136) Preiss, U. P.; Steinfeld, G.; Scherer, H.; Erle, A. M. T.; Benkmil, B.; Kraft, A.; Krossing, I. *Z. Anorg. Allg. Chem.* **2013**, *639*, 714-721.
- (137) Kunitake, T.; Takarabe, K.; Tsugawa, S.-i. *Polymer J.* **1976**, *8*, 363.
- (138) Brønsted, J. N. *Recl. Trav. Chim. Pays-Bas* **1923**, *42*, 718-728.
- (139) Paenurk, E.; Kaupmees, K.; Himmel, D.; Kütt, A.; Kaljurand, I.; Koppel, I. A.; Krossing, I.; Leito, I. *Chem. Sci.* **2017**, *8*, 6964-6973.
- (140) Brookhart, M.; Grant, B.; Volpe, A. F. *Organometallics* **1992**, *11*, 3920-3922.
- (141) Brookhart, M.; Rix, F. C.; Desimone, J. M.; Barborak, J. C. *J. Am. Chem. Soc.* **1992**, *114*, 5894-5895.
- (142) Mecking, S.; Johnson, L. K.; Wang, L.; Brookhart, M. *J. Am. Chem. Soc.* **1998**, *120*, 888-899.
- (143) Siu, P. W.; Gates, D. P. *Organometallics* **2009**, *28*, 4491-4499.
- (144) Juhasz, M.; Hoffmann, S.; Stoyanov, E.; Kim, K.-C.; Reed, C.A. *Angew. Chem. Int. Ed.* **2004**, *43*, 5352-5355.
- (145) Zhang, Y.; Huynh, K.; Manners, I.; Reed, C. A. *Chem. Commun.* **2008**, 494-496.
- (146) Hazin, K. From Main Group to Transition Metal-containing Brønsted Acid Initiators for the Cationic Polymerization of Olefins, PhD Thesis, University of British Columbia, Vancouver, 2018.
- (147) Arsenault, G.; Hazin, K.; Gates, D.P. Initiator System for the Cationic Polymerization of Olefins. WO2018/107295 A1, 21 June, 2018.
- (148) Piers, W. E.; Chivers, T. *Chem. Soc. Rev.* **1997**, *26*, 345-354.
- (149) Chen, E. Y.-X.; Marks, T.J. *Chem. Rev.* **2000**, *100*, 1205.
- (150) Metz, M. V.; Sun, Y. M.; Stern, C. L.; Marks, T. J. *Organometallics* **2002**, *21*, 3691-3702.
- (151) Engesser, T. A.; Lichtenthaler, M. R.; Schleep, M.; Krossing, I. *Chem. Soc. Rev.* **2016**, *45*, 789-899.
- (152) Krossing, I.; Bihlmeier, A.; Raabe, I.; Trapp, N. *Angew. Chem., Int. Ed.* **2003**, *42*, 1531-1534.
- (153) Stasko, D.; Hoffmann, S. P.; Kim, K. C.; Fackler, N. L. P.; Larsen, A. S.; Drovetskaya, T.; Tham, F. S.; Reed, C. A.; Rickard, C. E. F.; Boyd, P. D. W.; Stoyanov, E. S. *J. Am. Chem. Soc.* **2002**, *124*, 13869-13876.
- (154) Krossing, I. *J. Chem. Soc., Dalton Trans.* **2002**, 500-512.
- (155) Vijayaraghavan, R.; MacFarlane, D. R. *Chem. Commun.* **2004**, 700-701.
- (156) Vijayaraghavan, R.; MacFarlane, D. R. *Macromolecules* **2007**, *40*, 6515-6520.
- (157) Kapoor, R. N.; Prakash, S.; Kapoor, P. N. *Z. Anorg. Allg. Chem.* **1967**, *353*, 109-&.
- (158) Fairbrother, F.; Ahmed, N.; Edgar, K.; Thompson, A. *J. Less-Common Met.* **1962**, *4*, 466-475.
- (159) Funk, H.; Weiss, W.; Roethe, K.P. *Z. Anorg. Alg. Chem.* **1959**, 301.
- (160) Andrae, K. *J. Less-Common Metals* **1969**, *17*, 297.
- (161) Boyle, T. J.; Tribby, L. J.; Alam, T. M.; Bunge, S. D.; Holland, G. P. *Polyhedron* **2005**, *24*, 1143-1152.
- (162) Boyle, T. J.; Andrews, N. L.; Alam, T. M.; Rodriguez, M. A.; Santana, J. M.; Scott, B. L. *Polyhedron* **2002**, *21*, 2333-2345.
- (163) Marchetti, F.; Pampaloni, G.; Zacchini, S. *Eur. J. Inorg. Chem.* **2008**, 453-462.
- (164) Ihara, E.; Yoshida, N.; Ikeda, J. I.; Itoh, T.; Inoue, K. *J. Polym. Sci., Part A: Polym. Chem.* **2006**, *44*, 2636-2641.

- (165) Kanazawa, A.; Kanaoka, S.; Aoshima, S. *J. Polym. Sci., Part A: Polym. Chem.* **2010**, *48*, 2509-2516.
- (166) Bondi, A. *J. Phys. Chem.* **1964**, *68*, 441-&.
- (167) Vagedes, D.; Erker, G.; Fröhlich, R. *J. Organomet. Chem.* **2002**, *641*, 148.
- (168) Kanaoka, S.; Sawamoto, M.; Higashimura, T. *Macromolecules* **1992**, *25*, 6414-6418.
- (169) Kanazawa, A.; Kanaoka, S.; Aoshima, S. *Macromolecules* **2010**, *43*, 3682-3689.
- (170) Kanazawa, A.; Kanaoka, S.; Aoshima, S. *Macromolecules* **2010**, *43*, 2739-2747.
- (171) Fodor, Z.; Bae, Y. C.; Faust, R. *Macromolecules* **1998**, *31*, 5170-5170.
- (172) Yoshimitsu, H.; Kanazawa, A.; Kanaoka, S.; Aoshima, S. *J. Polym. Sci., Part A: Polym. Chem.* **2016**, *54*, 1774-1784.
- (173) Kigoshi, S.; Kanazawa, A.; Kanaoka, S.; Aoshima, S. *Polym. Chem.* **2015**, *6*, 30-34.
- (174) Sigma Aldrich Thermal Transitions of Homopolymers: Glass Transition & Melting Point, <https://www.sigmaaldrich.com/technical-documents/articles/materials-science/polymer-science/thermal-transitions-of-homopolymers.html> (Accessed 22 August 2018).
- (175) De, P.; Faust, R. Carbocationic Polymerization. In *Controlled and Living Polymerizations*, Muller, A.H.E.; Matyjaszewski, K. Eds.; Wiley-VCH Verlag GmbH & Co. KGaA: 2009; 57.
- (176) Higashimura, T.; Ishihama, Y.; Sawamoto, M. *Macromolecules* **1993**, *26*, 744-751.
- (177) Claudy, P.; Letoffe, J. M.; Camberlain, Y.; Pascault, J. P. *Polym. Bull.* **1983**, *9*, 208-215.
- (178) Wrasidlo, W. *Adv. Polym. Sc.* **1974**, *13*, 30.
- (179) Blanchard, L. P.; Hesse, J.; Malhotra, S. L. *Can. J. Chem.* **1974**, *52*, 3170-3175.
- (180) Li, S. J.; Xie, S. J.; Li, Y. C.; Qian, H. J.; Lu, Z. Y. *Phys. Rev. E* **2016**, *93*.
- (181) Dainton, F. S.; Ivin, K. J. *Nature* **1948**, *162*, 705-707.
- (182) Ramey, K. C.; Statton, G. L.; Jankowski, W. C. *J. Polym. Sci., Part C: Polym. Lett.* **1969**, *7*, 693.
- (183) Banerjee, S.; Paira, T. K.; Mandal, T. K. *Macromol. Chem. Phys.* **2013**, *214*, 1332-1344.
- (184) Higashimura, T.; Masami, K.; Kato, M.; Hasebe, T.; Sawamoto, M. *Macromolecules* **1993**, *26*, 2670.
- (185) Cowie, J. M. G.; Toporows.Pm *Eur. Polym. J.* **1968**, *4*, 621-&.
- (186) Cowie, J. M. G.; Bywater, S. *J. Polym. Sci., Part B: Polym. Phys.* **1968**, *6*, 499-&.
- (187) Ouardad, S.; Deffieux, A.; Peruch, F. *Pure Appl. Chem.* **2012**, *84*, 2065-2080.
- (188) Rozentsvet, V. A.; Kozlov, V. G.; Ziganshina, E. F.; Boreiko, N. P.; Kostjuk, S. V. *Polym. Int.* **2013**, *62*, 817-826.
- (189) McManus, N.T.; Penlids, A. *J. Appli. Polym. Sci.* **1998**, *70*, 1253.
- (190) Jackson, C. ; Chen, Y.-J.; Mays, J.W. *J. Appl. Polym. Sci.* **1996**, *61*, 865.
- (191) SAINT, Version 8.34 A, Bruker AXS Inc., Madisoc, WI, **1997-2013**.
- (192) SADABS, V2014/5, Krause,L; Herbst-Irmer, R.; Sheldrick, G.M.; Stalke, D. *J. Appl. Crystallogr.* **2015**, *48*, 3.
- (193) SHELXT, Sheldrick, G.M. *Acta Cryst. A.* **2015**, *71*, 3-8.
- (194) Sheldrick, G.M.; *SHELXL-97*, University of Göttingen, Germany, **1997**.
- (195) Herrmann, W.A.; Watzlowik, P. *J. Organomet. Chem.* **1992**, *441*, 265.
- (196) Rockwell, J. J.; Kloster, G. M.; DuBay, W. J.; Grieco, P. A.; Shriver, D. F.; Strauss, S. H. *Inorg. Chim. Acta* **1997**, *263*, 195-200.
- (197) Mehrotra, R. C.; Kapoor, P. N. *J. Less-Common Met.* **1965**, *8*, 419-&.
- (198) Cripps, W. S.; Willis, C. J. *Can. J. Chem.* **1975**, *53*, 817-825.
- (199) Cripps, W. S.; Willis, C. J. *Can. J. Chem.* **1975**, *53*, 809-816.

- (200) Willis, C. J. *Journal of the Chemical Society-Chemical Communications* **1974**, 117-118.
- (201) Middleton, W. J.; Lindsey, R. V. *J. Am. Chem. Soc.* **1964**, *86*, 4948-&.
- (202) Middleton, W. J. *J. Fluorine Chem.* **1999**, *100*, 207-216.
- (203) Allan, M.; Willis, C. J. *J. Am. Chem. Soc.* **1968**, *90*, 5343-&.
- (204) Atkins, P.; Overton, T.; Rourke, J.; Weller, M.; Armstrong, F., *Shriver and Atkins' Inorganic Chemistry*. Fifth ed.; Oxford University Press: Oxford, UK, 2010.
- (205) Friese, J.C.; Krol, A.; Puke, C.; Kirschbaum, K.; Giolando, D.M. *Inorg. Chem.* **2000**, *39*, 1496.
- (206) Martin, J.L.; Takats, J. *Can. J. Chem.* **1989**, *67*, 1914.
- (207) Karpishin, T.B.; Stack, T.D.P.; Raymond, K.N. *J. Am. Chem. Soc.* **1993**, *115*, 182.
- (208) Eisenberg, R.; Steifel, E.I.; Rosenberg, R.C.; Gray, H.B. *J. Am. Chem. Soc.* **1966**, *88*, 2874.
- (209) Morse, P.M.; Girolami, G.S. *J. Am. Chem. Soc.* **1989**, *111*, 4114.
- (210) Housecroft, C.E.; Sharpe, A.G. *Inorganic Chemistry*. Fourth ed. Pearson, 2012.
- (211) Vanseggen, D. M.; Hurlburt, P. K.; Anderson, O. P.; Strauss, S. H. *Inorg. Chem.* **1995**, *34*, 3453-3464.
- (212) Vanseggen, D. M.; Hurlburt, P. K.; Anderson, O. P.; Strauss, S. H. *J. Am. Chem. Soc.* **1992**, *114*, 10995-10997.

Appendices

Appendix A Supplementary Information for Chapter 2

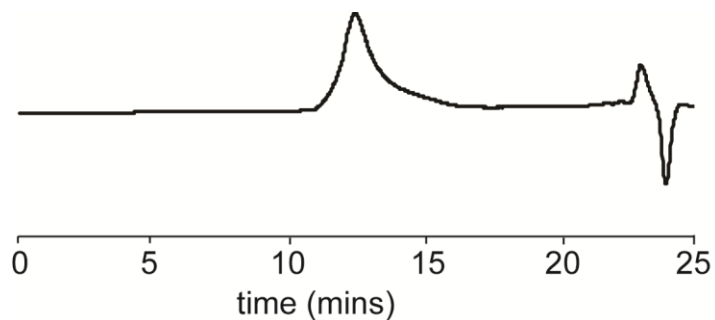


Figure A.1 GPC trace for H(OEt₂)₂[2.1]-initiated poly(*n*-butyl vinyl ether).

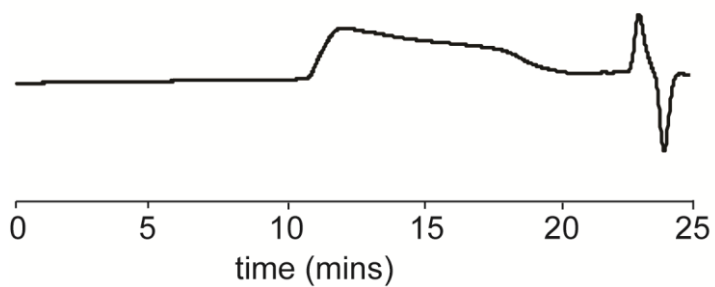


Figure A.2 GPC trace for H(OEt₂)₂[2.1]-initiated polystyrene.

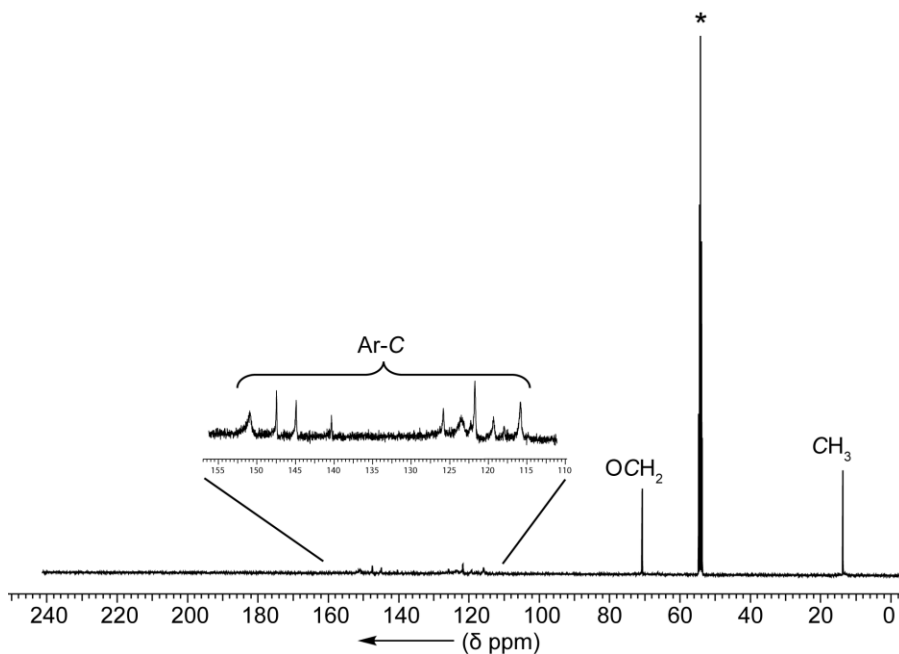


Figure A.3 ¹³C{¹H} NMR (100 MHz, CD₂Cl₂, -85 °C) spectrum of H(OEt₂)₂[2.2]. * indicates NMR solvent.

Temperature of
polymerization /°C

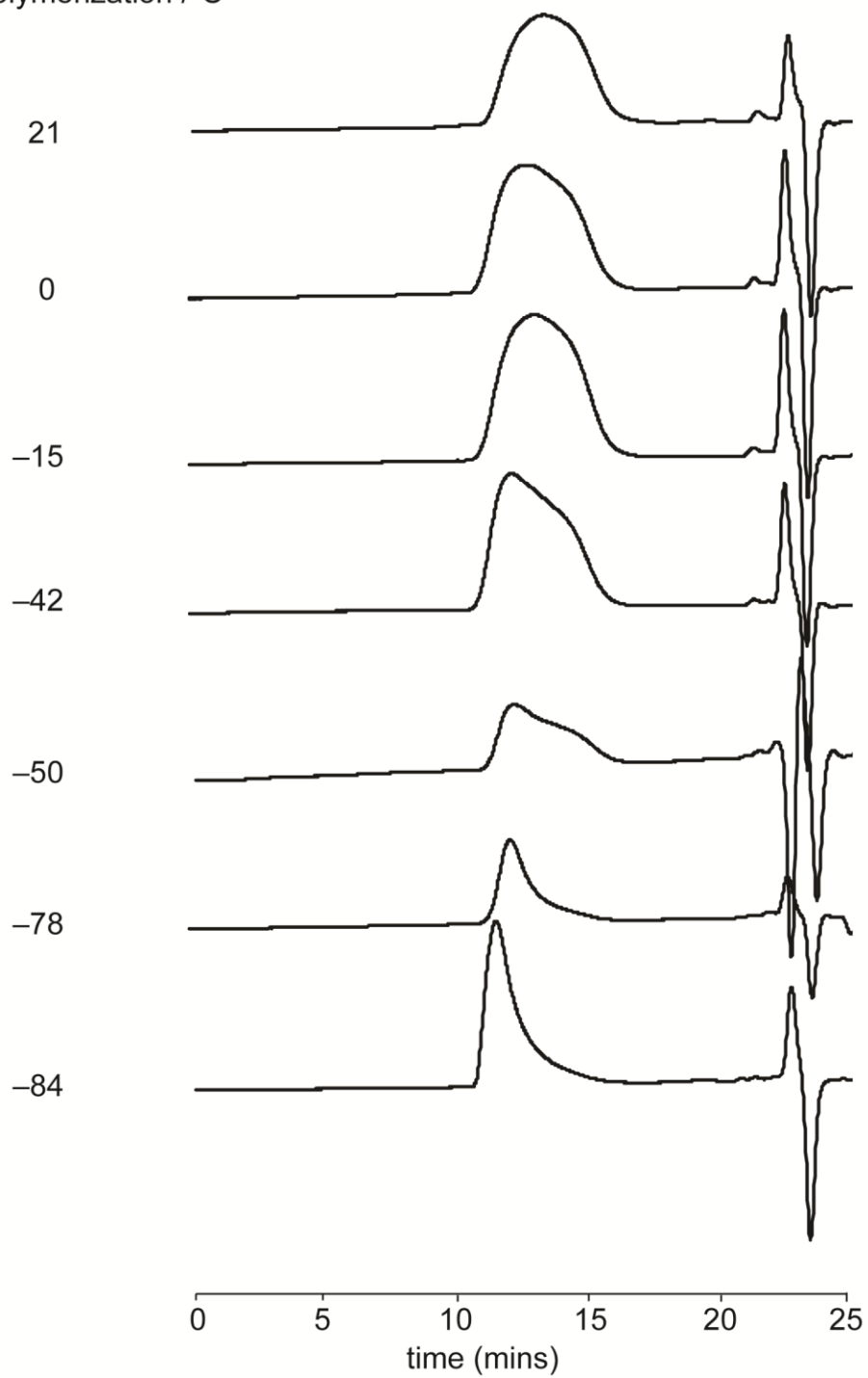


Figure A.4 GPC trace for $\text{H}(\text{OEt}_2)_2[2.2]$ -initiated poly(*n*-butyl vinyl ether).

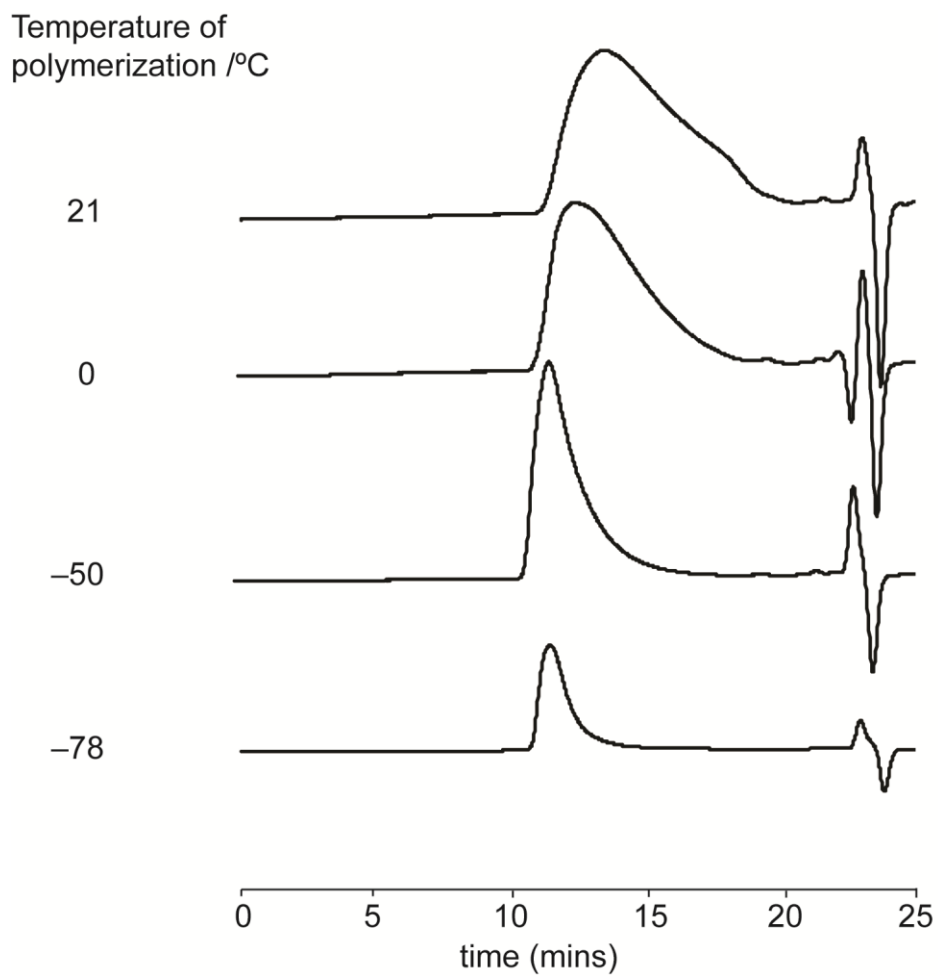


Figure A.5 GPC trace for H(OEt)₂[2.2]-initiated polystyrene.

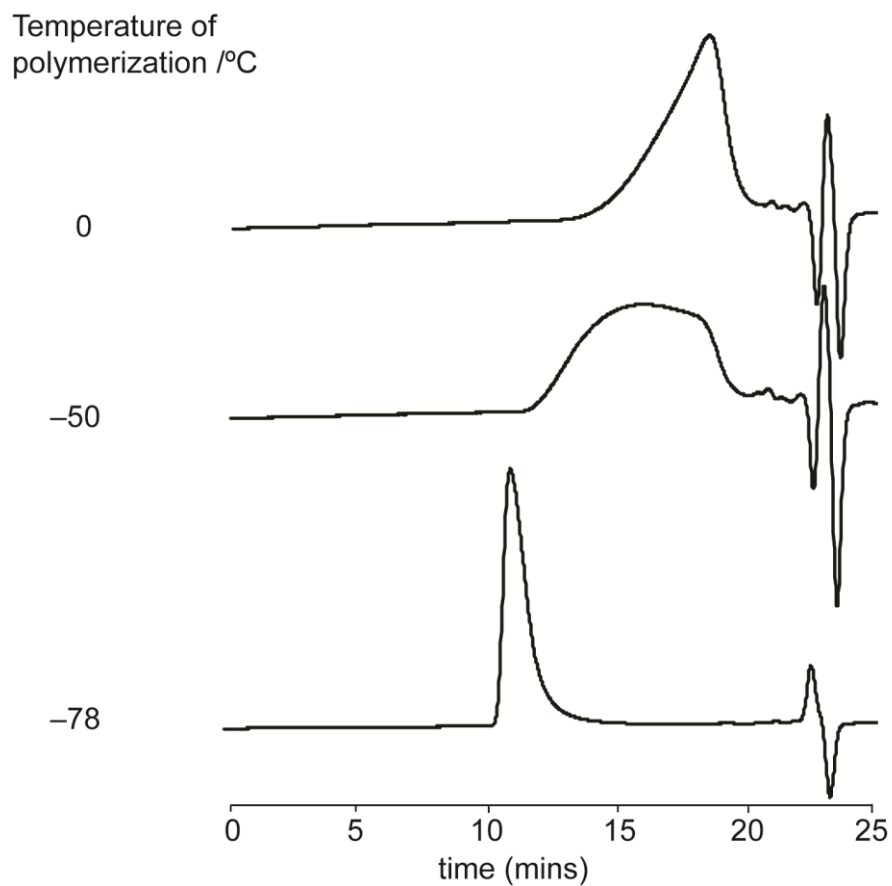


Figure A.6 GPC trace for H(OEt₂)₂[2.2]-initiated poly(α -methylstyrene).

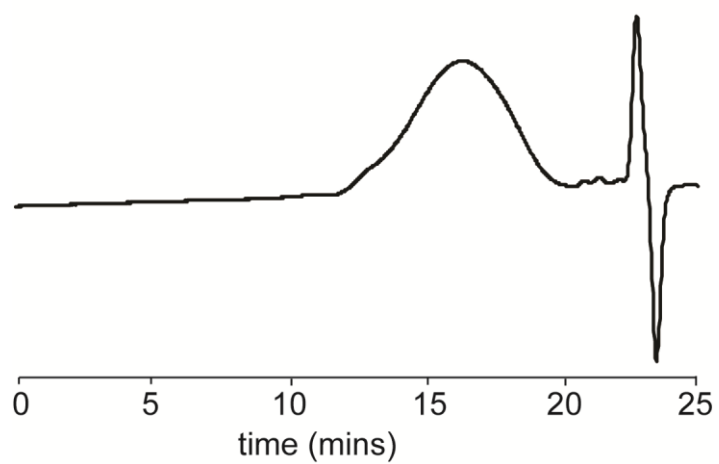


Figure A.7 GPC trace for H(OEt₂)₂[2.2]-initiated polyisoprene.

Appendix B Supplementary Information for Chapter 3

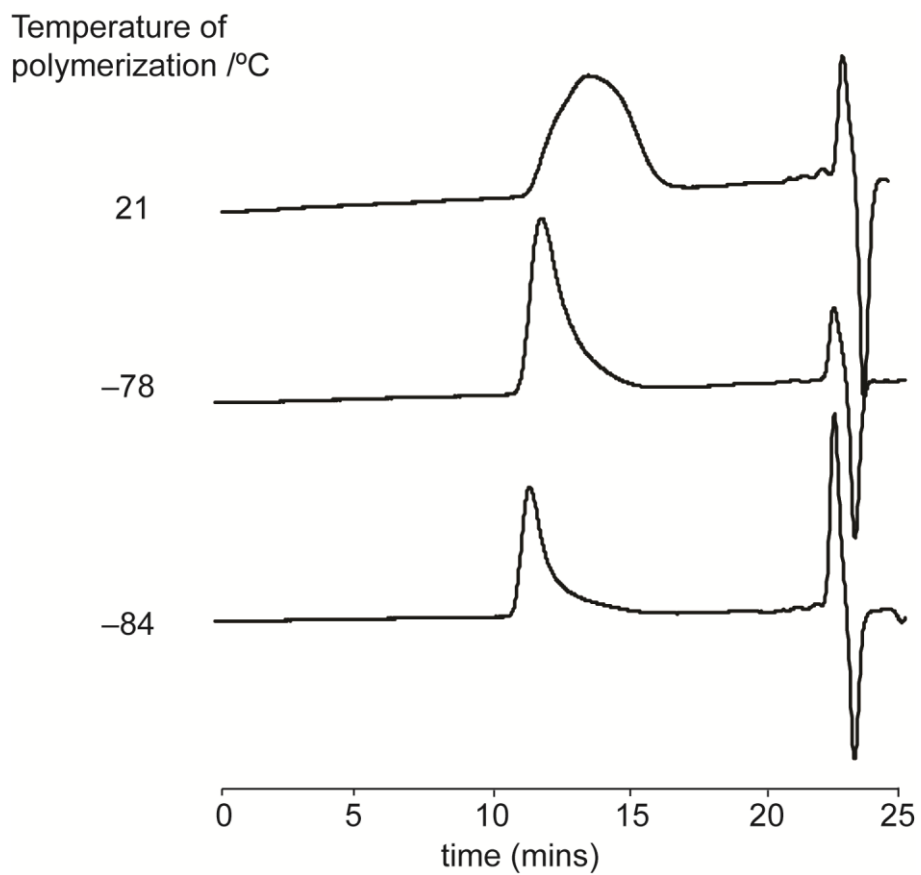


Figure B.1 GPC trace for H(OEt₂)₂[3.1]-initiated poly(*n*-butyl vinyl ether).

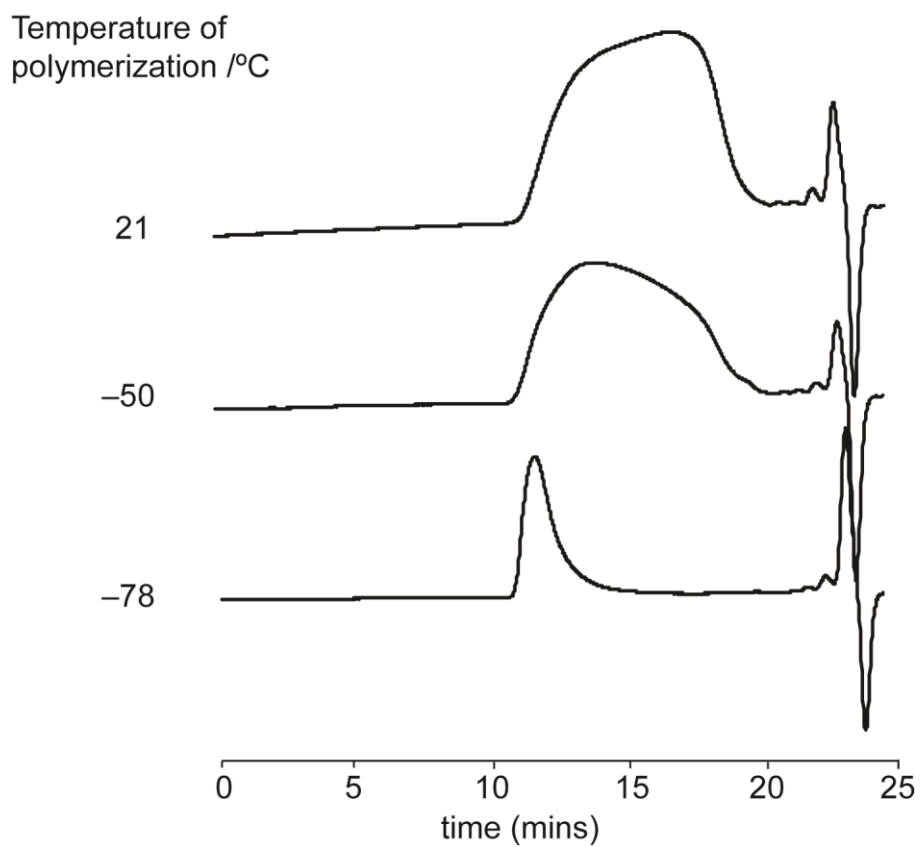


Figure B.2 GPC trace for H(OEt)₂[3.1]-initiated polystyrene.

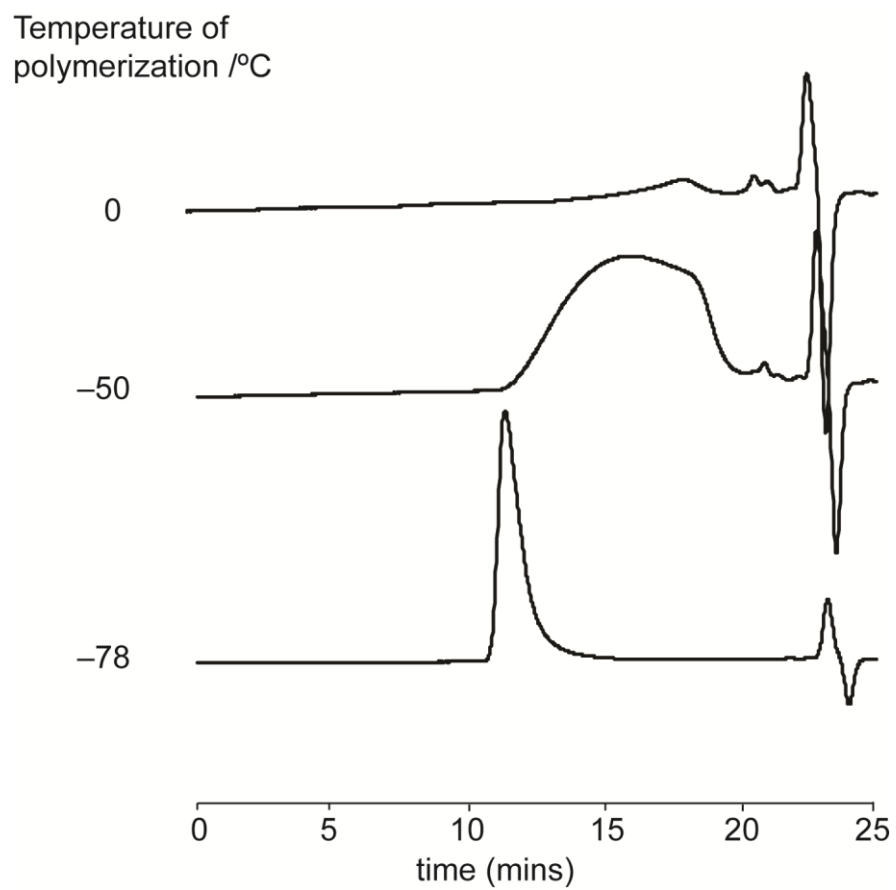


Figure B.3 GPC trace for $\text{H}(\text{OEt}_2)_2[3.1]$ -initiated poly(α -methylstyrene).

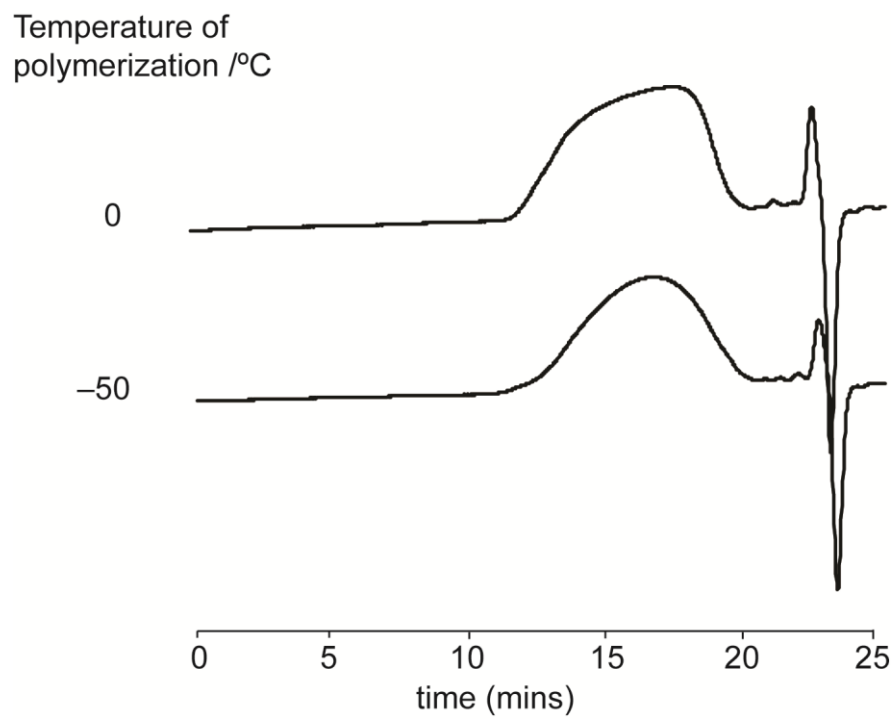


Figure B.4 GPC trace for $\text{H}(\text{OEt}_2)_2[3.1]$ -initiated polyisoprene.

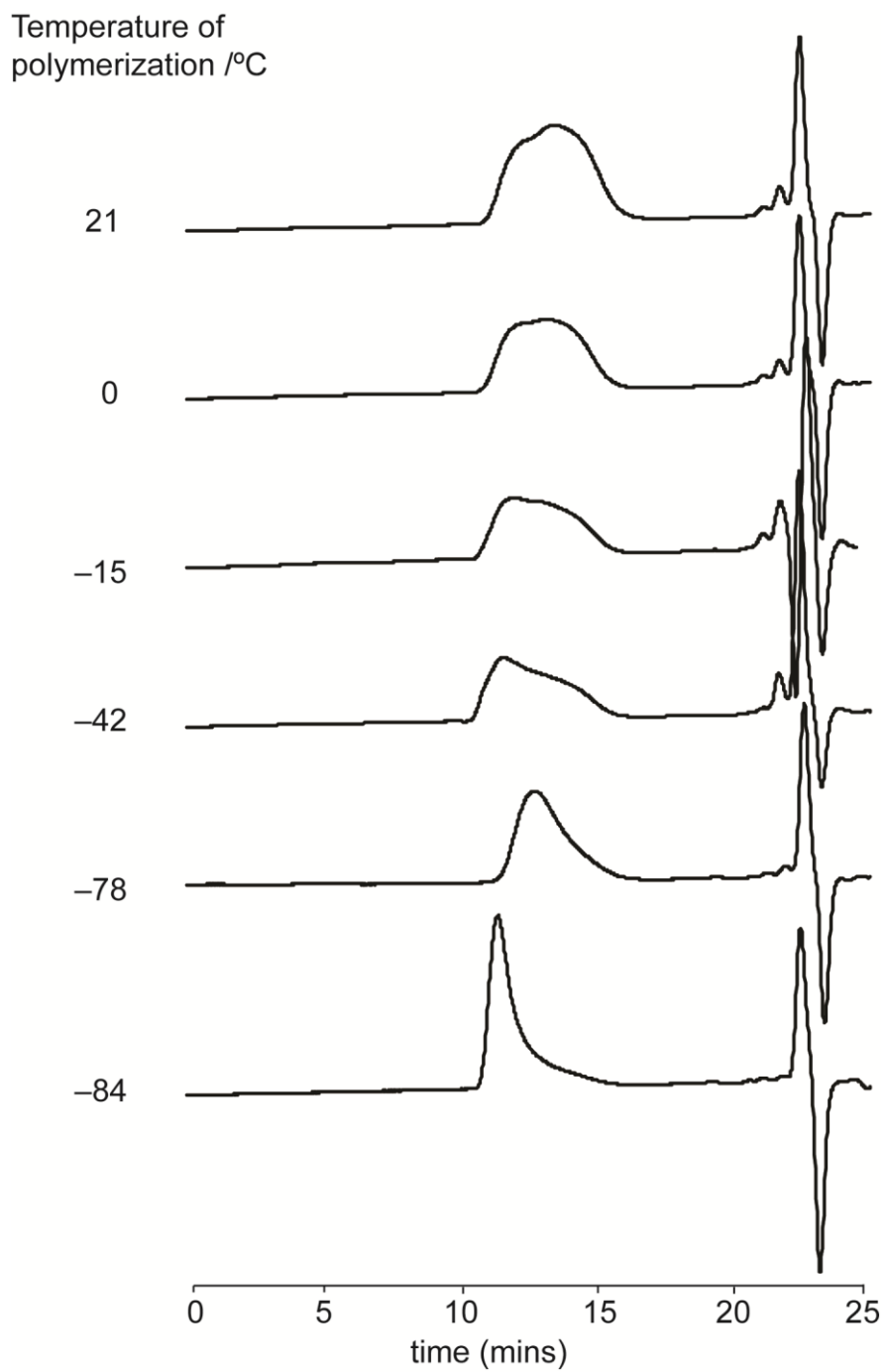


Figure B.5 GPC trace for H(OEt₂)₂[3.2]-initiated poly(*n*-butyl vinyl ether).

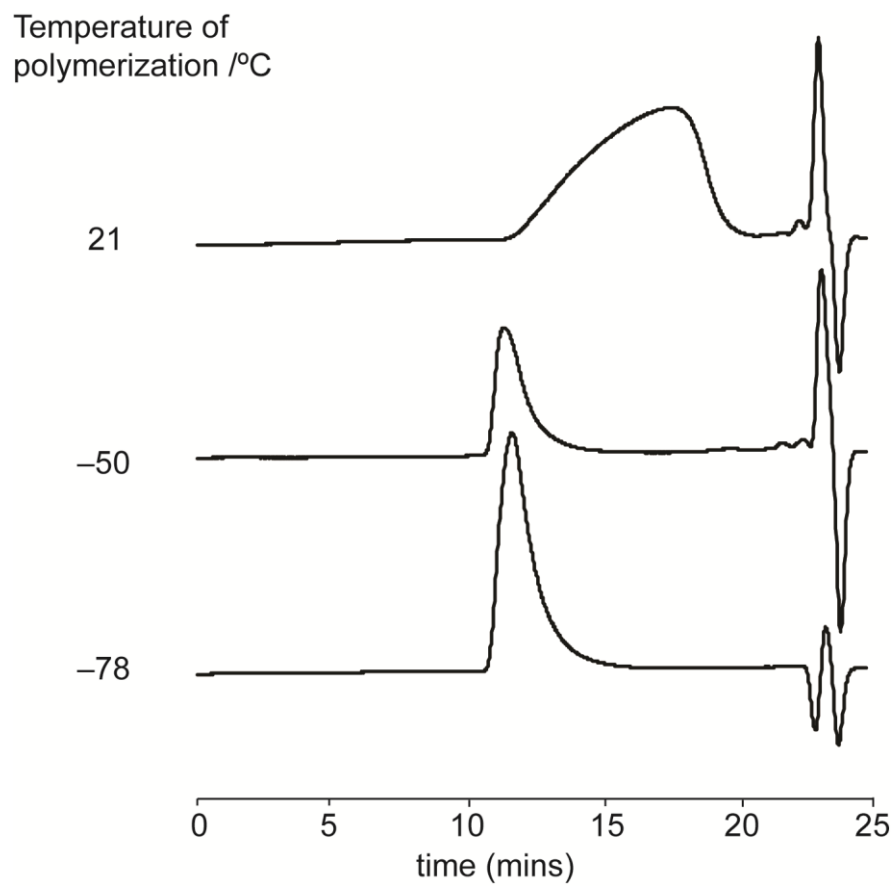


Figure B.6 GPC trace for H(OEt₂)₂[3.2]-initiated polystyrene.

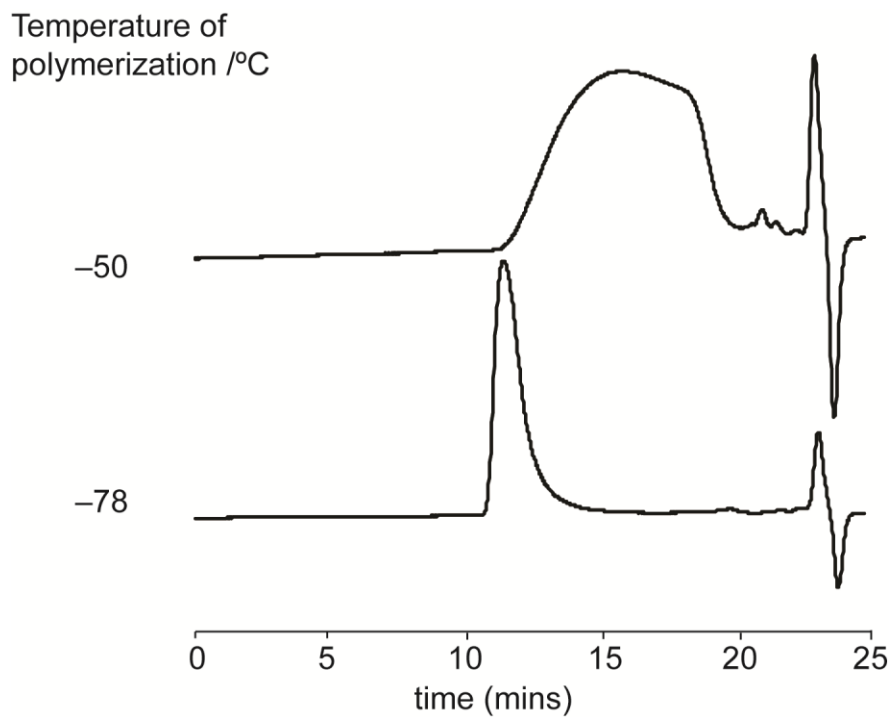


Figure B.7 GPC trace for H(OEt₂)₂[3.2]-initiated poly(α -methylstyrene).

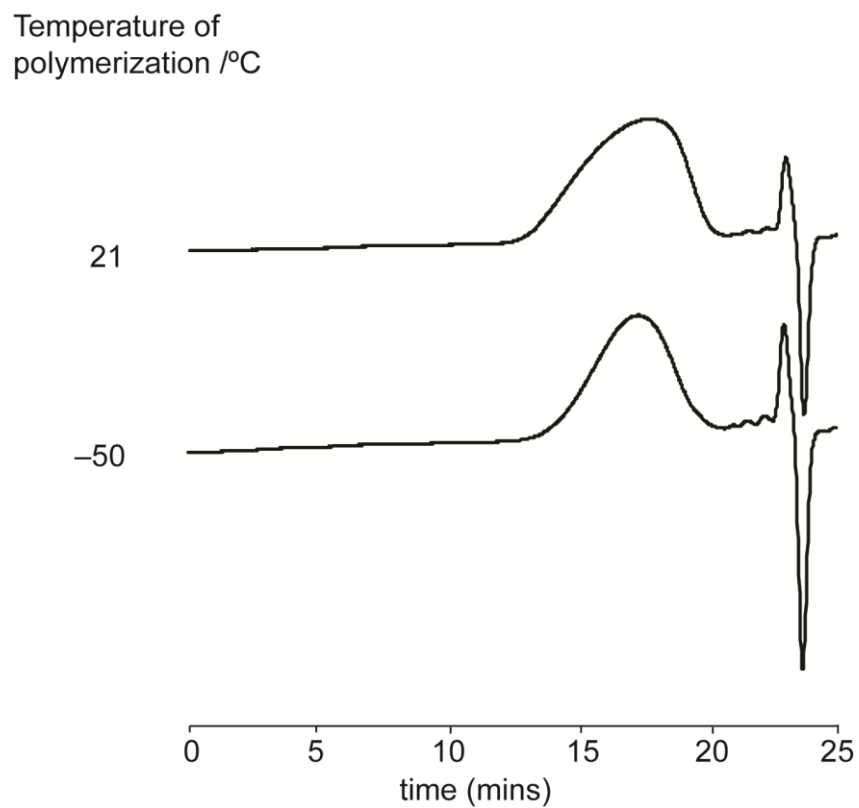


Figure B.8 GPC trace for H(OEt₂)₂[3.2]-initiated polyisoprene.